INFORMATION TO USERS

This material was produced from a microfilm copy of the original document. While the most advanced technological means to photograph and reproduce this document have been used, the quality is heavily dependent upon the quality of the original submitted.

The following explanation of techniques is provided to help you understand markings or patterns which may appear on this reproduction.

1. The sign or "target" for pages apparently lacking from the document photographed is "Missing Page(s)". If it was possible to obtain the missing page(s) or section, they are spliced into the film along with adjacent pages. This may have necessitated cutting thru an image and duplicating adjacent pages to insure you complete continuity.

2. When an image on the film is obliterated with a large round black mark, it is an indication that the photographer suspected that the copy may have moved during exposure and thus cause a blurred image. You will find a good image of the page in the adjacent frame.

3. When a map, drawing or chart, etc., was part of the material being photographed the photographer followed a definite method in "sectioning" the material. It is customary to begin photoing at the upper left hand corner of a large sheet and to continue photoing from left to right in equal sections with a small overlap. If necessary, sectioning is continued again — beginning below the first row and continuing on until complete.

4. The majority of users indicate that the textual content is of greatest value, however, a somewhat higher quality reproduction could be made from "photographs" if essential to the understanding of the dissertation. Silver prints of "photographs" may be ordered at additional charge by writing the Order Department, giving the catalog number, title, author and specific pages you wish reproduced.

5. PLEASE NOTE: Some pages may have indistinct print. Filmed as received.

Xerox University Microfilms

300 North Zeeb Road
Ann Arbor, Michigan 48106

73-21,079

KAYE, Stephen Edward, 1944-
ENTRANCE PRESSURE LOSSES FOR INELASTIC NEWTONIAN AND NON-NEWTONIAN FLUIDS.

Carnegie-Mellon University, Ph.D., 1973
Engineering, chemical

University Microfilms, A XEROX Company, Ann Arbor, Michigan

THIS DISSERTATION HAS BEEN MICROFLIMED EXACTLY AS RECEIVED

Carnegie-Mellon University

CARNEGIE INSTITUTE OF TECHNOLOGY

AND

MELLON INSTITUTE OF SCIENCE

THESIS

SUBMITTED IN PARTIAL FULFILLMENT OF THE REQUIREMENTS

FOR THE DEGREE OF Doctor of Philosophy

TITLE Entrance Pressure Losses for Inelastic Newtonian and Non-Newtonian Fluids

PRESENTED BY Stephen E. Kaye

ACCEPTED BY THE DEPARTMENT OF Chemical Engineering

Stephen L. Kaye — MAJOR PROFESSOR — 2/23/73 — DATE

R.R. Rothfus — DEPARTMENT HEAD — 2/23/73 — DATE

APPROVED BY THE COLLEGE COUNCIL

[signature] — DEAN — 4/10/73 — DATE

TABLE OF CONTENTS

ACKNOWLEDGEMENTS	ii
ABSTRACT	iii
NOMENCLATURE	iv
LIST OF FIGURES	vii
LIST OF TABLES	x
CHAPTER I. BACKGROUND	1
Introduction	1
Sudden Contraction--Newtonian Fluid	3
Conical Entrances	10
Sudden Contraction--Non-Newtonian Fluids	17
Entrance Losses--Summary	29
CHAPTER II. EXPERIMENTAL	31
Apparatus	31
Solutions	43
Experimental Procedures	47
Data Analysis	49
Sources of Error	52
CHAPTER III. RESULTS	54
Newtonian Fluids through a Sudden Contraction--Dependence on Contraction Ratio	54
Newtonian Fluids through Gradual Contractions--Dependence on Contraction Angle	65
Inelastic Non-Newtonian Fluids through a Sudden Contraction--Dependence on Flow Index	72
CONCLUSIONS	102
RECOMMENDATIONS	103
BIBLIOGRAPHY	104
APPENDICES	
A-1. Calculation of Least Squares for the Relative Error	110
A-2. Computer Program for Treating Data	111
A-3. Data	122

ACKNOWLEDGEMENTS

I wish to express appreciation to everyone who contributed toward the learning and accomplishment of this research. Specifically, to Professor Stephen Rosen for his time and interest through the work, to Messrs. Frank McMurtry and John Churchell for assisting in the construction of the apparatus, to Dow Chemical for donating polymers, to Harvey Cohen for helping prepare and evaluate solutions, to the department of Chemical Engineering for providing the funding that made this work possible, and, lastly, to my wife Cathy for bearing with me during the years of research and for typing the thesis.

Entrance Pressure Losses for Inelastic Newtonian
and Non-Newtonian Fluids by
Stephen E. Kaye - Dept. of Chemical Eng.
Carnegie-Mellon Univ.

ABSTRACT

Entrance pressure losses have been measured for inelastic fluids flowing through contractions in cylindrical tubes. The equation

$\frac{\Delta P_{ent}}{\rho v^2/2g_c} = K + K'/N_{Re}$ has been further shown to adequately describe

variation with Reynolds Number. For Newtonian fluids Hagenbach, K, and Couette, K', corrections were correlated with the ratio of tube areas, β, yielding $K = 2.32(1-\beta^2)$, $K' = 159(1-\beta^2)$, and with the contraction angle, α, showing an 11% decrease in K' for $\alpha = 45^\circ$ to 65°. Two different non-Newtonian inelastic fluids provided variation of K and K' with flow index, n, at $\beta = 0.041$ and $\beta = 0.636$. Linear correlations offered for $\beta = 0.041$: $K = 0.70n + 1.62$, $K' = 97n + 64$ and for $\beta = 0.636$: $K = 0.25n + 1.13$, $K' = 7n + 88$. A simple recoil method was developed to determine qualitative levels of elasticity in dilute polymer solutions.

TABLE OF NOMENCLATURE

A	area
C C'	parameters (analogous to K and K')
C	$= K'/64$
C'	$= K/64$
D	diameter
f_i	unknown functions
f_{ij}	unknown functions
f	Fanning Friction Factor
F	unknown function
g_c	gravitational constant
G	elastic modulus
H	power-law elastic modulus
K	Hagenbach correction
K'	Couette correction
L	length
m	elastic power-law index
n	power-law index
n_o	$K'/32$, form of Couette correction
N_e	$\dfrac{\kappa^2}{\rho G R^2 v^{2(1-n)}}$, Equation (1.28)
N_{Re}	Reynolds Number
P	pressure
$(P_{11}-P_{22})$	normal stress difference
Q	volumetric flow rate
r	radial coordinate
r_o	cone length from apex

R	radius
v, v_b	bulk velocity
X_{eff}	length of tube having an equilibrium pressure drop equal to ΔP_{ent}
z	axial coordinate
α	cone angle
α'	cone angle
α_3	proportionality constant in Equation (1.29)
β	contraction ratio
γ	shear strain
$\dot{\gamma}$	shear rate
$\dot{\gamma}_w$	wall shear rate
δ_i, δ_e	viscous entrance and exit correction proposed by Dorsey (22)
ΔK.E.	change in kinetic energy
ΔP_{cone}	pressure drop across a cone
$\Delta P_{elastic}$	elastic contribution to ΔP_{ent}
ΔP_{ent}	entrance pressure loss
ΔP_{tot}	total pressure drop
θ	spherical coordinate
κ	consistency
μ	viscosity
π	3.14159
ρ	density
σ_w	first normal stress difference at the wall
τ	shear stress
τ_w	wall shear stress

ϕ	spherical coordinate
ϕ	adjustable parameter
$\phi_1(n)$	function of n, Equation (1.27)
$\phi_2(n)$	function of n, Equation (1.27)

Subscripts

ij	indices
t	test section
e	entrance section

LIST OF FIGURES

Figure No.	Title	Page
1.1	Qualitative Representation of Pressure over a Sudden Contraction	2
1.2	Coordinate System for Theoretical Considerations of Flow in Tapered Tubes	12
1.3	K'_{cone} vs. Cone Angle for Slow Flow through a Cone with Small r/r_o. Calculated from Solution by Bond (13)	15
1.4	Comparison of Work on K = K(n)	18
1.5	Functions $\phi_1(n)$ and $\phi_2(n)$ from Tomita and Yamane (67)	27
2.1	Schematic of Apparatus for Studying K and K'	32
2.2	Flange Design for Entrance Section of Test Section	34
2.3	Cross-Section of Entrance Section	35
2.4	Manometer Arrangement	46
2.5	Cross-Section of 15° Conical Insert	41
2.6	Schematic for Recoil Apparatus	42
2.7	Viscosity Dependence on Temperature for Representative Fluids	50
3.1	Entrance Pressure Loss for Newtonian Flow through a Sudden Contraction, $\beta = 0.635$	55
3.2	Entrance Pressure Loss for Newtonian Flow through a Sudden Contraction, $\beta = 0.411$	56
3.3	Entrance Pressure Loss for Newtonian Flow through a Sudden Contraction, $\beta = 0.213$	57
3.4	Entrance Pressure Loss for Newtonian Flow through a Sudden Contraction, $\beta = 0.109$	58
3.5	Entrance Pressure Loss for Newtonian Flow through a Sudden Contraction, $\beta = 0.062$	59

Figure No.	Title	Page
3.6	Entrance Pressure Loss for Newtonian Flow through a Sudden Contraction, $\beta = 0.041$	60
3.7	Entrance Pressure Loss for Newtonian Flow through a Sudden Contraction, $\beta = 0.026$	61
3.8	K and K' vs. Ratio of Tube Areas	63
3.9	Entrance Pressure Loss for Newtonian Flow through a Conical Contraction, $\alpha = 7\ 1/2^{\circ}$	66
3.10	Entrance Pressure Loss for Newtonian Flow through a Conical Contraction, $\alpha = 15^{\circ}$	67
3.11	Entrance Pressure Loss for Newtonian Flow through a Conical Contraction, $\alpha = 30^{\circ}$	68
3.12	Entrance Pressure Loss for Newtonian Flow through a Conical Contraction, $\alpha = 60^{\circ}$	69
3.13	K and K' vs. Contraction Angle	70
3.14	Flow Curve for Separan	75
3.15	Flow Curves for Methocel	75
3.16	Flow Curve for Polyox	76
3.17	Flow Curve for Polyox	76
3.18	Flow Curve for Polyox	77
3.19	Flow Curves for Polyox	77
3.20	Flow Curves for Polyox	78
3.21	Representative Friction Factor-Reynolds Number Data	82
3.22	Recoil vs. Shear Degradation Time for Polyox and Recoil vs. Concentration for Methocel	84
3.23	Entrance Pressure Loss for Inelastic Non-Newtonian Methocel Flowing through a Sudden Contraction with $\beta = 0.041$	86

Figure No.	Title	Page
3.24	Entrance Pressure Loss for Inelastic Non-Newtonian Methocel Flowing through a Sudden Contraction with $\beta = 0.041$	87
3.25	Entrance Pressure Loss for Inelastic Non-Newtonian Polyox Flowing through a Sudden Contraction with $\beta = 0.041$	88
3.26	Entrance Pressure Loss for Inelastic Non-Newtonian Polyox Flowing through a Sudden Contraction with $\beta = 0.041$	89
3.27	Entrance Pressure Loss for Inelastic Non-Newtonian Polyox Flowing through a Sudden Contraction with $\beta = 0.041$	90
3.28	Entrance Pressure Loss for Inelastic Non-Newtonian Polyox Flowing through a Sudden Contraction with $\beta = 0.041$	91
3.29	Entrance Pressure Loss for Inelastic Non-Newtonian Polyox Flowing through a Sudden Contraction with $\beta = 0.041$	92
3.30	Entrance Pressure Loss for Inelastic Non-Newtonian Polyox Flowing through a Sudden Contraction with $\beta = 0.636$	93
3.31	Entrance Pressure Loss for Inelastic Non-Newtonian Polyox Flowing through a Sudden Contraction with $\beta = 0.636$	94
3.32	K vs. Power-Law Index	97
3.33	K' vs. Power-Law Index	98
3.34	Entrance Pressure Loss for Separan Flowing through a Sudden Contraction with $\beta = 0.041$	101

LIST OF TABLES

Table No.	Title	Page
1.1	Summary of Values for K and K'	29
2.1	Entrance Section Dimensions	38
3.1	Values of K and K' for Newtonian Fluids	62
3.2	K and K' vs. Cone Angle for Gradual Contractions	71
3.3	Non-Newtonian Fluids	73
3.4	Entrance Loss Parameters for Non-Newtonian Fluids	96

CHAPTER 1. BACKGROUND

Introduction

Fluid flowing through a contraction from one cylindrical tube to another will result in a pressure drop. Parallel to Sylvester's work (62) this study defines the entrance pressure loss as the difference between the actual pressure drop between a section upstream and one far downstream, and the pressure drop that would exist if only losses from fully developed flow in the tube were present. This is graphically depicted for a sudden contraction in Fig. 1.1.

The entrance pressure loss, ΔP_{ent}, is commonly written in dimensionless form as

$$\frac{\Delta P_{ent}}{\rho v^2/2g_c} \tag{1.1}$$

where v is the average downstream fluid velocity. For a fluid with shear stress, τ, shear rate, $\dot{\gamma}$, behavior describable by the power-law approximation

$$g_c \tau = \kappa \dot{\gamma}^n$$

dimensional considerations indicate that

$$\frac{\Delta P_{ent}}{\rho v^2/2g_c} = F\left[\left(\frac{v^{2-n} D^n \rho}{\kappa}\right), f_i(\beta,\alpha,n)\right] \tag{1.2}$$

where the $f_i(\beta,\alpha,n)$ are a set of unknown functions of β, the ratio of tube areas, of α, the contraction geometry, and of n, the power-

Fig. 1.1. Qualitative Representation of
Pressure Drop Over a Sudden Contraction

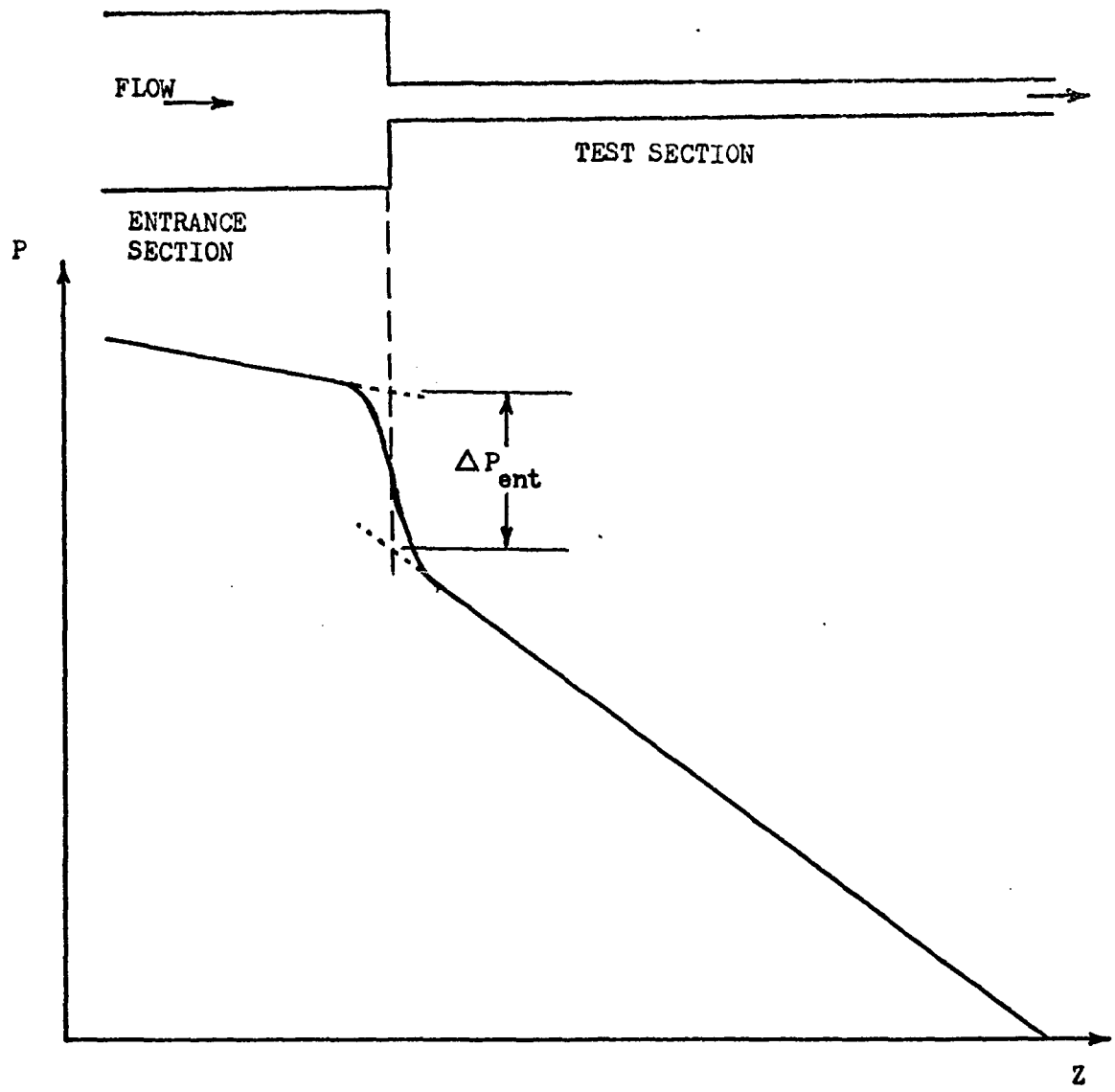

law index. The group $\frac{v^{2-n}D^{n}\rho}{\kappa}$ is a generalized Reynolds number.

Research on flow through contractions has attempted to determine or model a dependence of $\frac{\Delta P_{ent}}{\rho v^2/2g_c}$ on measurable parameters. In general most of this work has ignored the $f_i(\beta,\alpha,n)$ and has restricted study to either very low N_{Re} (less than 10) or reasonably high laminar N_{Re} (500 to 2000). To achieve this workers had to make assumptions or design experiments that were insensitive to undesirable (and unexplainable) phenomena.

The objective of this study is to experimentally determine the dependence of ΔP_{ent} on first β and α for Newtonian fluids and second on n for inelastic non-Newtonian fluids, over a wide range of Reynolds Numbers.

Sudden Contraction--Newtonian Fluid

The problem of predicting pressure entrance losses has been studied since Poiseuille's famous work (49) on the flow of liquids in capillary tubes, in which he observed experiments that deviated from a common law. Two types of corrections have been proposed: one for kinetic energy changes (Hagenbach correction)[1]

$$g_c \Delta P_{tot} = \frac{8\mu L v}{R^2} + K\rho\frac{v^2}{2} \qquad (1.3)$$

---

1. Observe that $\frac{8\mu L v}{R^2}$ represents pressure drop due to developed laminar flow and that $\frac{1}{2}K\rho v^2$ accounts for entrance pressure losses due to changes in kinetic energy. Thus $\Delta P_{tot} = \Delta P_{laminar} + \Delta P_{ent}$.

which gives

$$\frac{\Delta P_{ent}}{\rho v^2/2g_c} = K \tag{1.4}$$

and one for viscous effects (Couette correction)[1]

$$g_c \Delta P_{tot} = \frac{8\mu(L + n_o R)v}{R^2} \tag{1.5}$$

which gives

$$\frac{\Delta P_{ent}}{\rho v^2/2g_c} = \frac{K'}{N_{Re}} \; ; \; (K' = 32n_o) \tag{1.6}$$

Knibbs (39) presented an extensive review of work on this. He also proposed a form that combined these effects:

$$g_c \Delta P_{tot} = \frac{8\mu(L + n_o R)v}{R^2} + K\frac{\rho v^2}{2} \tag{1.7}$$

which gives

$$\frac{\Delta P_{ent}}{\rho v^2/2g_c} = K + K'/N_{Re} \tag{1.8}$$

Knibbs applied Poiseuille's data to Equation (1.7) to get values for K and n_o. Large differences in the magnitude and sign of n_o (or K') led Knibbs to decide that it should be ignored since "no constant value could be assigned to it except zero." For K he obtained an average value of 2.28. Hosking (34) admits obtaining values for K and n_o which he does not publish. Perhaps these were calculated from data reported in earlier papers (35, 36). However,

---

1. This has been written in many ways: as n_oR, n_oD, or e, each giving rise to a different numerical factor in the last equation. Notice that n_o is dimensionless and e had dimensions of length.

he did conduct experiments at high flow rates (up to turbulent flow)[1] in which he found $n_o = 0$ for all tests and the kinetic energy correction responsible for up to 55-60% of the viscosity. This is the expected result, since at large N_{Re} kinetic energy effects dominate and the term n_o/N_{Re} becomes negligible.

Bond (12) showed that a Couette correction could be measured at low Reynolds numbers ($N_{Re} < 16$), getting $K' = 36.7$. However, to do this, he neglected kinetic energy effects. Bond measured ΔP_{ent} by observing flows through tubes of the same radius but different lengths--some being very short. This may have adversely effected his results, especially if the short tubes did not allow full development of velocity profiles.

Dorsey (22) enlarged on Bond's work (12) giving added consideration to his data. Dorsey presented an argument against the possibility of a kinetic energy correction for reservoir-to-reservoir viscometers. Although this is valid (that ΔK.E. = 0) for such a design, not all viscometers exit into a reservoir of fluid. Also, as Dorsey showed, there are still two <u>different</u> corrections necessary for an accurate representation of ΔP_{ent}, i.e.:

$$g_c \Delta P_{ent} = \frac{8\mu(\delta_i + \delta_o)v}{R^2} \qquad (1.9)$$

where δ_i and δ_o are the viscous entrance and exit corrections.

---

1. Hosking (10) observed a "sudden change in values" above certain flow rates. Calculation shows these conditions to give Reynolds numbers in the transition region to turbulent flow.

From Bond's data (12), Dorsey concluded that for $N_{Re} < 10$, $K = 0$, $K' = 36.7$; for $N_{Re} > 10$, two situations were possible: the same values for K and K' held as for $N_{Re} < 10$, or $K = 2.0$ and $K' = 18.3$.

Rieman (52) measured entrance losses, with the opposite approach of Bond's: his experiment was designed to maximize K.E. effects. Rieman based the validity of this on the result that inclusion of Dorsey's value for K' in Knibbs' equation affected the value for K by about 0.1%.

Astarita and Greco (3) were the first to conduct an experimental study aimed at determining both K and K'. They fitted data to Equation (1.8) in the form of two asymptotes, which gave a questionable sharp break at $N_{Re} = 146$. Sylvester (62) has also taken entrance pressure loss data but his form a smooth curve which can be described by Equation (1.8). Sylvester predicted that both K and K' should be functions of β, the ratio of tube areas ($\beta<1$). To support this, Sylvester and Rosen (63) presented the data of many workers illustrating that different contraction ratios yielded different values for K and K'. In this presentation the data showed K and K' increasing with β for $0<\beta<0.1616$. Sylvester suggested that K and K' would have to pass through a maximum to satisfy K and K' vanishing as β went to zero. He also indicated the need for a study of $K = K(\beta)$ and $K' = K'(\beta)$. Han (30) misinterpreted this as a statement of the functionality of $K(\beta)$ and $K'(\beta)$. As an alternative Han presented polyethylene data (30) which showed K' monotonically increasing with decreasing β for $0.003<\beta<0.1$. Kaye and Rosen (38) noted that entrance loss data for a molten polymer

would contain elastic contributions that could obscure the true dependence of K' on β. Further, they presented $K = K(\beta)$ and $K' = K'(\beta)$ data for Newtonian fluids (glycerine-water solutions) that showed both functions attaining essentially constant values for $\beta < 0.25$.

The problem has also received much attention in a theoretical sense. However, most treatments have been concerned with the limiting cases of either high Reynolds number flow (for K) or creeping flow (for K') through an infinite contraction. None of these works considers a combination of kinetic energy and unsimplified viscous effects, which could equally influence intermediate flows. Generally, these works ignore the dependence of ΔP_{ent} on β by simplifying to the case of an infinite contraction, $\beta = 0$.

Treatments at higher Reynolds numbers are usually based on three common assumptions:

1. Neglect of the possibility that a vena contracta may form immediately past the entrance, and of its associated energy losses.
2. A flat velocity profile at the tube entrance.
3. No dissipation of energy upstream from the entrance plane.

Methods of solution can be divided into four categories: A) Applying an integral representation of the equations of motion and continuity to the boundary layer which develops along the tube walls. This method is attributed to Schiller (53) and has been extended by Campbell and Slattery (14). They repeat Schiller's computations,

but now instead of assuming $P = P(z)$ obtain pressure from a macroscopic mechanical energy balance on all the fluid in the tube. Their results include a theoretical plot of $\frac{\Delta P_{tot}}{\rho V^2/2g_c}$ vs. $\frac{z}{D}\left(\frac{1}{N_{Re}}\right)$, which, in terms of Equations (1.3) and (1.4) gives $K = 2.18$.

B) Patching of a boundary layer solution and a perturbation to developed flow solution. This method has been applied by Atkinson and Goldstein (29), who obtain $K = 2.41$.

C) Numerical methods. Christiansen and Lemmon (17) performed a finite difference solution of the equations of motion and continuity. They obtained $K = 2.274$, and $K = 2.015$ when the radial term was eliminated from their analysis. Hornbeck (33) solved the equations of motion for laminar flow in the entrance region of a pipe without linearization assumptions. His finite difference procedure calculated axial velocity and pressure from upstream values and converged reducing the grid size. He computed $K = 2.14$. Schmidt and Zeldin (55) solved the Navier-Stokes equations for laminar flows in the inlet sections of tubes and ducts by finite differences. They computed K as a function of axial distance for various Reynolds numbers obtaining asymptotic K values ranging from $K = 2.31$ ($N_{Re} = 10{,}000$) to $K = 2.40$ ($N_{Re} = 100$). Similarly Schmidt and Wimmer (54) computed K for a contraction with $\beta = 0.25$. They obtained $K = 2.27$ ($N_{Re} = 100$), $K = 2.32$ ($N_{Re} = 200$), and $K = 2.18$ ($N_{Re} = 2000$). Weissberg (69) applied a variational treatment to creeping flow. As the limiting case for $L/D \to \infty$ he obtained $K' = 43.6$. For smaller L/D Weissberg proposed that K' approaches 37.5, the

value calculated for creeping flow through a thin orifice. Christiansen et al. (18) obtained a finite difference solution for ΔP_{ent} as a function of N_{Re} and β for $1 \geq \beta \geq 1/64$ and $0.01 \leq N_{Re} \leq 500$. For $N_{Re} > 100$ they studied only the case of $\beta = 1$, which was treated as a comparison for their other results. They presented entrance losses in terms of an equivalent length of downstream tube measured in diameters having a developed flow pressure loss equal to ΔP_{ent}. Extrapolating their results to higher Reynolds numbers ($N_{Re} > 700$) yields good agreement (being less than 3%) with Sylvester's (62). At low Reynolds numbers ($N_{Re} = 0.01$) their results are 10% lower than Weissenberg's (69) analysis. Christiansen et al. do not correlate their results according to any particular equation, but display them as plots of $\frac{X_{eff}}{D}$ vs. N_{Re}. This complicates any direct comparison with results presented in terms of pressure loss parameters. Still their results do adopt a form describable by

$$\frac{X_{eff}}{D} = C + C'N_{Re} \tag{1.10}$$

Since this equation readily converts (63) to

$$\frac{\Delta P_{ent}}{\rho v^2/2g_c} = K + K'/N_{Re} \tag{1.8}$$

With the aid of the Hagen-Poiseuille equation where

$$C = \frac{K'}{64} \quad \text{and} \quad C' = \frac{K}{64}$$

it lends additional support for its validity.

D) Linearization methods. Langhaar (43) linearized the

equation of motion getting solutions for developing velocity profiles in terms of Bessel functions. He also obtained K = 2.28. Lundgren et al. (44) obtained a relatively simple equation for K in terms of the fully developed velocity profile. Their approach assumes the shape of the velocity profile at the entrance to have no effect on ΔP_{ent}, and it approximates the equations by linearizing them. Yet, their result yields a value of K for Newtonian flow in a circular tube consistent with previous work (K = 2.33).

Holmes (32) deserves a separate mention, as his approach is more intuitive than theoretical. He obtained Equation (1.8) by simply equating to ΔP_{ent} the sum of effects that would be responsible for entrance pressure losses. It is noteworthy that he analyzed the problem in terms of a finite contraction with viscous dissipation in the large tube. Also, his analysis indicates a dependence on β, i.e. $K = K(\beta)$.

Conical Entrances

Little has been done on laminar flow of Newtonian fluids through conical contractions. Studies have been made on creeping flow into a closed apex (1) and extensive data have been taken for turbulent flow through converging pipe fittings (27). The flow of polymer solutions (16) and polymer melts (56) through a conical entrance has been considered. Tanner (65) suggested use of conical flows to obtain estimations of non-Newtonian fluid parameters. Sutterby (60, 61) has done this for dilute polymer solutions. He developed a new three-parameter viscosity model from dimensional arguments. Ballenger and White (6) observed that molten polymers approaching

an abrupt contraction adopt a "wineglass" shaped velocity field, with stagnant circulating fluid in the corners. From data on such flows he developed a relation between the angle of this conical velocity field and the entrance pressure loss.

Some theoretical work has been done on laminar flow in tapered tubes, but this is limited by assumptions of radial flow only and slight taper. Yet, it affords an insight and may provide a starting point for parallel efforts on gradual contractions.

Theoretical solutions for flow in tapered tubes adopt a spherical coordinate system as shown in Fig. 1.2. Geometry shows the definition of cone angle in tapered tube studies to be identical to that in this work.

Gibson (28) was the first to consider laminar converging flow in a slightly tapered tube. He assumed radial flow and uniform pressure at constant radius (from the apex). His solution, which retains the inertial terms, unfortunately confuses coordinates. This yields a relation for ΔP that is dependent on angular position, which violates his second assumption. Harrison (31) obtained a slow-flow solution for pressure variations in a cone by assuming radial flow, slight taper, and negligible inertial effects. Bond (13) developed this work further to obtain an expression for $\frac{\partial P}{\partial r}$. Integrating Bond's result over the length of a cone and simplifying for an axial pressure drop ($\theta = 0$) gives:

$$g_c \Delta P_{cone} = \frac{2\mu(-Q)}{\pi(1-\cos\alpha)^2(1+2\cos\alpha)} \left[\frac{1}{r^3} - \frac{1}{r_o^3}\right] \qquad (1.11)$$

Fig. 1.2. Coordinate System for Theoretical Considerations of Flow in Tapered Tubes

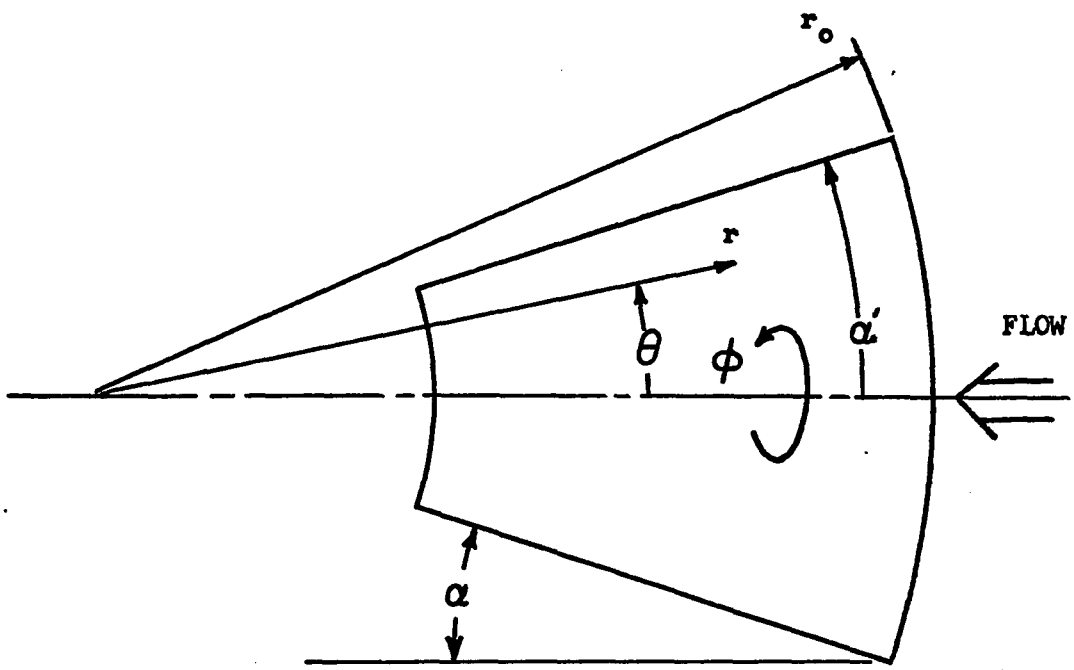

WHERE:

r_o = CONE LENGTH FROM APEX

α' = CONE ANGLE

α = CONE ANGLE AS DEFINED IN THIS WORK

where a negative volumetric flow rate implies flow toward the origin. Oka (47) derives a similar relation in a study of velocity, pressure, and stress distributions for creeping flow through tapered tubes.

Sutterby (58) obtained a solution for fast radial flow in a slightly conical tube.

$$g_c \Delta P_{cone} = \frac{\rho}{2} \left[\frac{Q}{2\pi(1-\cos\alpha)} \right]^2 \left[\frac{1}{r^4} - \frac{1}{r_o^4} \right] \tag{1.12}$$

Equations (1.11) and (1.12) can be rewritten with the following substitutions. The area receiving radial flow in a cone is

$$A = 2\pi r^2 (1-\cos\alpha) \tag{1.13}$$

and thus the volumetric flow rate becomes

$$Q = 2\pi r^2 v (1-\cos\alpha) \tag{1.14}$$

where v is the bulk velocity of fluid leaving the cone at r. Similarly, a radial flow Reynolds number can be written as

$$N_{Re} = \frac{4\rho v \alpha r}{\mu} \tag{1.15}$$

Then, for a tapered tube described by[1]

$$\frac{r}{r_o} = \sqrt{\beta} \tag{1.16}$$

equation (1.11) becomes

$$\frac{\Delta P_{cone}}{\rho v^2 / 2 g_c} = (1 - \beta^2) \tag{1.17}$$

---

1. Notice that for an abrupt contraction ($\alpha = 90^\circ$) r^2/r_o^2 is β as defined earlier. Also, for the same contraction ratio (of tube areas) geometry shows r/r_o to be constant for all angles.

Equation (1.12) becomes[1]

$$\frac{\Delta P_{cone}}{\rho v^2/2g_c} = \frac{1}{N_{Re}} \left[\frac{32 \left(\frac{\pi\alpha}{180}\right)}{(1-\cos\alpha)(1+2\cos\alpha)} (1-\beta^{3/2}) \right] \qquad (1.18)$$

$$\frac{\Delta P_{cone}}{\rho v^2/2g_c} = \frac{K'_{cone}}{N_{Re}} \qquad (1.19)$$

This shows that the slow and fast flow solutions for a tapered tube have the same form as analogous expressions (1.4 and 1.6) for a sudden contraction. However, because of the assumption of radial flow a complete description of ΔP_{cone} may not come from a sum of slow and fast solutions, as was done for ΔP_{ent}. Dryden et al. (24) have pointed out that radial flow is a special occurrence, even in slight tapers. For creeping flow it would only occur far from the apex (large r) and for fast flows only near the apex (small r). At intermediate r the flow is not radial since the streamlines must be curved so as to produce the change in velocity distribution.

It is noteworthy that the fast flow solution is independent of cone angle. As with fast flow through an abrupt contraction, the pressure drop depends on the change in kinetic energy and not on the geometry. The slow flow solution, which represents viscous losses, does depend on cone angle, as shown in Fig. 1.3.

---

1. α is written in degrees instead of radians.

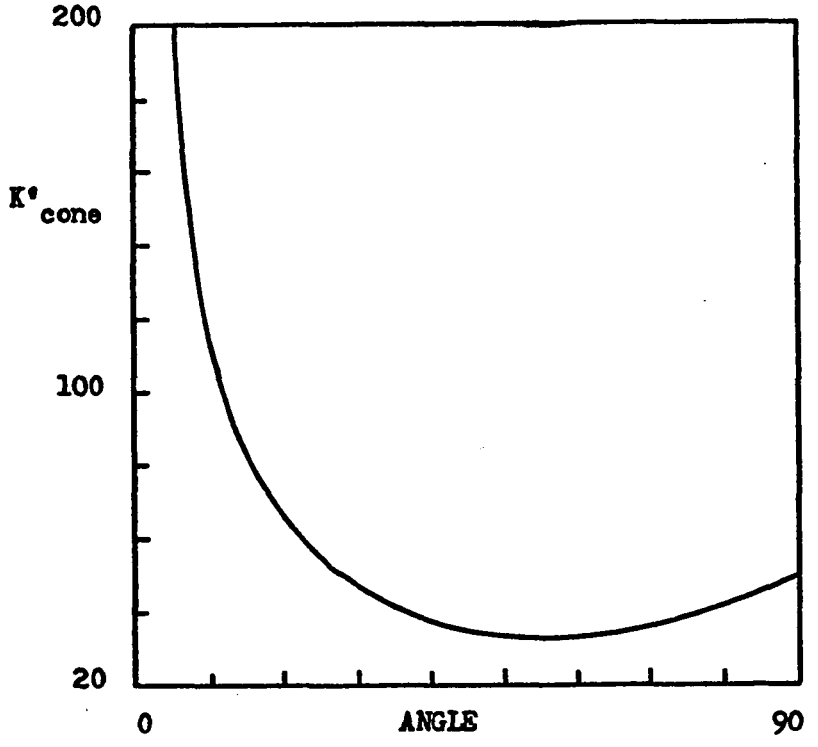

FIG. 1.3. K'_{cone} VS. CONE ANGLE FOR SLOW FLOW THROUGH A CONE WITH SMALL r/r_o. CALCULATED FROM SOLUTION BY BOND (13).

This shows that a contraction angle of 55° offers a maximum reduction in ΔP_{cone} of about 35%. Then ΔP_{cone} begins to increase, reflecting increased pressure losses due to an effective constriction of the entrance region.

Sutterby (59) has also performed a finite difference analysis of flow through a slightly tapered tube with $r = \frac{1}{4}r_o$. His solution is presented as a $\frac{P}{\rho V^2}$ vs. N_{Re} plot which asymptotically approaches the analytical solutions for slow (13) and fast (58) flow. At intermediate flow rates (e.g. $N_{Re} \approx 10$) the finite difference result differs from a total ΔP_{cone} written as $\Delta P_{cone,\ slow} + \Delta P_{cone,\ fast}$.

This may result from limitations of the radial flow approximation. Dependence on cone angle is included in the Reynolds Number, which Sutterby defines as

$$N_{Re} = \frac{r_o \alpha^2 (-v)\rho}{\mu} \qquad (1.20)$$

Ashino (2) developed an entrance correction for creeping flow through a conical inlet in terms of an effective distance $\frac{X_{eff}}{D} = C$. This is the low Reynolds number equivalent of $\frac{\Delta P_{ent}}{\rho v^2/2g_c} = K'/N_{Re}$. Ashino computed C vs. cone angle values which show a steady increase in entrance loss with cone angle. Large angles appear to have little effect on ΔP_{ent} (12% increase between 90° and 45°), but as α decreases further, $\frac{X_{eff}}{D}$ begins to increase rapidly (over 100% between 45° and 15°). For the limiting case of an abrupt contraction (α = 90°) Ashino's results (K = 44.8 or C = 0.70) compare well with Weissberg's (69) solution for flow through an orifice (K = 43.5 or C = 0.68).

Boles et al. (11) studied the flow of a Newtonian oil through a conical contraction. They obtained good agreement with Weissberg (69) at α = 90° and with Oka (47) at large angles, but not at small angles.

Related to conical entrance pressure losses is work by Caw and Wylie (15). They designed capillary viscometers with long flared ends that required no kinetic energy correction. If each end allowed the same velocity profile, then the kinetic energy change for these

viscometers should have been zero, thus leading to negligible kinetic energy effects.

Sudden Contraction--Non-Newtonian Fluids

Work on non-Newtonian flow through abrupt contractions can be divided into three parts: studies of $K = K(n)$ for power law fluids, comparisons of elastic and inelastic fluids, and investigations of elastic contributions to entrance losses.

Different theoretical predictions of $K = K(n)$ for an infinite contraction ($\beta = 0$) are compared in Fig. 1.4. The works yielding these results are extensions of Newtonian flow calculations for the kinetic energy correction, this time applied to a power-law fluid.

Bogue (10) assumed a plug-like velocity profile at the entrance of the pipe and treated the velocity profile in the boundary layer with a cubic approximation. His results predict $K = K(n)$ such that $K = 2.16$ at $n = 1.0$. Tomita (66) solves the boundary layer equations for flow in the inlet region of a tube by a variation method. For Newtonian fluids his results yield $K = 2.20$. Collins and Schowalter (20) combine boundary layer techniques at the entry and perturbation techniques in the region where fully developed flow appears. At $n = 1$ they obtain $K = 2.33$. Sestak and Charles (57) apply the procedure of Lundgren et al. (44) to a power-law fluid. They obtain

$$K(n) = \frac{8n(3n + 1)}{(2n + 1)(5n + 3)} \qquad (1.21)$$

Fig. 1.4. Comparison of Work on K = K(n).

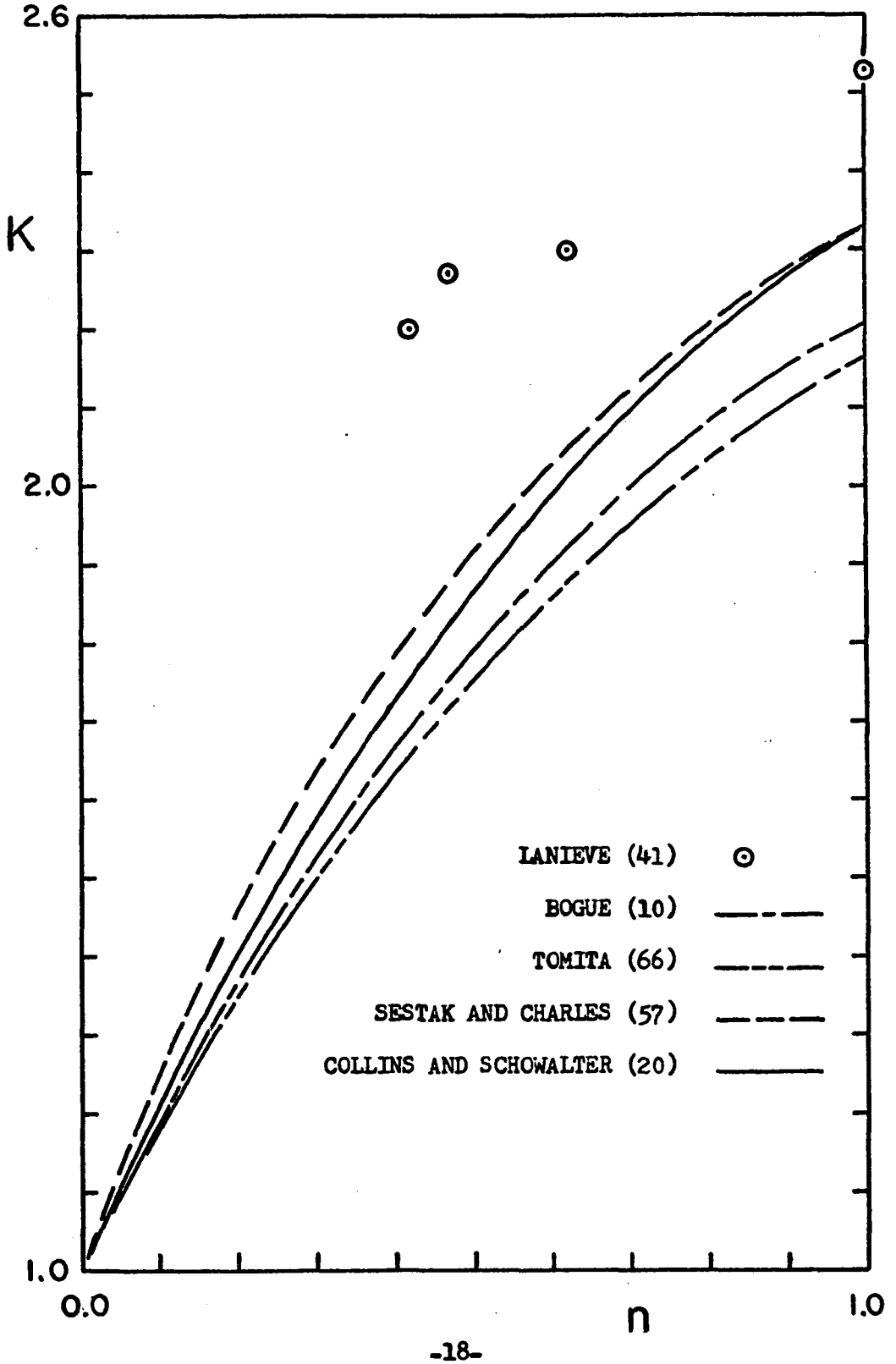

which becomes $K(1) = 2.33$.

LaNieve (41) has measured ΔP_{ent} for an 85% solution of ethylene glycol ($n = 1$) and for neutralized solutions of Carbopol ($n < 1$). Modeling flow behavior with the power-law approximation and correlating ΔP_{ent} in terms of only the kinetic energy correction, i.e.

$$\frac{\Delta P_{ent}}{\rho v^2/2g_c} = K$$

he obtains the following values for $K(n)$.

n	1.00	0.62	0.47	0.42
K	2.53	2.30	2.27	2.20

These are slightly larger than any of the predictions for $K(n)$ perhaps because only the kinetic energy correction, K, was considered or because of elastic effects. If LaNieve had evaluated his data in terms of

$$\frac{\Delta P_{ent}}{\rho v^2/2g_c} = K + \frac{K'}{N_{Re}} \qquad (1.8)$$

he might have obtained better agreement. Taking a value of $K'(n = 1) = 160$ as reported by Kaye and Rosen (38) suggests $K(n = 1) = 2.53$ too large by 0.3 to 0.1 for the Reynolds number range studied by LaNieve. Reducing $K = 2.53$ by 0.1 to 0.3 would bring it closer to or within agreement of predicted values. The non-Newtonian results

are also larger than predicted, but by increasing amounts (about 25% at n = .42 compared to less than 8% at n = 1.0). This may be attributed to elastic effects. Tests on Carbopol indicated that neutralized solutions possessed a gel-like quality even at concentrations as low as 1/3 % and were slightly elastic. This introduces an elastic contribution that could make ΔP_{ent} larger.

It would be expected that works comparing inelastic and elastic fluids offer an insight to the contribution of elasticity to ΔP_{ent}. But the difficulty of gathering ΔP_{ent} data and the complexity of the inter-relationship between viscous and elastic effects generally masks a true comparison. Part of this may be due to opposing influences of flow index, n, and elasticity. Lower n's result in flatter velocity profiles requiring less rearrangement through the contraction and thus less chance of a vena contracta which should lead to smaller ΔP_{ent}. Elasticity causes a storage of energy in the fluid which is carried out of the system, thus increasing ΔP_{ent}. How much energy leaves will depend on the Weissenberg Number, a ratio of elastic and viscous stresses. It may therefore be possible to achieve combinations of these effects in proportions that yield unexpected results. As will be seen in the following sections, the contradictions arising between different efforts support this.

Astarita et al. (4) have studied highly elastic (with $0.53 \leq n \leq 0.875$) and slightly elastic (with $0.79 \leq n \leq 0.89$) fluids flowing through a sudden contraction. Since the high viscosities of their test fluids limited testing to $N_{Re} < 100$ (with the exception of one point) they were only able to obtain values for K'. They present

the elastic and slightly elastic results plus a Newtonian value ($K = 795$) from another study (3) on the same graph. Within the limits of scatter, all their non-Newtonian results can be described by a straight line extending from about $K'(n = 0.53) = 400$ to about $K'(n = 0.89) = 1130$. Yet, to include the one Newtonian point they draw a curve with a maximum at $n = 0.85$. Since both highly and slightly elastic fluids yielded data describable by this smooth curve they suggested that elasticity has no effect on ΔP_{ent}. This ignores that elastic fluids (with $0.745 \leq n \leq 0.89$) produced entrance losses up to almost a third larger than the Newtonian fluid. It is well possible these K' values are larger because of elastic effects. It is also noteworthy that only one highly elastic fluid point overlaps the slightly elastic fluid data. Since Astarita et al. offer no measure of elasticity for their fluids it is questionable if a significant difference in elasticity exists between these points. Further, their presentation of $\frac{\Delta P_{ent}}{\rho v^2/2g_c}$ vs. N_{Re} indicates that they determined the K' values from straight lines through three to five data points. The works of Sylvester (62) and Kaye and Rosen (38) show these lines to be curved even at $N_{Re} < 10$ and especially for $10 < N_{Re} < 100$ which is the region containing most of their data. Thus, Astarita et al. may not be obtaining accurate values of K' from their data.

Sylvester (62) has measured entrance pressure losses for fluids

with varying levels of elasticity over a wide range of Reynolds numbers ($0.1 < N_{Re} < 1600$). Although he offered no measure of elasticity, Sylvester did show that elastic fluids (water solutions of Separan and CMC) could yield significantly larger ΔP_{ent} than Newtonian fluids. Sylvester also tested Polyox solutions which, due to shear degradation in pumping, had lost much of their original elasticity. These fluids, though possibly still slightly elastic, produced lower entrance losses than Newtonian fluids. Sylvester combined the data from tests with five such polyox solutions ($0.382 \leq n \leq 0.523$) to form one curve from which he computed K and K'. At an average flow index of n = 0.4, Sylvester reports: $K(n = 0.4) = 2.1$ and $K'(n = 0.4) = 185$. These are lower than his Newtonian values of $K(n = 1) = 2.4$ and $K'(n = 1) = 295$, and thus support a decrease in ΔP_{ent} with n. Sylvester's value of $K(n = 0.4) = 2.1$ compares well with LaNieve's (41) data but is (similarly) higher than predicted (10, 20, 57, 66). Tests for this study on shear degraded polyox were unable to produce an inelastic fluid with a flow index with $n < 0.6$, although significant losses in elasticity were obtained even for n = 0.4. Thus, Sylvester's non-Newtonian values for K and K' are probably larger than they would be for a truly inelastic fluid with the same power-law index.

Bodger and Rama Murthy measured entrance losses (9) and velocity profile development (51) for inelastic and elastic Methocel solutions. Inelasticity was confirmed by observing no measurable normal stress differences with a rheogoniometer. Like LaNieve (41), they evaluate ΔP_{ent} in terms of only the kinetic energy correction, K.

For the inelastic fluids their results lie between the predictions of Bogue (10) and Collins and Schowalter (20). However, if Bodger and Rama Murthy had correlated ΔP_{ent} with both parameters K and K', their results for K would be lower than predicted. Their results on elastic fluids show considerable scatter and, interestingly, are all less than the inelastic fluid values. Some of their elastic fluid data even suggest K = 0. This is contrary to observations by Sylvester (62) of increased ΔP_{ent} due to elastic effects.

Works dealing exclusively with contributions to ΔP_{ent} due to fluid elasticity generally are unable to offer workable answers. They either contain unmeasurable parameters or require knowledge of the elastic behavior of the fluid. However, these efforts do propose suggestions of how ΔP_{ent} may be influenced by elasticity.

Many works have demonstrated that fluid elasticity could lead to increased entrance losses. Philippoff and Gaskins (48) proposed that in steady flow a viscoelastic fluid acquires an elastic energy. In a capillary this energy is imparted at the entrance and then carried out of the tube by the flowing fluid, thus causing a larger ΔP_{ent}. Pruitt and Crawford (50) studying drag reduction in turbulent flow and Feig (25) measuring entrance losses for dilute polymer solutions, both report elasticity causing increased ΔP_{ent}. Metzner et al. (46) have obtained an expression showing ΔP_{ent} to be related to normal stresses. For fast flows ($N_{Re} > 500$) they offer

$$\Delta P_{ent} = \phi \rho v^2 + (P_{11} - P_{22}) \qquad (1.22)$$

where ϕ is an adjustable parameter, analogous to K, and $(P_{11} - P_{22})$

is a normal stress difference. Since positive non-zero normal stress differences are an indication of fluid elasticity, this suggests larger ΔP_{ent} with increased elasticity. Markovitz (45) has reviewed experimental works that show the first normal stress difference to be positive.

Kobayashi and Tomita (40) indicate that elasticity may increase ΔP_{ent}. Starting with the Maxwell model of elasticity, then neglecting normal stresses, and making the boundary layer simplifications they obtain an expression for K. Elastic effects are represented in terms of "relaxation distance" which is actually the product of relaxation time and bulk fluid velocity. Their result predicts larger ΔP_{ent} for finite relaxation distances. Also it shows elasticity having an increasing effect on ΔP_{ent} as the flow index decreases. In comparison, this work offers smaller purely viscous values of K than predicted by Bogue (10) and elastic values of K only slightly larger than the $K = K(n)$ calculated by Sestak and Charles (57). Kobayashi and Tomita (40) present data for two elastic and two inelastic (as determined from normal stress data on a rheogoniometer) fluids that demonstrates increased ΔP_{ent} due to elasticity, but has no consistent agreement with the theory presented. This may be a result of choosing a simple model for fluid elasticity and of neglecting normal stresses. Equivalent to assuming a Maxwell model in equilibrium flow Sylvester and Rosen (64) applied Hooke's Law in shear and equated rate of elastic energy added to rate lost to show the elastic contribution, $\Delta P_{elastic}$, related to the

wall shear stress.

$$\Delta P_{elastic} = \frac{\tau_w^2}{G} \left[\frac{(3n + 1)}{4(5n + 1)} \right] \qquad (1.23)$$

They test this relation with entrance loss data on elastic fluids, where $\Delta P_{elastic}$ was obtained by subtracting a purely viscous contribution from ΔP_{ent}, i.e.

$$\Delta P_{elastic} = \Delta P_{ent} - \Delta P_{viscous} \qquad (1.24)$$

Since frictional losses for inelastic and elastic fluids (with same n) may not be equal, their values of $\Delta P_{elastic}$ may not be accurate. However, their plots of $\Delta P_{elastic}$ vs. τ_w^2 have slopes equal to one at low shear rates, and thus confirm the form of Equation (1.23). A complete verification of their model was not possible because reliable values of the elastic modulus, G, are not available for dilute polymer solutions. It is noteworthy that if a power-law elastic model is assumed

(1.25)

which gives

$$\Delta P_{elastic} = \frac{\tau_w^{\frac{m+1}{m}}}{H^{1/m}} \left[\frac{2m^2(3n+1)}{3m^3(4n+1)+m^2(19n+4)+m(8n+1)+n} \right] \qquad (1.26)$$

then their data for the entire range of shear rate studied can be fitted to a straight line with slope of $\frac{m+1}{m}$. Until values of G, or H and m, are known independently it will not be possible to predict $\Delta P_{elastic}$ from these equations. Yet, they do suggest elasticity

increases ΔP_{ent} since all the terms in Equations (1.24) and (1.27) are positive.

Tomita and Yamane (67) have developed an expression for the Hagenbach correction that accounts for the elasticity of a power-law fluid. They apply boundary layer theory, assume the second normal stress differences equal to zero, and make other simplifications to obtain a relatively simple relation for K.

$$K = \left(\frac{3n+1}{n+1}\right)^2 - 4\left(\frac{3n+1}{n}\right)^n \left[\phi_1(n) + N_e^* \phi_2(n)\right] \qquad (1.27)$$

where

$$N_e^* = \frac{\kappa^2}{\rho G R^2 v^{2(1-n)}} \qquad (1.28)$$

Plots of the functions $\phi_1(n)$ and $\phi_2(n)$ appear in Fig. 1.5. It is interesting that $\phi_2(n)$ suggests elasticity having both an additive and negative effect on ΔP_{ent}. Notice also that $\phi_2(n)$, and thus the elastic contribution, is equal to zero at n = 0.54. Although these predictions may not be entirely accurate because of the assumptions and simplifications applied in the derivation, these results do suggest a complex dependence of ΔP_{ent} on elasticity. Since N_e^* depends on shear rate, it may be possible to obtain negative or positive contributions from the fluid depending on flow conditions.

LaNieve and Bogue (42) also suggest the possibility of additive and negative elastic contributions to ΔP_{ent}. They observed a linear dependence between the first normal stress

Fig. 1.5. Functions $\phi_1(n)$ and $\phi_2(n)$ from Tomita and Yamane (67).

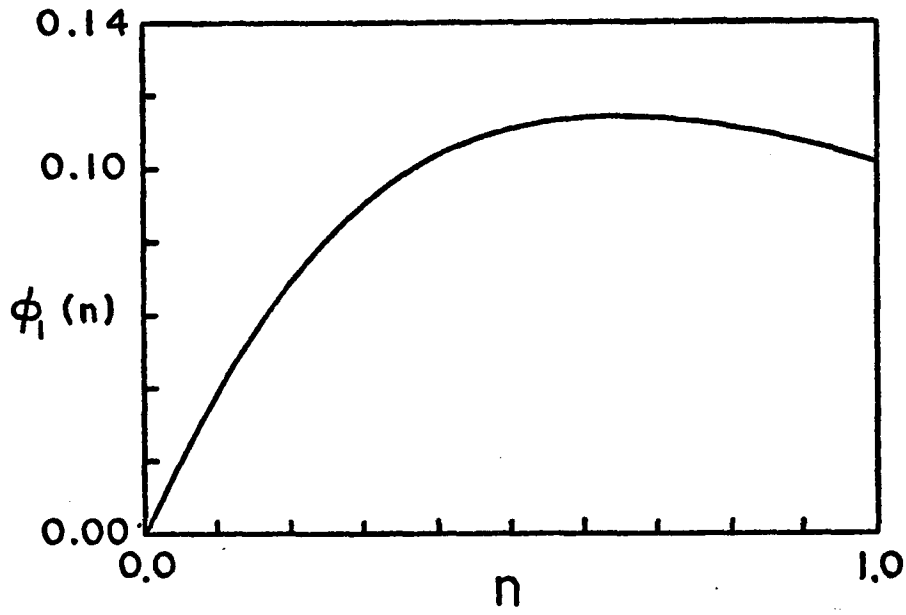

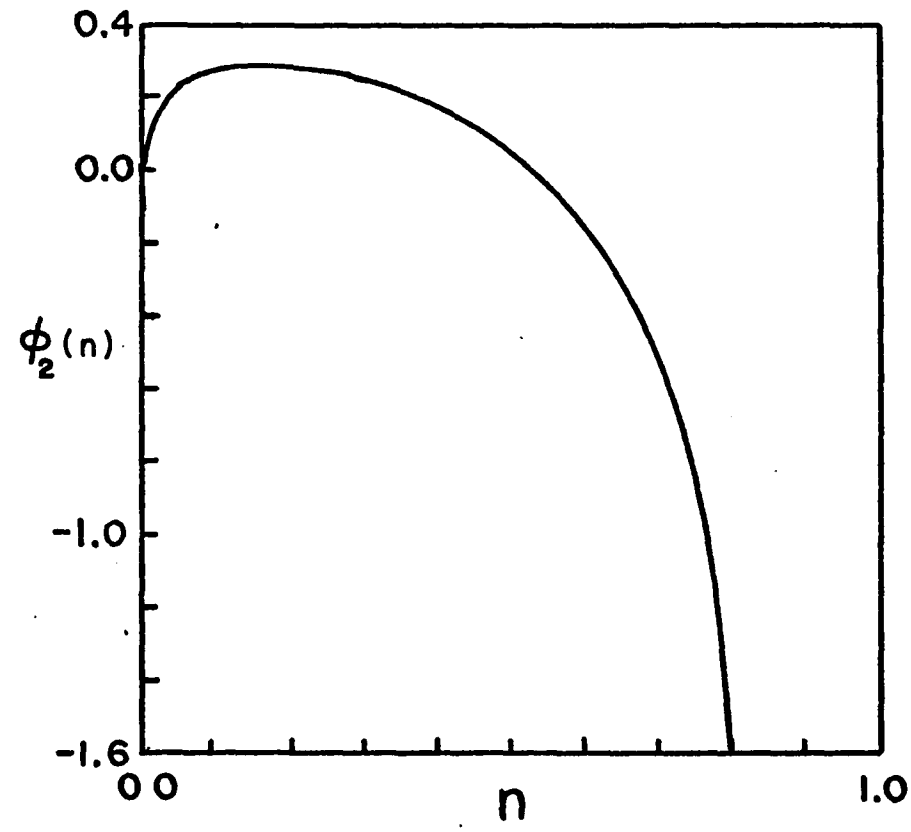

difference as measured on a rheogoniometer and the elastic portion of ΔP_{ent} for elastic fluids.

$$\Delta P_{elastic} = \alpha_3(P_{11} - P_{22}) \tag{1.29}$$

Difficulties in separating viscous effects made it impossible to determine α_3 accurately. However, they found that the theory of a second-order fluid could predict either small positive or small negative values for α_3, depending on the assumed flow field and the assumed relationship between the material constants.

Ballenger and White (6) have observed that polymer melts adopt a "wineglass" structured velocity field when flowing through a contraction. They develop an empirical relation between the angle of this flow pattern (2α)[1], the entrance pressure loss, and the principal normal stress difference at the tube wall (σ_w) which can be written as

$$\Delta P_{ent} = \sigma_w \left[\frac{\ln\left(\frac{2\alpha}{178.5}\right)}{\ln(0.9644)} \right] \tag{1.30}$$

where the numerical constants can be regarded valid only for the melts tested. This equation contains two variables (σ_w and α) that will exert opposite influences on ΔP_{ent} with changes in elasticity. Although increased elasticity implies a large σ_w, it also causes a smaller α.

---

1. This is written with α, the cone angle, as defined earlier.

Entrance Losses--Summary

The following tabulation summarizes Newtonian flow values obtained for K and K' at $\beta = 0$.

TABLE 1.1. SUMMARY OF VALUES FOR K AND K'.

Reference		K	K'
Ashino (2)			44.8
Astarita and Greco (3)		5.48	795
Bogue (10)		2.16	
Bond (12)			36.7
Campbell and Slattery (14)		2.18	
Christiansen and Lemmon (17)		2.274, 2.015	
Collins and Schowalter (20)		2.33	
Dorsey (22)	$N_{Re} < 10$	0	36.7
	$N_{Re} > 10$	2.0	18.3
Goldstein (29)		2.41	
Hornbeck (33)		2.14	
Hosking (34)			0 at large N_{Re}
Kaye and Rosen (38)		2.32	159
Knibbs (39)		2.28	
Kobayashi and Tomita (40)		2.16 calc.	
LaNieve (41)		2.53	
Langhaar (43)		2.28	
Lundgren et al. (44)		2.33	
Rieman (52)		2.25	
Schiller (53)		2.16	

TABLE 1.1 (Continued)

Reference	K	K'
Schmidt and Wimmer (54)	2.32 - 2.18	
Schmidt and Zeldin (55)	2.40 - 2.31	
Sestak and Charles (57)	2.33	
Sylvester (62)	2.4	295
Tomita (66)	2.20	
Tomita and Yamane (67)	2.365	
Weissberg (69)		43.6 - 37.5

CHAPTER 2. EXPERIMENTAL

Apparatus

This research modified the apparatus built by Sylvester (62) to increase efficiency of experimentation and to allow variation of the entrance region. The apparatus is a closed-loop flow system with a by-pass line around the pump as shown in Fig. 2.1. Liquid in the feed tank, a 55-gallon drum, is pumped through 3-in. standard schedule 40 pipe to a 12-in. diameter by 15-in. high surge tank. From this it passes through the entrance section, a removable acrylic tube, thus allowing a variety of entrance diameters, to the test section, an 8-ft. length of 3/8-in. standard schedule 80 polyvinyl chloride tube. Fluid leaving the test section is directed back into the storage tank by an acrylic shield. The test section has removable pressure taps 12 inches apart that allow a bank of manometers to measure pressure drops over different portions of the section, or at different intervals.

Sylvester (62) encountered severe degradation of polymer solutions upon prolonged shear due to pumping. To reduce this, the old pump, an Eco-series 400 Gear chem pump, was replaced by a helical rotor Moyno Pump, model 1L4, type CDF. The Moyno pump was driven by a 1/2-h.p. Varidrive U.S. Electric Motor through a Falk 5-to-1 ratio gear reducer, type AA112, with sure flex couplings connecting the shafts. This equipment was mounted on a base constructed from 8-in. wide steel channel. The base was placed

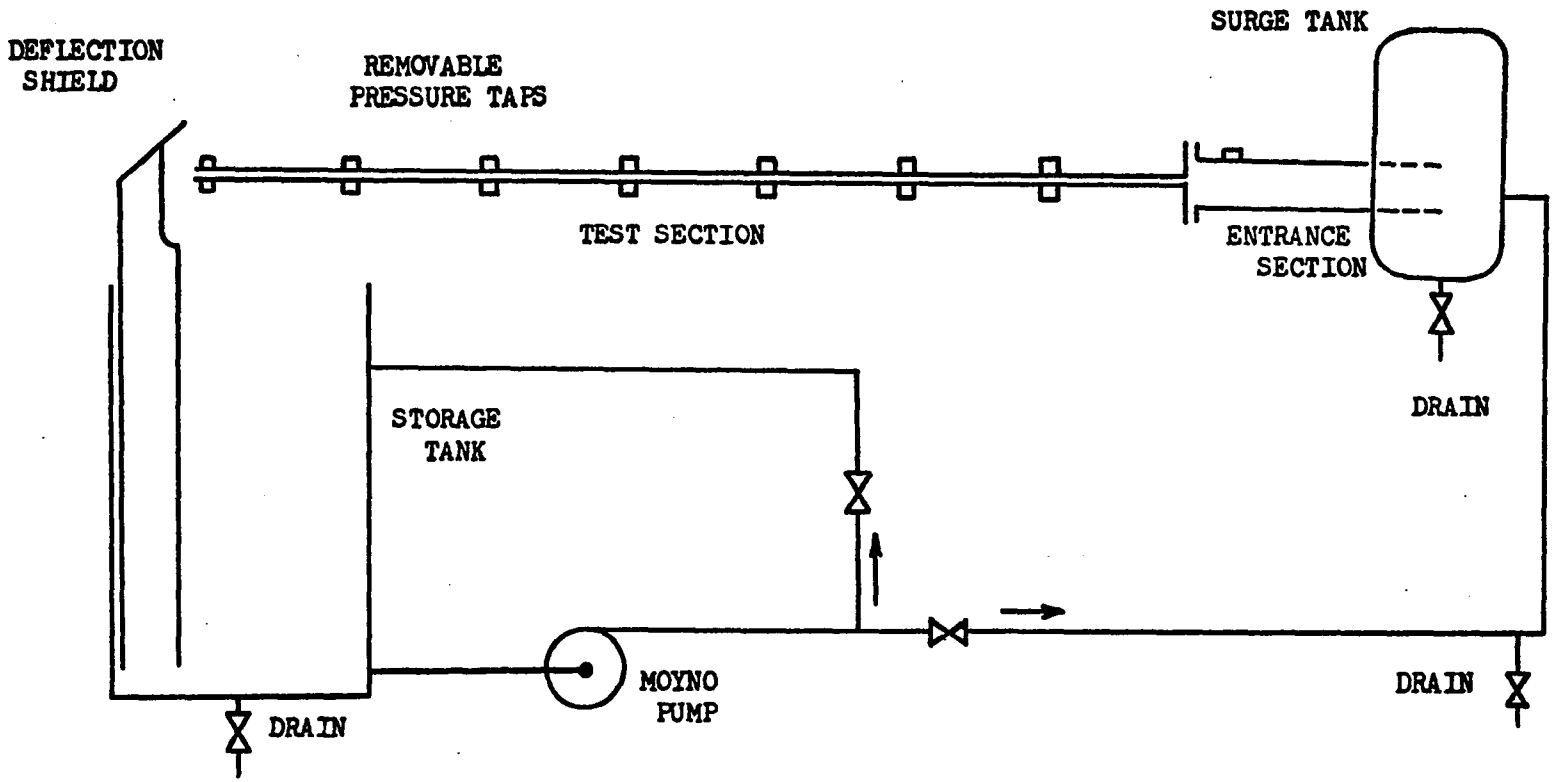

Fig. 2.1. Schematic of Apparatus for Studying K and K'.

on 1/8-in. thick rubber sheet pads and secured to the floor with expansion bolts.

Seven entrance sections with internal diameters from 2½-in. to ½-in. were constructed from acrylic tubing. Tube supports, pressure tap blocks, and the 7-in. diameter flanges were also made from acrylic plastic and cemented to the tube. The flange on the end mating with the test section (Fig. 2.2) was designed with a 4-in. diameter by 3/8-in. high raised surface having a slightly beveled edge that aided in aligning the two sections on the same center line. This fit snugly into a ¼-in. deep by 4-in. diameter depression in the flange on the test section (Fig. 2.3). Care was taken in machining the beveled edge to insure that the faces of the flanges still made contact around the contraction, thus providing a sharp 90° square entrance. This face-to-face contact was sufficiently snug that no gasketing material except a thin layer of stopcock grease was necessary to make the contraction leakproof.

To provide uniformity of testing, a fully developed velocity profile in the entrance region is preferrable to a series of semi-flat profiles reaching the contraction in various stages of development. The length of the entrance region was extended--Sylvester's (62) study was on a 4-in. long entrance section--to attempt to obtain a fully developed velocity profile before the contraction. For purely viscous fluids in laminar flow, Goldstein (29) offers L/D = 0.035 Re as an approximate means of predicting

Fig. 2.2. Flange Design for Entrance Section and Test Section

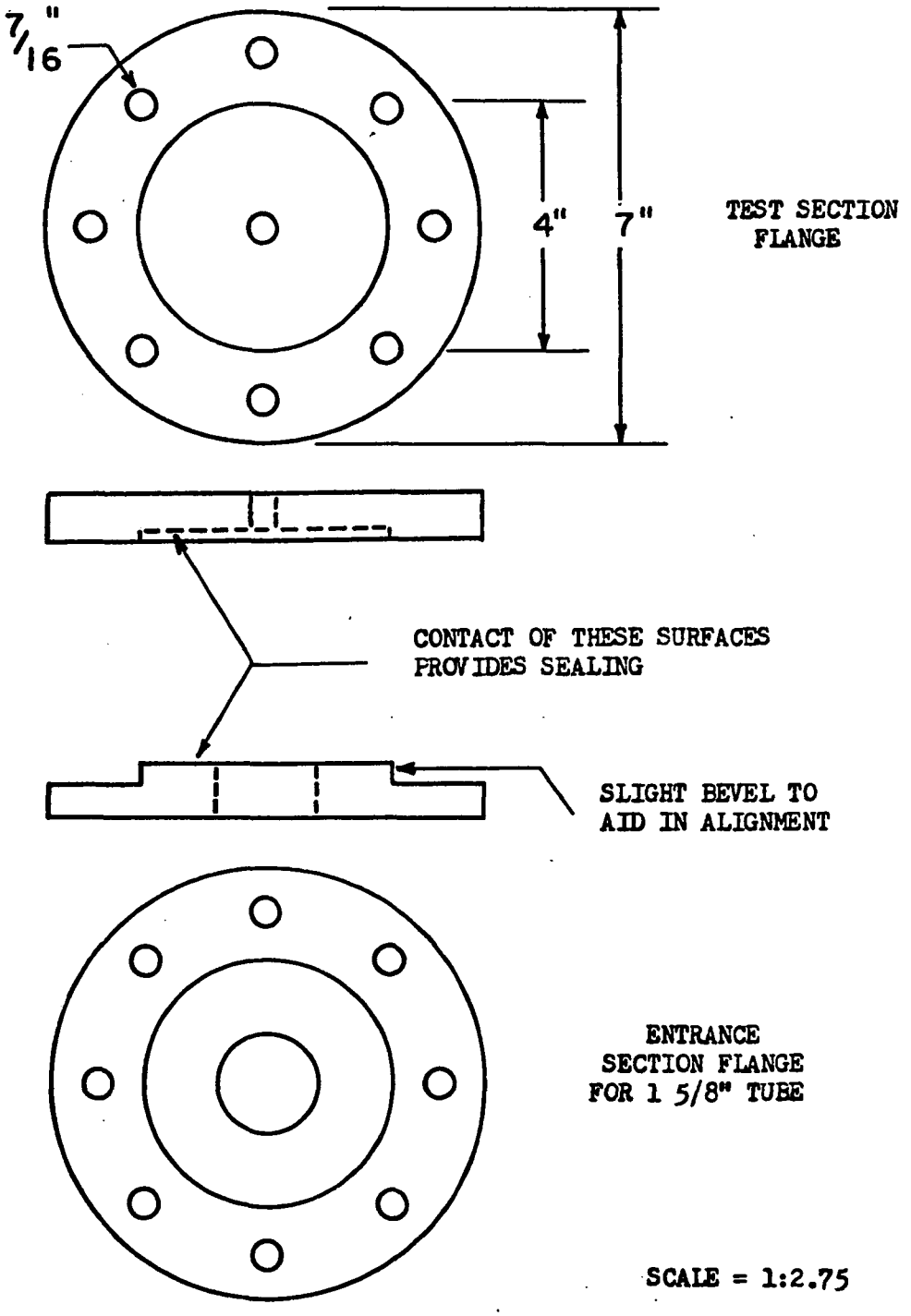

Fig. 2.3. Cross Section of Entrance Section

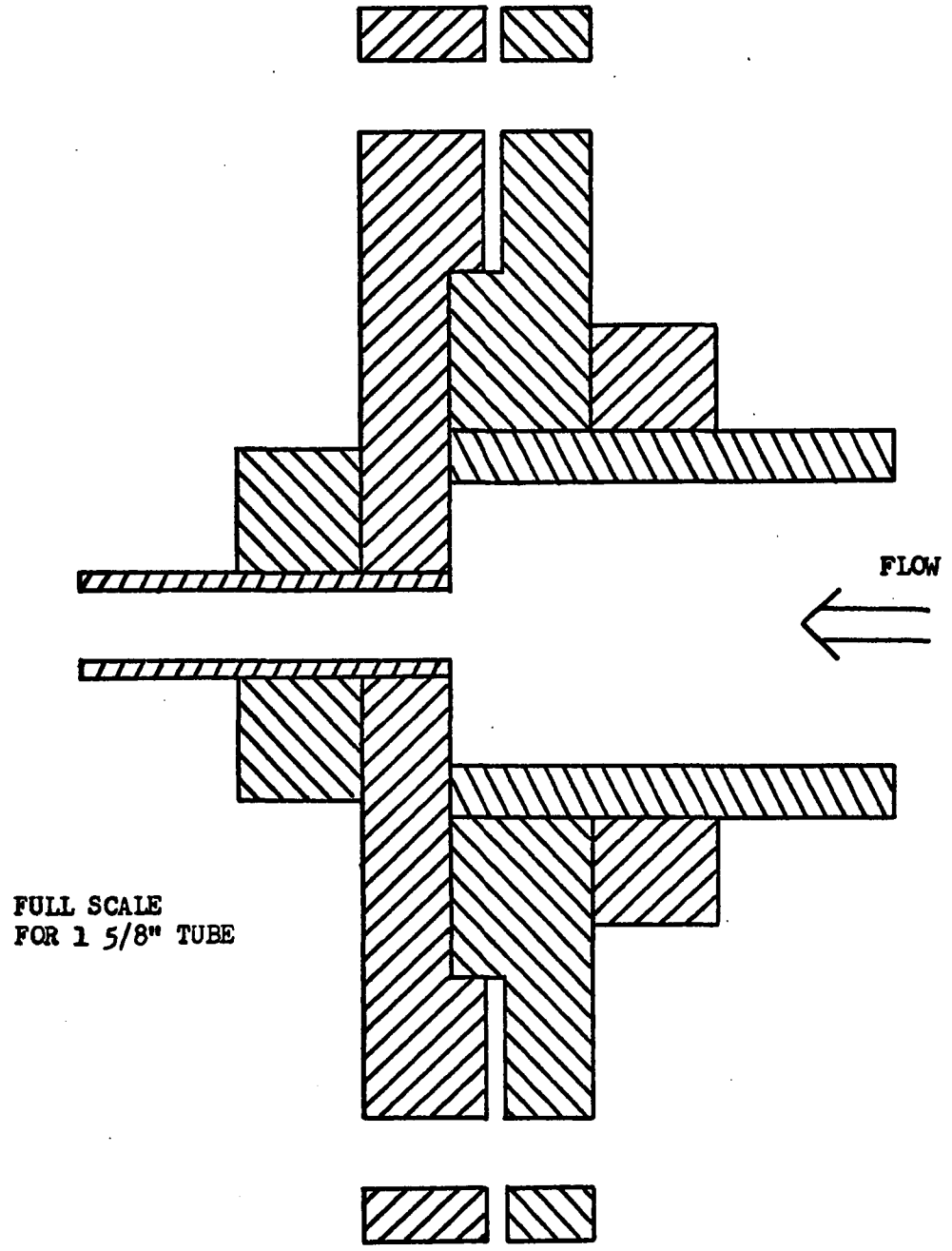

the distance (L) to reach fully developed flow at a Reynolds number of N_{Re} in a tube of diameter D. The maximum Reynolds number will occur in the 0.4-in. I.D. downstream tube and this was not expected to exceed 1500. Consider the ratio of the lengths in the two sections

$$\frac{L_t}{L_e} = \frac{(N_{Re}D)_t}{(N_{Re}D)_e}$$

since $N_{Re} = \frac{\rho v D}{\mu}$ and $Q = \frac{\pi D^2 v}{4}$

$$\frac{L_t}{L_e} = \frac{(vD^2)_t}{(vD^2)_e} = \frac{Q_t}{Q_e}$$

and since the volumetric flow rate in both tubes is the same, $L_1 = L_2$, i.e. they both require the same distance to establish a fully developed velocity profile. For a Reynolds number of 1500 in the 9.4-in. I.D. tube, the above equation gives a length of 30-in. Sylvester and Rosen (64) observed that in laminar flow viscoelastic and purely viscous fluids require approximately the same distance to develop a velocity profile. Any length of the entrance region in excess of 30 inches would serve as a safety margin. So, as an optimum between maximizing the entrance length and the limits of laboratory space, the entrance regions were designed 42 inches long. The entrance ends of the entrance sections were rounded to aid in flow development.

As shown in Fig. 2.1 the upstream end of the entrance section extended into the surge tank through the 4-in. I.D. pipe Sylvester (62) used as his entrance section. Flanges were placed about 12 inches from the end of the entrance section and gasketed with a 1-in. wide ring of 1/8-in. thick rubber sheet.

Choice of a minimum placement distance for the entrance section pressure tap was based on stress birefringent data collected by Fields and Bogue (26). Their studies on flows of viscoelastic fluids through sharp-edge channels indicated that all variations of stress fields occurred well within one channel-width from the contraction. To insure that the pressure tap tested undisturbed flow it was placed a minimum of two tube diameters from the contraction. Table 2.1 lists the entrance section internal diameters, their β values, and placement of pressure tap distances.

Tube diameters were obtained by filling with a measured volume of water. Diameters were calculated from the averages of three trials and then compared with Vernier readings (accurate to 0.001-in.) taken on both axes at each end. In all cases diameter values compared within ±1%.

The test section was a 96 1/2-in. length of schedule 80 3/8-in. PVC pipe, with an internal diameter of 0.406-in. The pressure tap holes, made with a number 60 drill (0.04-in. diameter), were located at the centerline on alternating sides of the tube. Checks made with a cathetometer showed all pressure tap holes to be ±0.01-in. of the centerline. The tap holes were spaced 12.00 inches

TABLE 2.1. ENTRANCE SECTION DIMENSIONS

Tube	Tube Internal Diameter	β	Distance of Pressure tap from Contraction
1/2"	0.509	0.636	2.015
5/8"	0.633	0.411	2.000
7/8"	0.879	0.213	2.000
1 1/4"	1.231	0.109	3.190
1 5/8"	1.631	0.062	4.760
2"	1.997	0.041	5.000
2 1/2"	2.512	0.026	6.000

apart, measuring from the contraction. Any burrs that might have been caused by drilling were removed by passing an acrylic plug machined with a slight cutting edge through the tube.

The manometers were air over test fluid in Imperial Eastman PVC-60 tubing connected with Imperial Eastman "Poly-Flo" fittings so as to read differential pressures (Fig. 2.4). This arrangement allowed for rapid changing of test fluids, cleaning, and replacement of manometer tubes. Manometer scales were obtained from Meriam Standard (Model 10AA25WM) U-tube manometers and could be read to ±0.01-in. with the aid of a vernier. A valve connected to a "T" at the top of each manometer allowed control of fluid levels in the manometers.

Test fluids exiting the test section were caught by acrylic collection shields that extended down below the test fluid surface in the 55-gal. drum. This virtually eliminated any of the foaming that can easily develop when viscous fluids are poured into one another. The bottoms of these collection shields were covered with two layers of cheese cloth to act as filters for any dirt that may enter the apparatus and also to further retard bubble formation. At high flow rates some air bubbles would get mixed into the test fluid. These bubbles, barely visible with the naked eye, could be observed in the dark if a light beam was directed perpendicularly to flow through the clear acrylic entrance section. The author feels these bubbles were small enough not to have influenced fluid properties or the common assumptions of continuity and incompressibility.

Fig. 2.4. Manometer Arrangement

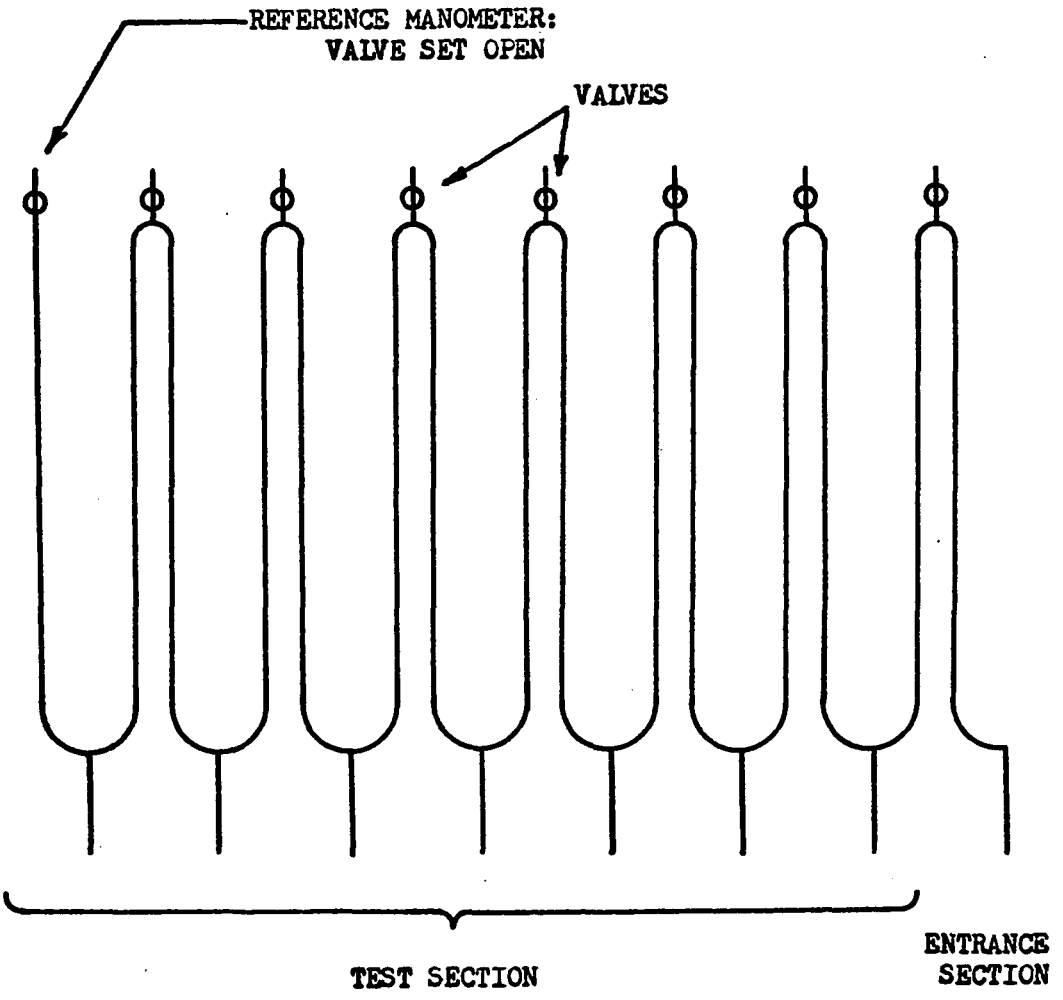

To study the influence of contraction angle on ΔP_{ent} a series of 2-in. diameter cylinders with an internal conical face were machined out of acrylic plastic (Fig. 2.5).

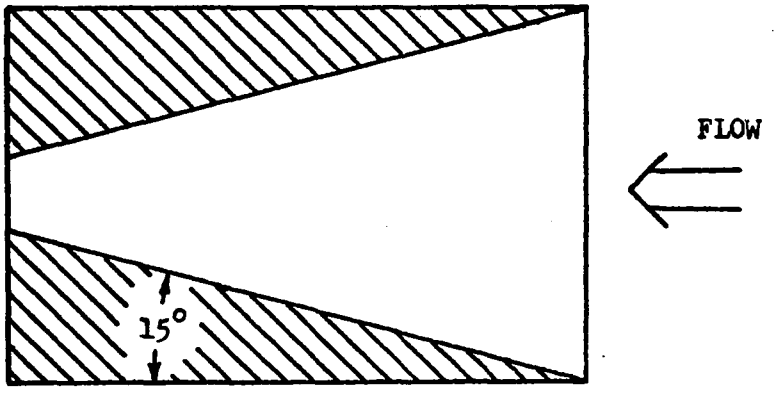

FIG. 2.5. CROSS-SECTION OF 15° CONICAL INSERT

These cylinders were inserted in the 2-in. tube with the flat face flush against the test section flange. Dow Corning stopcock grease was applied as an adhesive to keep the insert in place during installation. The inserts provided contraction angles, as defined in Fig. 2.5 of 60°, 30°, 15° and 7 1/2°. The internal cone surfaces were polished to the same smoothness as inside the entrance section.

Elasticity was measured in terms of the fluid's ability to recoil after an applied stress was suddenly released. A schematic of the apparatus built for this appears in Fig. 2.6. Pint-size jars of test fluid were secured to a disk that freely rotated on a ring of ball bearings. The jars had an inside diameter of 7.0-cm. and were 13.5-cm. deep. A 229-gm. weight attached to the wheel by

Fig. 2.6. Schematic for Recoil Apparatus

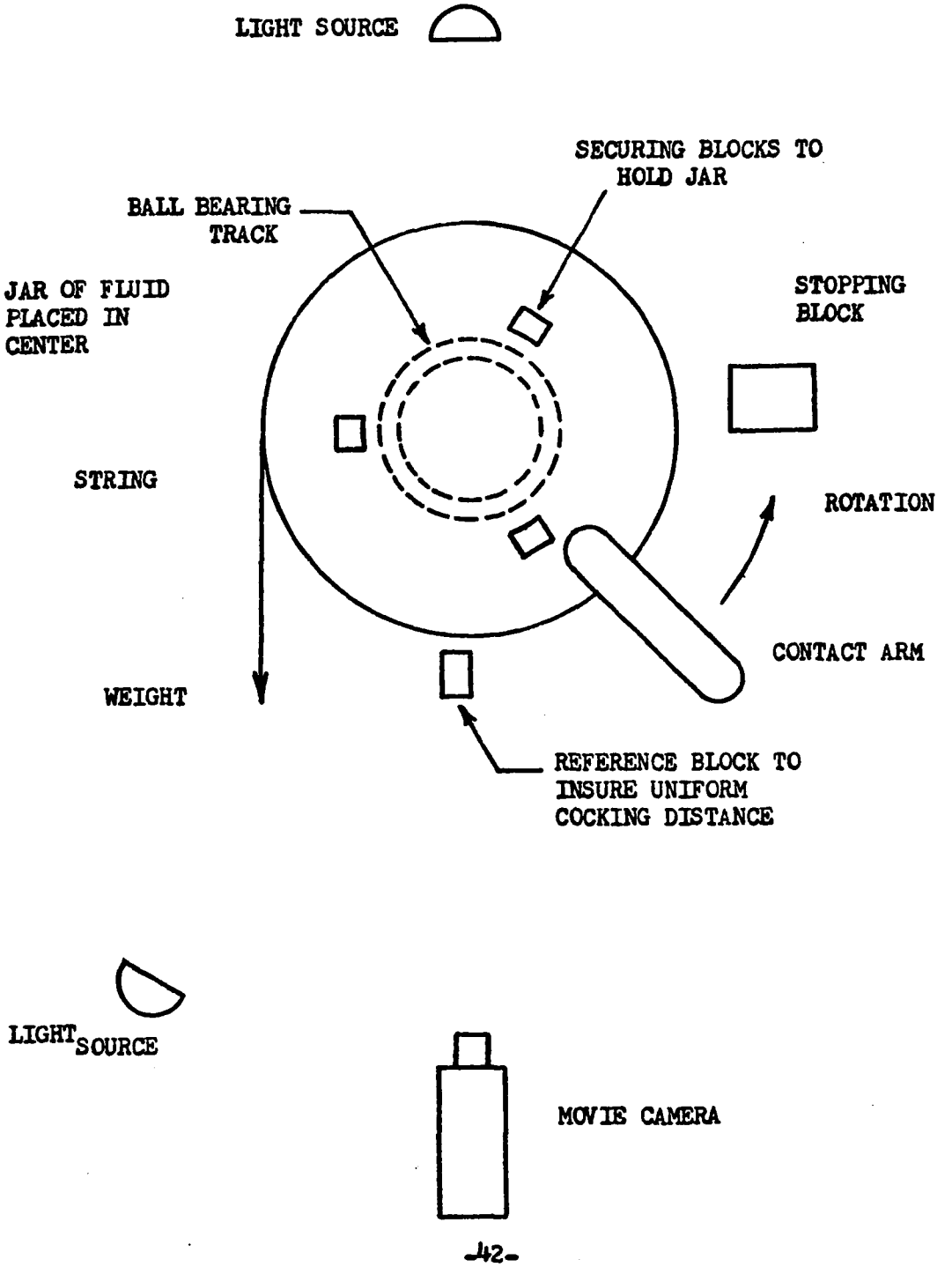

heavy string provided a uniform force that was abruptly terminated when the extended arm on the disk contacted the stopping block. The reference block insured a uniform turning angle for all tests. A fine line of Sheafers blue ink was injected at a uniform depth (10 inches) and wall distance (1.3 cm.) in all fluid samples with a 21 gauge, 2-in. hypodermic needle. Dow Corning silicone stopcock grease was generously applied to the ball bearings to damp out any tendency to bounce or shake that the disk and sample may have had on impact. This was effective enough to render such secondary movements unnoticeable. Recoil movement was observed with a Cannon 518, 5-1 zoom, super-8 movie camera outfitted with a +2 close-up lens and running at 36 frames/sec.[1] Filming was done on Kodachrome II, super-8 movie film, ASA 40, with lighting provided by strategically placed flashlights--one behind the jar to illuminate the ink line and one off to the side to light the reference scale (a strip of 1-cm. x 1-cm. K and E graph paper) on the jar.

Solutions

The Newtonian fluids were glycerine-water solutions. The non-Newtonian inelastic fluids were water solutions of Methocel or blends of different shear degraded Polyethylene Oxide (type WSR-301) water solutions and glycerine. Separan AP-30 water solutions provided the viscoelastic fluids used as a comparison against the inelastic fluids.

---

1. The standard filming speed for a super-8 movie camera is 18 frames/sec.

Methocel (51) and shear degraded Polyox (40, 62) were chosen because they have served as inelastic fluids for other works. In two of these works (40, 51) inelasticity was determined by observing zero normal stress differences for the fluids.

Methocel, a product of Dow Chemical is available in a wide variety of grades and molecular weights. Bodger (8) reports Methocel 90 HG as the type used by Rama Murthy and Bodger (51) and thus was adopted for this work. The basic structure for Methocel is (23):

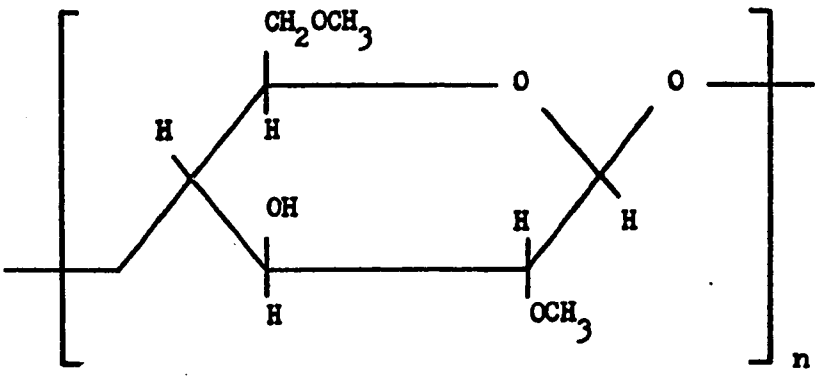

The Methocel HG products differ from this in that they contain some hydroxypropoxyl ($-OCH_2CHOHCH_3$) units in addition to the methoxyl ($-OCH_3$) groups. Varying the ratio of these substituents yields different degrees of organic solubility and, in aqueous solutions, different thermal gel points. The nomenclature 90 HG implies a gel point at 90°C. Bench scale testing yielded a viscosity grade of 15,000 cps (2% water solution at 20°C) as the best candidate for this work. Methocel 90 HG, 15,000 cps, has an average molecular weight of 1.2×10^5.

Polyethylene oxide (WSR-301 supplied by Union Carbide) is a very high molecular weight (approximately 4×10^6) linear polymer with the repeating unit

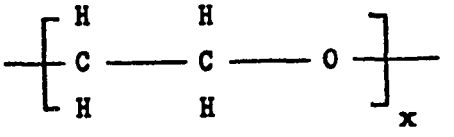

that imparts non-Newtonian behavior to solutions even when present in low concentrations. In aqueous solutions, hydrogen bonding is responsible for the polymer's solubility. Under shear, polyethylene oxide solutions degrade markedly with strong losses of elasticity and viscosity. Researchers have found it necessary to prepare solutions "by gentle rolling" (5) so as to preserve maximum levels of pseudoplastic behavior.

Polyethylene oxide solutions were occasionally diluted with glycerine because it allowed variation of the power-law index without great changes in viscosity. Addition of glycerine always reduced solution viscosity because it is not a solvent for polyethylene oxide and thus the resulting glycerine-water mix was a poorer solvent for the polymer than pure water.

Separan AP-30 (from Dow Chemical) is a partially hydrolyzed polyacrylamide, average molecular weight of about 2×10^6, with the repeating unit:

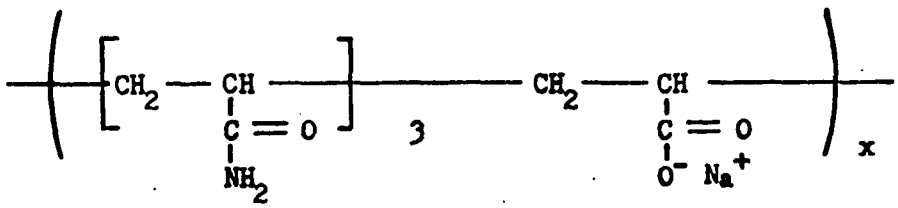

It is readily soluble in water yielding solutions of high elasticity and low shear sensitivity.

The inelastic fluids were prepared in a 55-gal. drum with a 1/3-h.p. Typhoon mixer providing agitation. Methocel was obtained in granular form which allowed rapid dispersion in water. However, considerable air entrainment occurred due to the porous granules, thus making it necessary to wait one to two days before testing with the fluid. Dispersion of the Polyox in water was fastest when ice was added as part of the water weight fraction. This lowered the solubility of the Polyox and thus reduced clump formation while the powder was added. Rapid agitation maintained the dispersion as the water warmed up and the Polyox dissolved.

Degradation of Polyox solutions was effected by pumping through a Northern, size 4387-02-A139, gear pump. Obtaining inelastic fluids with viscosities compatible with apparatus capabilities and yet possessing different power-law index values required careful watching of the duration of this high shear pumping. Insufficient degradation yielded fluids that were still elastic while excessive pumping could render low viscosity fluids that were almost Newtonian. Bench scale testing was conducted on 1-gal. quantities to determine Polyox concentrations. Blends of inelastic Polyox solutions were developed by further spot testing with a Contraves AG cone-and-plate viscometer

(made by the Olkon Corporation, Zurich) to yield the desired viscosity and power-law index combinations.

Experimental Procedures

Raw data consisted of the set of steady state differential pressure readings taken from the manometers, the steady state volumetric flow rate, and the specific gravity of the test fluid. Attainment of a steady state was determined by observing fluid levels in the manometers with the vernier and/or a cathetometer. When these remained within the error of a pressure reading (±0.01-in.) for the time needed to take data (about 10 minutes) a steady state was assumed.

Pressure readings were taken relative to atmospheric pressure as observed by the open reference tube in the manometer system. This allowed the pressure at the exit end to be arbitrarily set equal to zero in computing the equilibrium pressure gradient, $\frac{dP}{dZ}$. The manometers were read twice--once left to right, then right to left--so as to balance any error that might develop due to gradual system changes. To reflect data scatter better each reading was taken as one point. Thus the data appear as pairs of points, each pair representing one set of experimental conditions.

Depending on the flow rate, volumetric flow rates were obtained either by collecting a timed 1000-ml. sample or by collecting timed bucket quantities and then weighing them. In all cases, volumetric flow rates were measured while reading the manometers. At least one rate measurement was taken for each point. While collecting

volumetric flow rates a holding tank return system delivered a comparable volume of fluid back to the 55-gal. storage tank. A valve on the holding tank allowed an approximate match of fluid return rate to fluid collection rate, thus effecting a constant head of fluid above the pump. Volumetric flow rates were timed with a Sears stop watch, accurate to ±0.1-sec. The bucket sized samples were weighed on an Ohaus, heavy duty solution balance to ± 1-gm.

Specific gravities were measured with hydrometers accurate to ±0.1% on fluid collected in measuring the volumetric flow rate.

New fluids were prepared in a separate 55-gal. drum and pumped to the apparatus for testing. At least one day of circulating within the system was allowed to insure steady state temperature. After testing, fluids were drained and the apparatus rinsed with water.

Data on Newtonian fluids were collected from study of three different glycerine-water solutions, thus allowing a wide range of flow rates. Only one fluid was run for each non-Newtonian study since a correlation versus power-law index was being sought. It would have been quite difficult to obtain fluids possessing almost identical power-law index values but different viscosities.

When setting up the apparatus for a run, cathetometers assisted in leveling the test and entrance sections and in placing the entrance section pressure tap on the tube center-line.

For the Newtonian flow studies no strict attention was paid to achieving the same temperature over an entire run since fluid

properties were obtained at the same time that ΔP_{ent} was measured. However, temperature control was very important for the non-Newtonian studies where fluid properties were determined from a flow curve of τ_w vs. $\dot{\gamma}_w$ data gathered over many runs. With the aid of a room air conditioner, ambient air temperatures could be generally maintained within $\pm 0.5^{\circ}C$ as observed by mercury thermometers, accurate to $\pm 0.1^{\circ}C$. On occasions when room temperature variations exceeded $\pm 0.5^{\circ}C$ the run was terminated. Temperature fluctuations within the $1^{\circ}C$ range should have little effect on experimental results. The amount of test fluid, 20 to 30 gallons, was large enough to be insensitive to rapid fluctuations in temperature. To appreciate the influence of gradual temperature changes representative test fluids were studied for their viscosity dependence on temperature.

These data appear in Fig. 2.7 showing capillary viscometer times vs. temperatures. (These points were taken on a size 3C Cannon viscometer in a constant temperature bath.) This demonstrates that a $1^{\circ}C$ change in temperature represents at most a 2% change in fluid viscosity, which is well within experimental error.

Data Analysis

The raw data were analyzed by a computer program written in Fortran for this thesis. Input to the program consisted of the fluid level readings from the manometers, the volumetric flow rate in terms of time (sec.) required for 10^5-cm.^{3} of fluid, and the

Fig. 2.7. Viscosity Dependence on Temperature for Representative Fluids

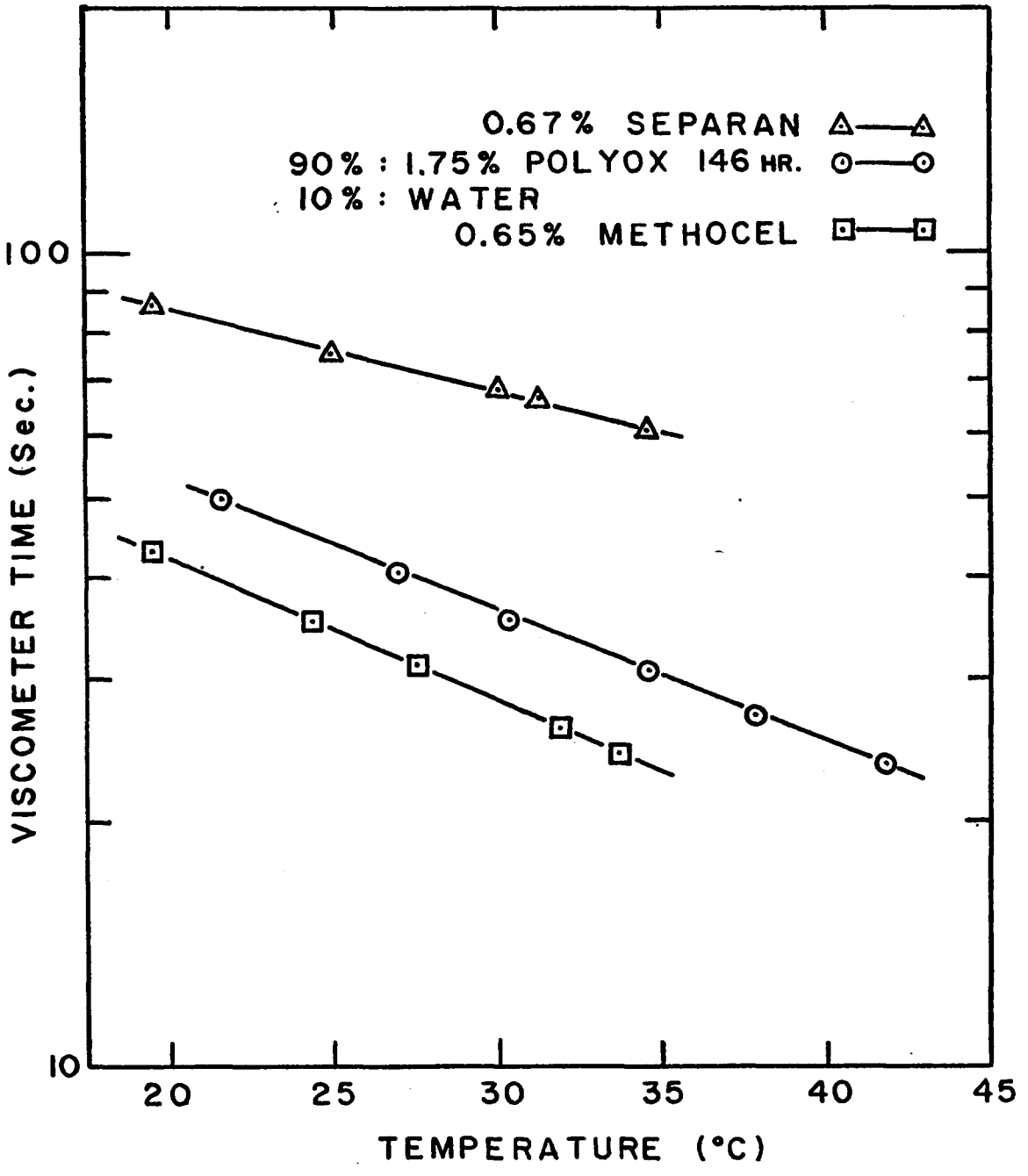

specific gravity. A flow chart, definition of symbols, and discussion of these computer programs appear in the Appendix.

The computer program for Newtonian flow data treated each data point separately, yielding pairs of ΔP_{ent}, N_{Re} values. A second program then computed the parameters K and K'. For non-Newtonian flow, these two programs were combined and enlarged upon so as to treat non-Newtonian flows. The data analysis discussed below is for the non-Newtonian flow program.

For each set of data, the following were computed. The manometer readings yielded a set of equilibrium pressure gradients $\left\{\frac{dP}{dZ}\right\}_i$, and then a set of wall shear stresses $\left\{\tau_w\right\}_i = \frac{D}{4}\left\{\frac{dP}{dZ}\right\}_i$. Friction factors were computed from $\left\{f\right\}_i = \frac{2\left\{\tau_w\right\}_i g_c}{\left\{v_b\right\}_i^2}$. A least squares fit of $\left\{\ln \tau_w\right\}_i$ with $\left\{\ln v_b\right\}_i$ led to $1/n' = \frac{d(\ln v_b)}{d(\ln \tau_w)}$ and then the wall shear rates $\left\{\dot{\gamma}_w\right\}_i = \left\{v_b\right\}_i \left[\frac{3n'+1}{r_t n'}\right]$. A least squares fit of $\left\{\ln \tau_w\right\}_i$ and $\left\{\ln \dot{\gamma}_w\right\}_i$ produced n, the power-law index (slope) and K, the consistency (value of τ_w at $\dot{\gamma}_w = 1$). Assuming flow properties to be similar in the entrance section, equilibrium pressure drops were computed as $\left\{\left(\frac{dP}{dZ}\right)_e\right\}_i = \left\{\left(\frac{dP}{dZ}_t\right)\right\}_i \left(\frac{r_t}{r_e}\right)^{3n+1}$.

Then the entrance pressure drops were computed

$$\left\{\Delta P_{ent}\right\}_i = \left\{\Delta P_{tot}\right\}_i - \left\{\left(\frac{dP}{dZ}\right)_e\right\}_i Z_e - \left\{\left(\frac{dP}{dZ}\right)_t\right\}_i Z_t$$

and the Reynolds numbers

$$\left\{N_{Re}\right\}_i = \frac{2\rho D_t^{\,n}\left[2\left\{v_b\right\}_i\right]^{2-n}}{K\ (3 + 1/n)^n}$$

The parameters K and K' were obtained from a least squares fit minimizing the relative errors of $\left\{\frac{\Delta P_{ent}}{\rho v^2/2g_c}\right\}_i$ vs. $\left\{1/N_{Re}\right\}_i$ yielding K' as the slope and K as the intercept. The equations for this method appear in the appendix. Then to obtain a comparison curve, values of $\frac{\Delta P_{ent}}{\rho v^2/2g_c}$ vs. N_{Re} were calculated from K and K'.

Sources of Error

The major source of error existed in the absolute magnitude of the entrance pressure loss relative to the error of reading the manometers. For Reynolds numbers less than 10 the entrance pressure loss can be of the order of 0.10-in. of test fluid, which is then accurate to about 10% when read to 0.01-in. Consequently, no testing was conducted at flow rates when ΔP_{ent} was small enough to cause large errors. At higher flow rates, ΔP_{ent} was the order of

inches of test fluid in magnitude, reducing this error to less than 1%.

Volumetric flow rate readings were dependent on the stop watch (read to ±0.1-sec.) and the amount of fluid that flowed as the watch was stopped or the bucket withdrawn. When collecting 1000-ml. samples, the watch could be stopped within 1-ml. or 0.1% and times were the order of 100-sec. Bucket-size quantities with minimum weights of 1500-gm. could be weighed to 1-gm. At higher flow rates (5000-gm. in 50 sec.) the bucket could be removed from the exit stream in about 0.1 sec. causing a collection error of ± 10 gm. or 0.4%. Collectively this suggests that volumetric flow rates should be accurate to 0.5% which is borne out by the scatter in the data.

The manometer scales could be read to ±0.01-in. and the minimum differential pressure reading was 1-in. so that the error in reading a manometer was less than 1%.

Sylvester (62) computed the maximum temperature rise due to viscous heating to be 0.5°C for his fluids. Since this study was conducted at similar flow conditions with similar fluids it is assumed that this source of error is of the same order for this study. As shown earlier, such a rise in temperature is within the limits of temperature control and related to about a 1% error in viscosity.

CHAPTER 3. RESULTS

Newtonian Fluids Through a Sudden Contraction--Dependence on Contraction Ratio

When a fluid in laminar flow passes through a contraction of cylindrical tubes, Sylvester and Rosen (63, 64) have shown that the excess entrance pressure loss can be expressed by

$$\frac{\Delta P_{ent}}{\rho v^2/2g_c} = K + K'/N_{Re} \qquad (1.8)$$

where

$$K = K(\beta, \alpha, n, \text{elasticity})$$

$$K' = K'(\beta, \alpha, n, \text{elasticity})$$

For the case of Newtonian flow (n = 1 and no elasticity) through a sudden contraction ($\alpha = 90^\circ$) these parameters simplify to $K = K(\beta)$ and $K' = K'(\beta)$.

Data taken for a series of glycerine-water solutions at seven different contraction ratios ($\beta = 0.636, 0.411, 0.213, 0.109, 0.062, 0.041$, and 0.026) appear in Fig. 3.1-3.7. All of these data further verify the relationship in Equation (1.8) as can be seen by the close agreement between data and the curve calculated from the K and K' values. Also, it demonstrates that for Newtonian fluids flowing through a sudden contraction K and K' are only functions of β.

Values of K and K' are presented in Table 3.1. These were obtained from a least squares fit of the data that minimized the relative errors. The equations for such a calculation appear in Appendix A-1. A kinetic energy balance yields $K = 2(1-\beta^2)$. Thus the K data were fit by least squares to an equation of that form

Fig. 3.1. Entrance Pressure Loss for Newtonian Flow through a Sudden Contraction, $\beta = 0.636$

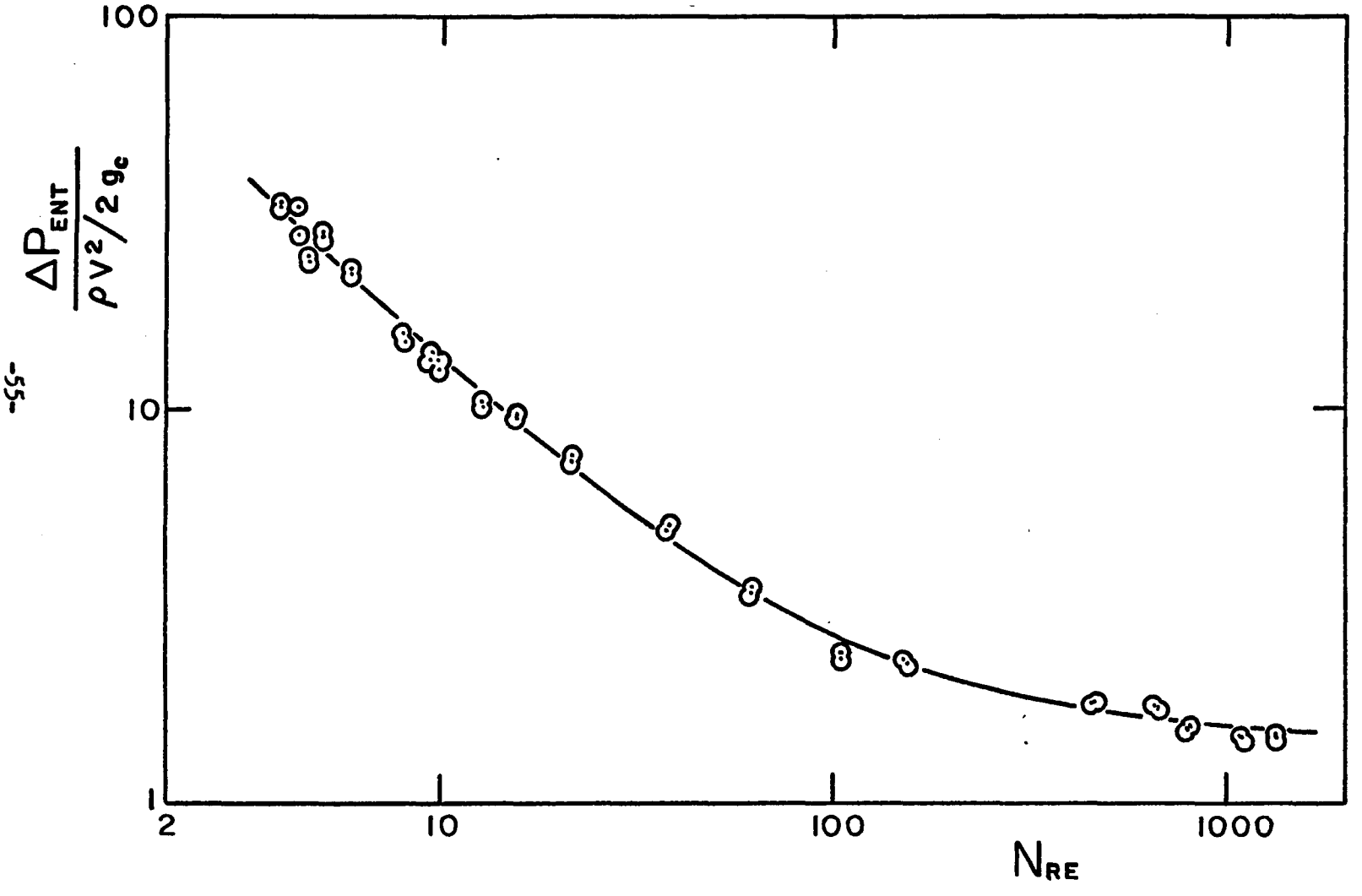

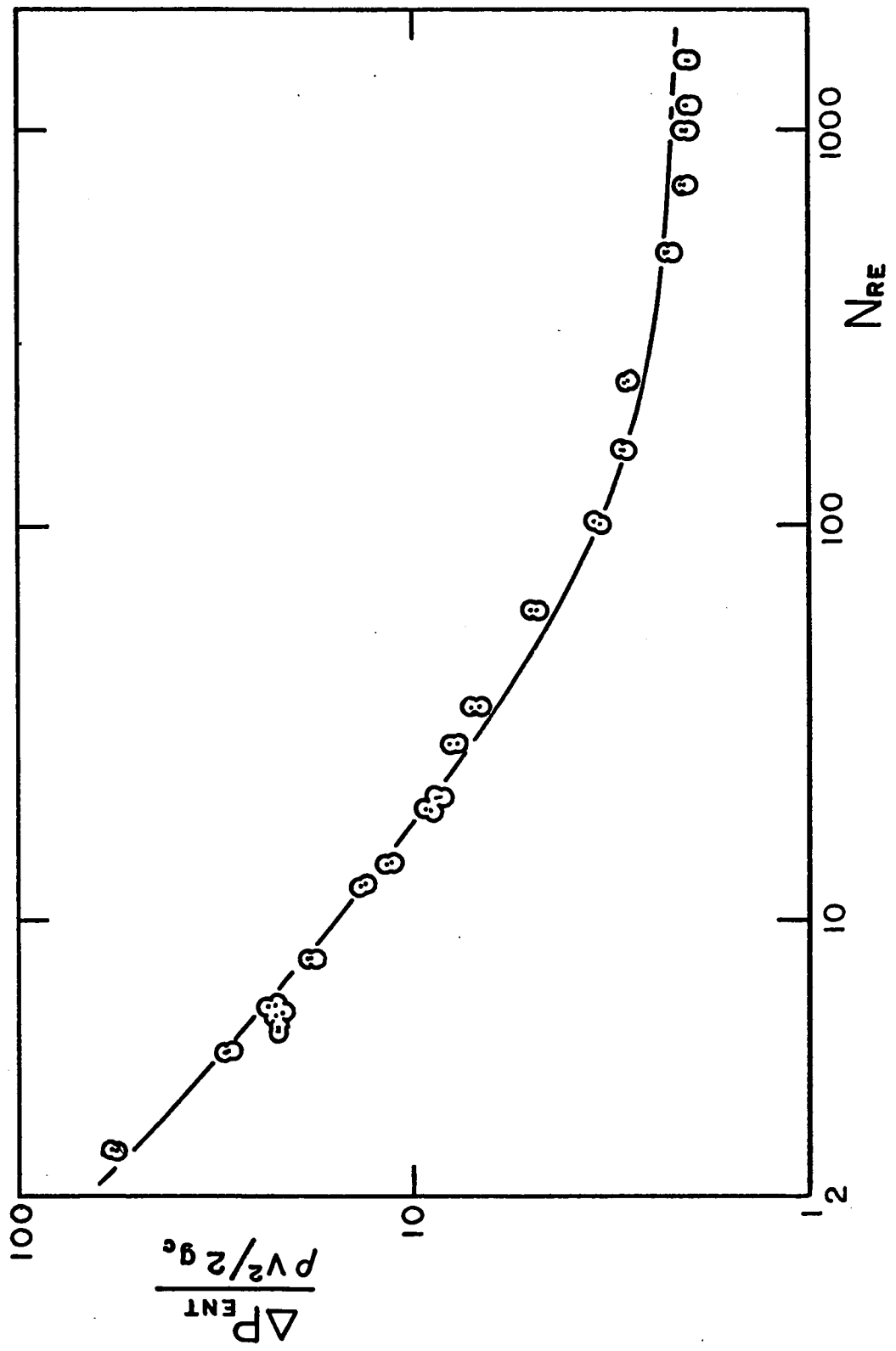

Fig. 3.2. Entrance Pressure Loss for Newtonian Flow through a Sudden Contraction, $\beta = 0.411$

Fig. 3.3. Entrance Pressure Loss for Newtonian Flow through a Sudden Contraction, $\beta = 0.213$

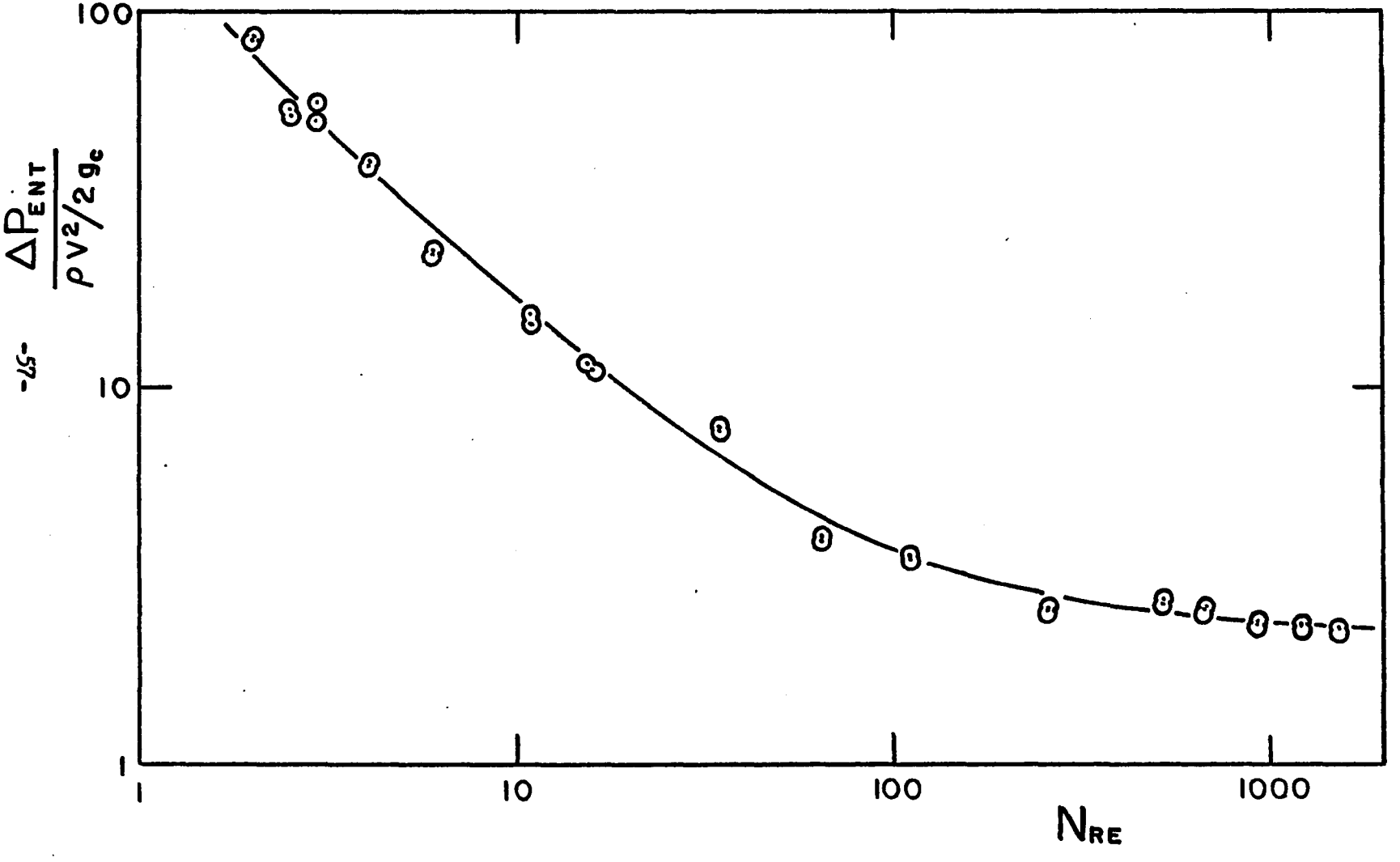

Fig. 3.4. Entrance Pressure Loss for Newtonian Flow through a Sudden Contraction, $\beta = 0.109$

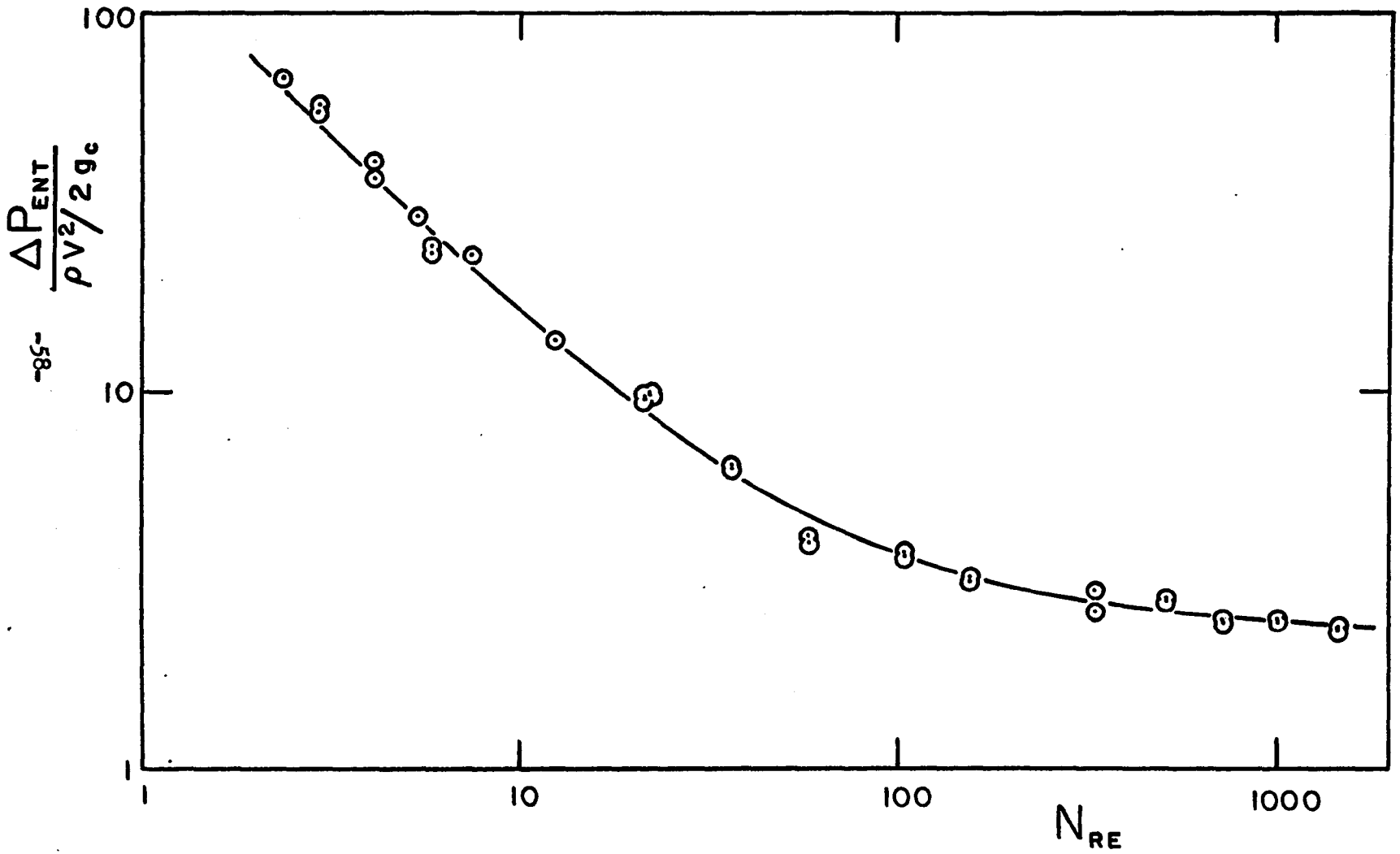

Fig. 3.5. Entrance Pressure Loss for Newtonian Flow through a Sudden Contraction, $\beta = 0.062$

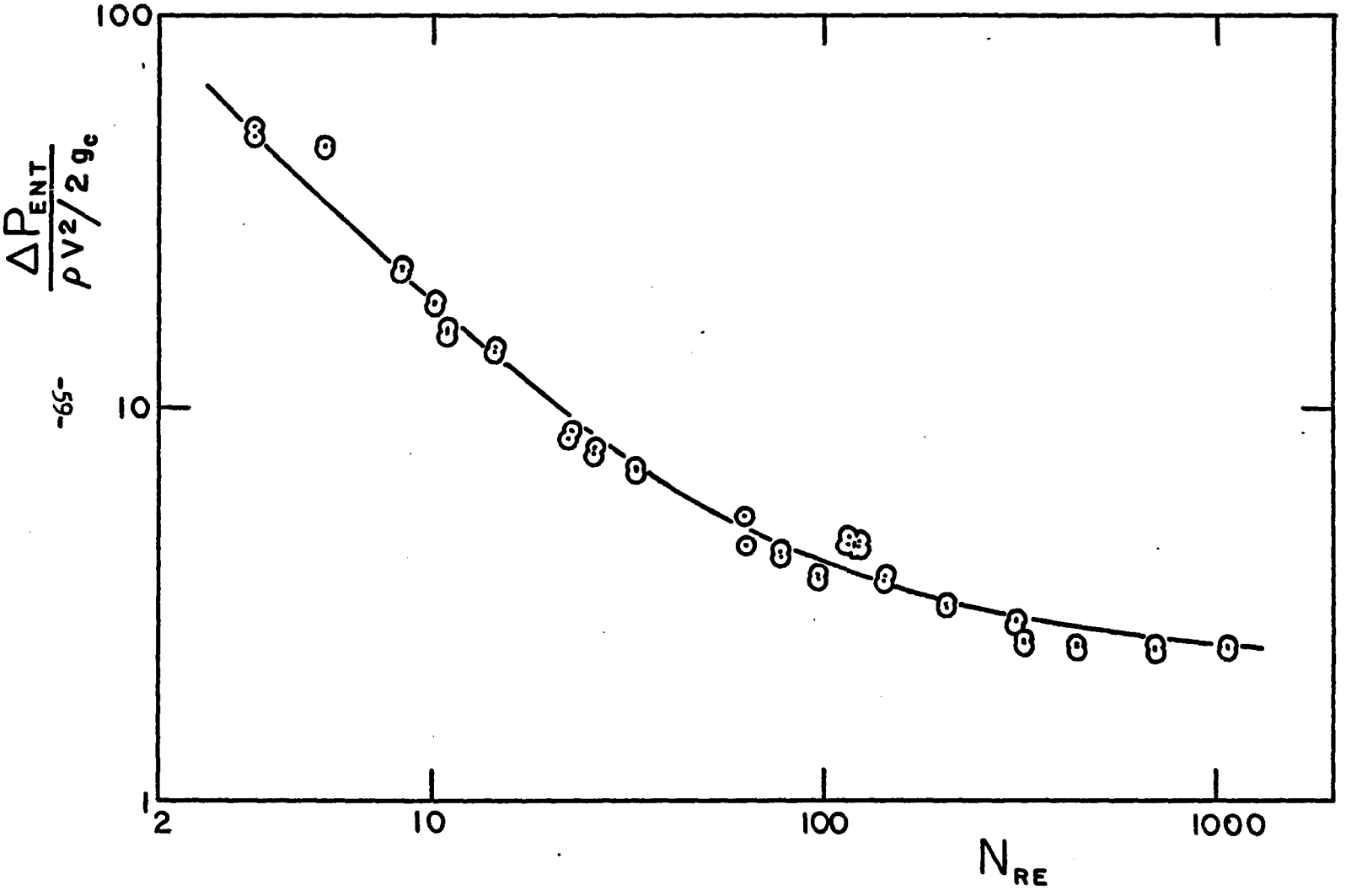

Fig. 3.6. Entrance Pressure Loss for Newtonian Flow through a Sudden Contraction, $\beta = 0.041$

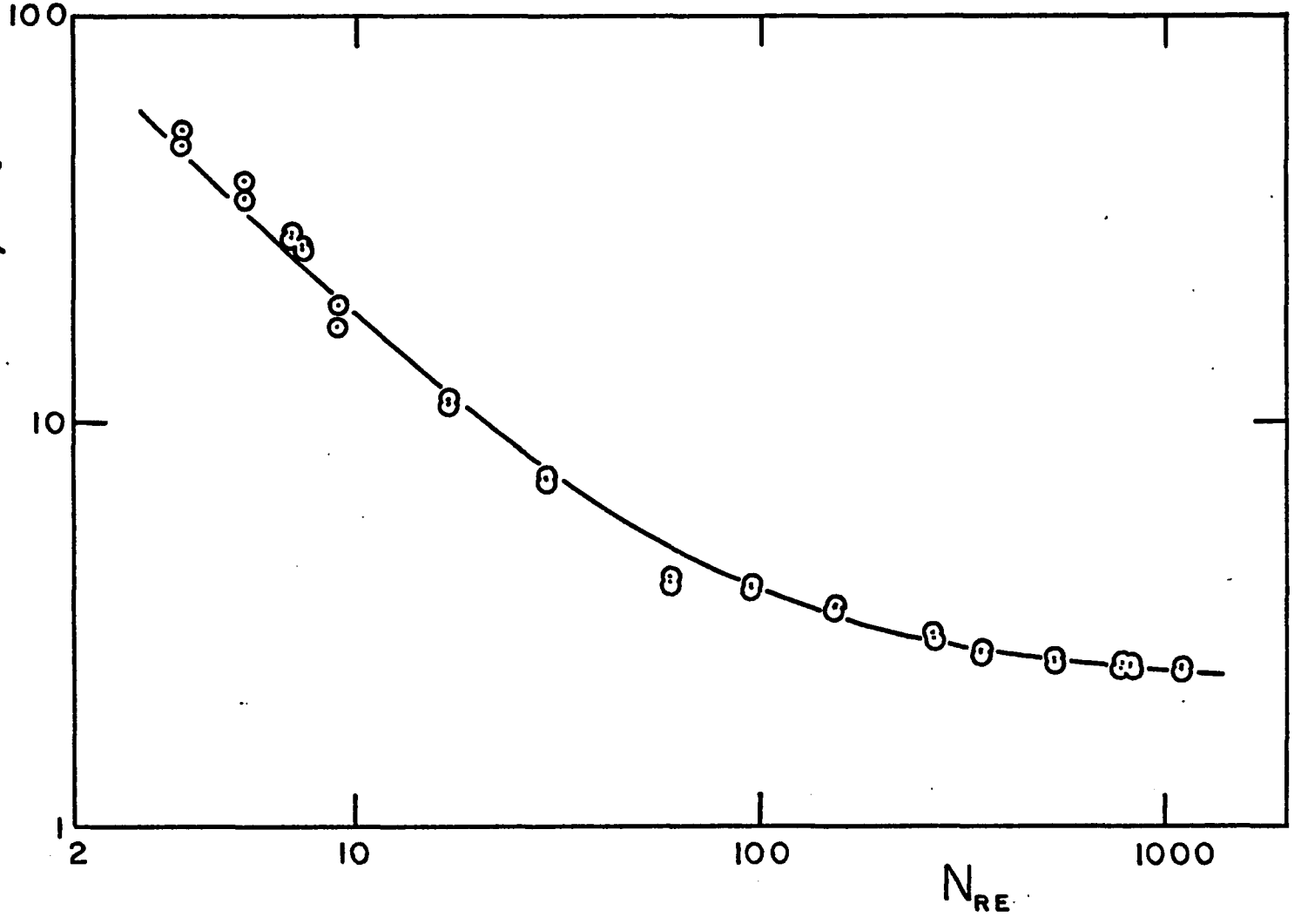

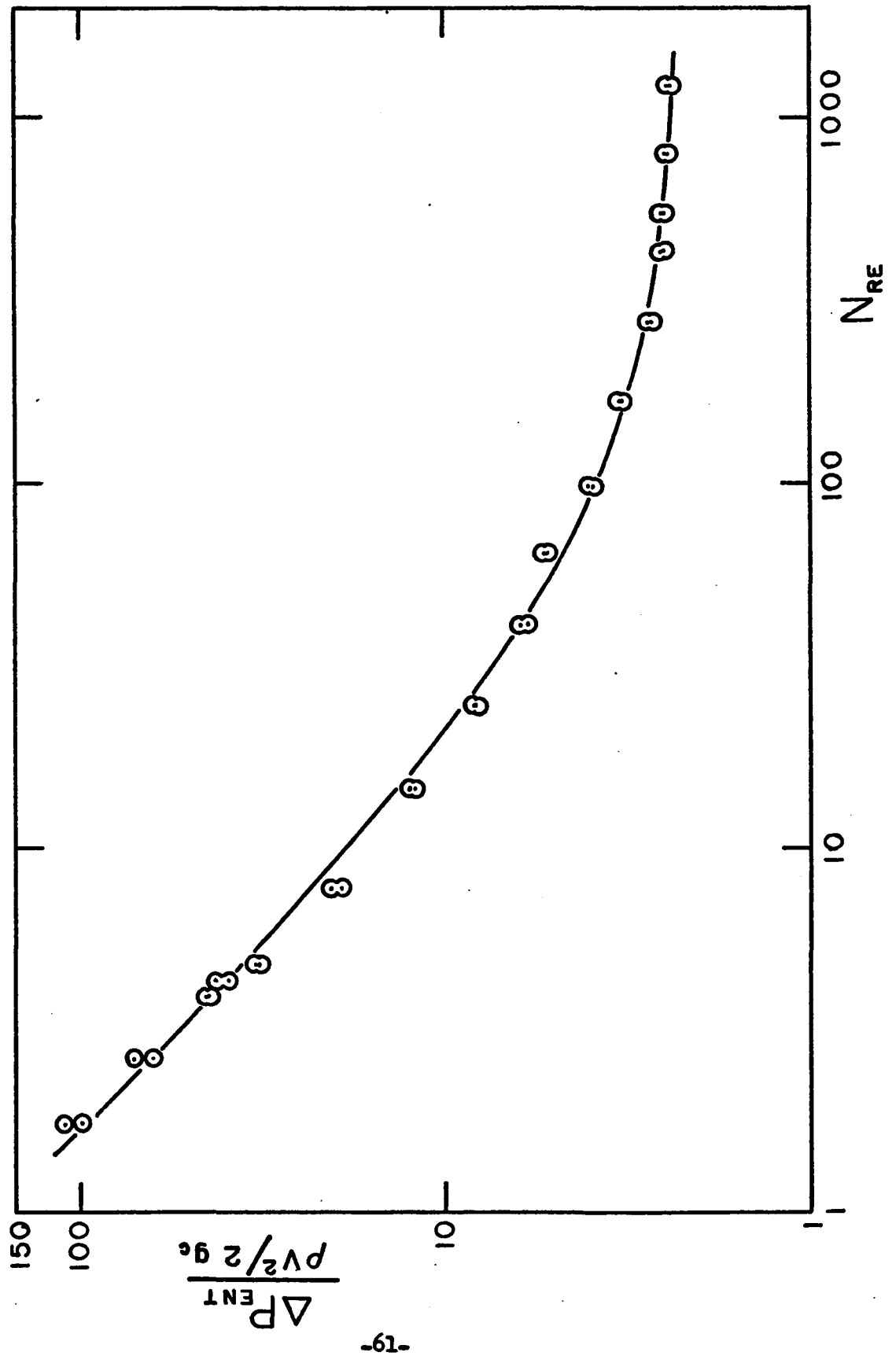

Fig. 3.7. Entrance Pressure Loss for Newtonian Flow through a Sudden Contraction, $\beta = 0.026$

Table 3.1. Values of K and K' for Newtonian Fluids.

Tube	β	K	K'
1/2"	0.636	1.46	120
5/8"	0.411	2.06	129
7/8"	0.213	2.20	147
1 1/4"	0.109	2.28	144
1 5/8"	0.062	2.34	164
2"	0.041	2.23	161
2 1/2"	0.026	2.25	158

giving

$$K = 2.32 \pm 0.05(1-\beta^2) \qquad (3.1)$$

For K' the data were fit to a similar equation, although there is no theoretical justification for this.

$$K' = 159 \pm 20(1-\beta^2) \qquad (3.2)$$

These curves appear in Fig. 3.8.

For the limiting case of an infinite contraction ($\beta=0$) the value K = 2.32 is in agreement with the boundary-layer analysis of Collins and Schowalter (19). These results also agree with that of Sylvester and Rosen (63), K = 2.4±0.1 (β = 0.0156) within experimental precision. Reanalyzing Sylvester's data (62) with the statistical techniques applied in this work gives a value of K' = 241(β = 0.0156), which appears to be somewhat higher than the present results. This may be due to the fact that Sylvester's entrance section was not long

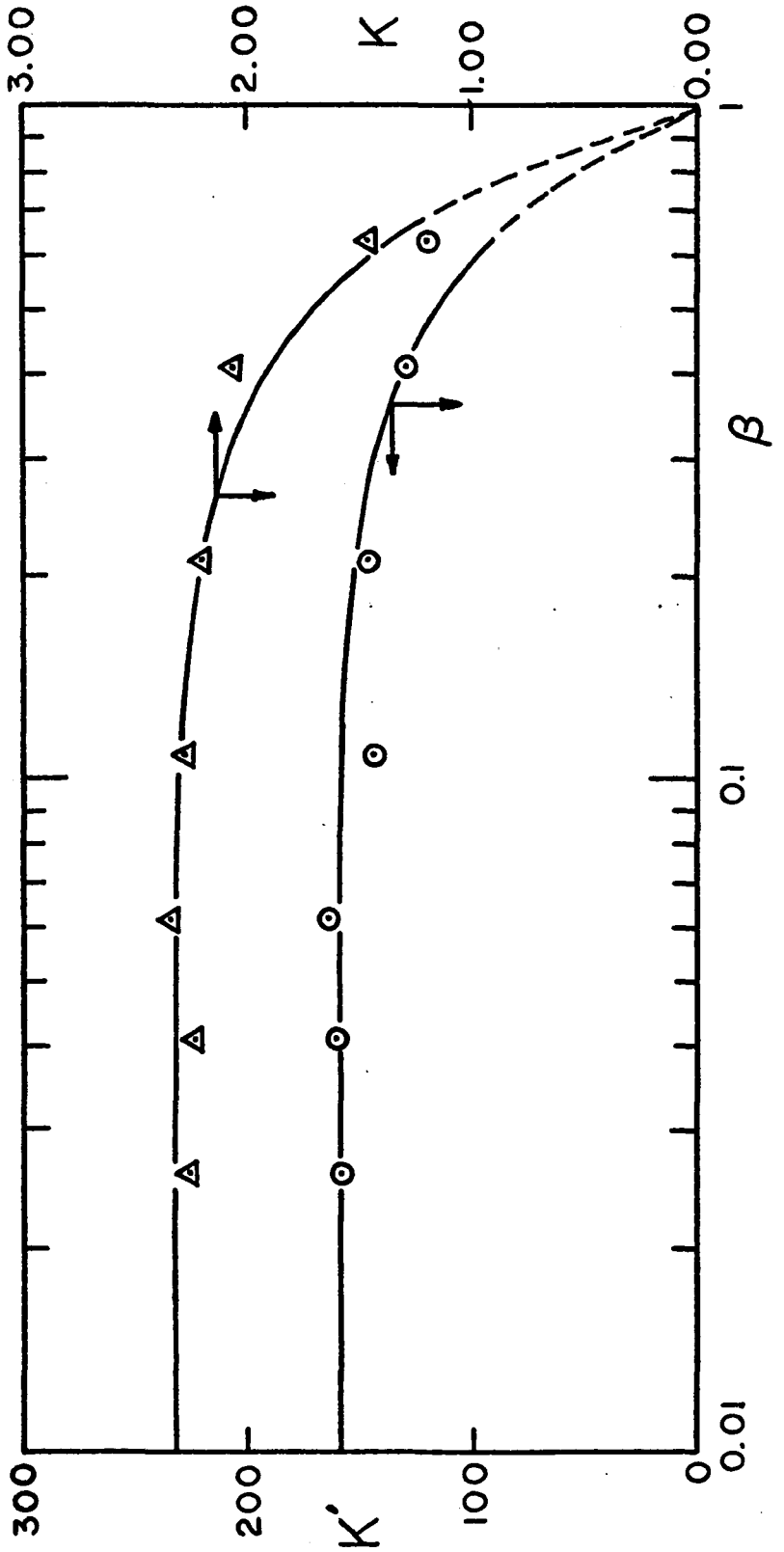

Fig. 3.8. K and K' vs. Ratio of Tube Areas

enough to permit fully developed flow before reaching the contraction, and K' may be particularly sensitive to the nature of the profile in the entrance region. The infinite contraction ($\beta = 0$) value of K' differs greatly from low Reynolds numbers studies of flow through an orifice. Generally, K' has had the broadest range of reported values--from K' = 795 (3) to K' = 44 (69). The results of this work need to be carried forward toward a better understanding of K'. Questions regarding its sensitivity to velocity profile development and sharpness of contraction need to be examined.

From a practical standpoint, this work demonstrates that an upstream tube of greater than twice the diameter of the downstream tube ($\beta = 0.25$) may be considered an infinite reservoir, K = 2.32, K' = 159, with less than 4% error. In many applications this may be an acceptable assumption.

In designing pipe systems it is common practice (7) to express pressure losses due to fittings, valves, and other restrictions in terms of a length of pipe having an equivalent pressure loss due to fully developed flow. This effective length, X_{eff}, is conveniently stated as $\frac{X_{eff}}{D}$ giving a measure of pressure loss in terms of tube diameters. Dodge (21) suggested $\frac{X_{eff}}{D} = 0.05N_{Re}$, but Sylvester and Rosen (63) pointed out that $\frac{X_{eff}}{D} = C + C'N_{Re}$ is equivalent to $\frac{\Delta P_{ent}}{\rho v^2/2g_c} = K + K'/N_{Re}$ where $C = K'/64$ and $C' = K/64$.

To allow comparisons with other X_{eff} data, C and C' can be correlated with the same $(1-\beta^2)$ relation as were K and K'.

$$C = 2.48(1-\beta^2) \tag{3.3}$$

$$C' = 0.0362(1-\beta^2) \tag{3.4}$$

The finite difference solution of Christiansen et al. (18) is within 2% agreement of $\frac{X_{eff}}{D} = 2.48 + 0.0362N_{Re}$ at high (> 700) Reynolds numbers, but is about a factor of six less at very low Reynolds numbers.

Newtonian Fluids Through Gradual Contractions--Dependence on Contraction Angle

To understand further the influence of contraction geometry on ΔP_{ent}, entrance loss data were collected for conical entrance sections having angles of 60°, 30°, 15° and 7 1/2° for $\beta = 0.041$. These data were correlated by

$$\frac{\Delta P_{ent}}{\rho v^2/2g_c} = K + K'/N_{Re} \tag{1.8}$$

and are presented in Fig. 3.9-3.12. Values for K and K' appear in Table 3.2 and they are plotted vs. cone angle, α, in Fig. 3.13. The close fit of the $\frac{\Delta P_{ent}}{\rho v^2/2g_c}$ vs. N_{Re} data verifies the application of this relation to gradual contractions.

As expected, the parameter representing kinetic energy changes has remained almost constant within experimental error because this depends on the change in fluid velocity and not on how such is

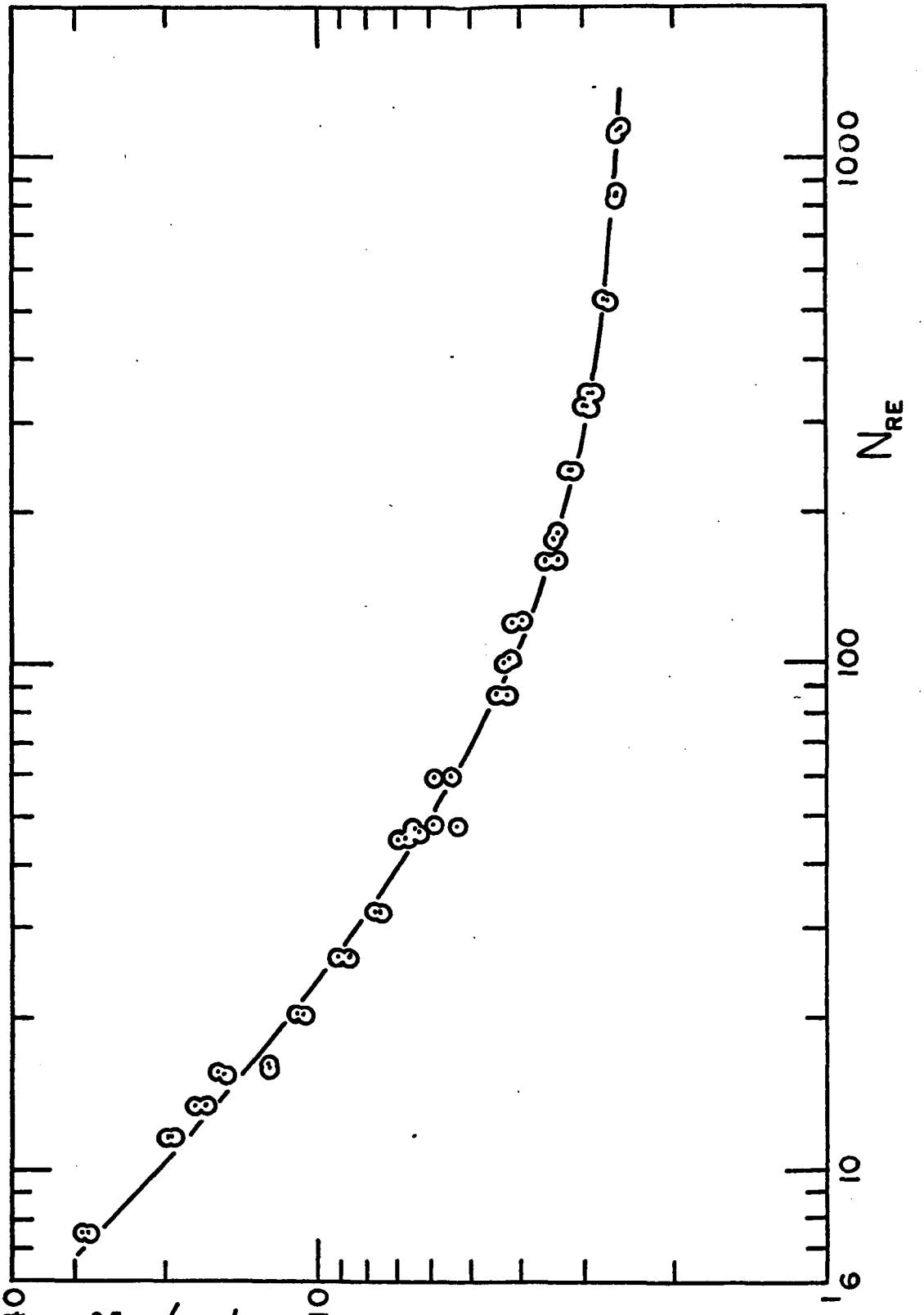

Fig. 3.9. Entrance Pressure Loss for Newtonian Flow through a Conical Contraction, $\alpha = 7\ 1/2^{\circ}$

Fig. 3.10. Entrance Pressure Loss for Newtonian Flow through a Conical Contraction, $\alpha = 15^{0}$

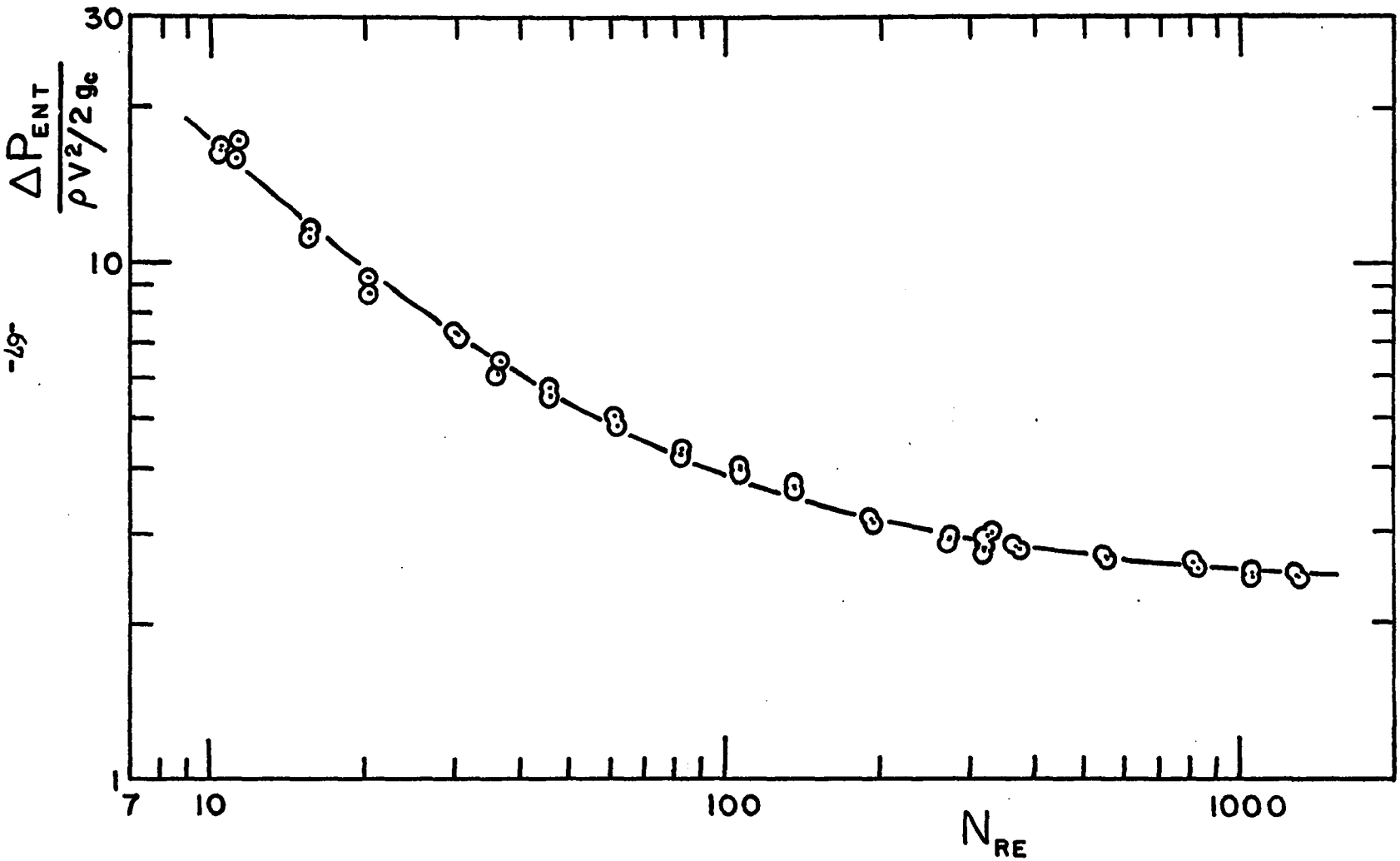

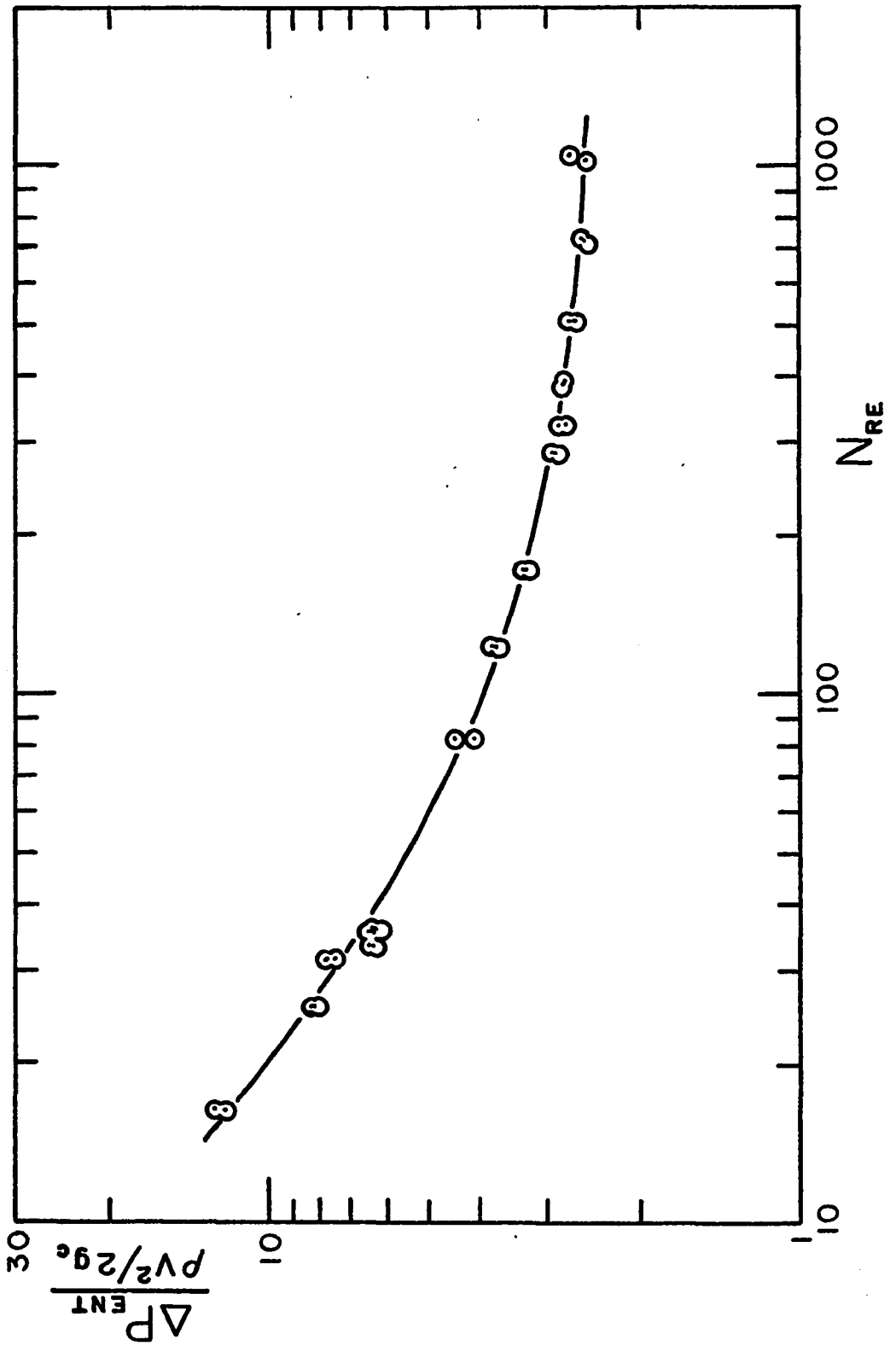

Fig. 3.11. Entrance Pressure Loss for Newtonian Flow through a Conical Contraction, $\alpha = 30°$

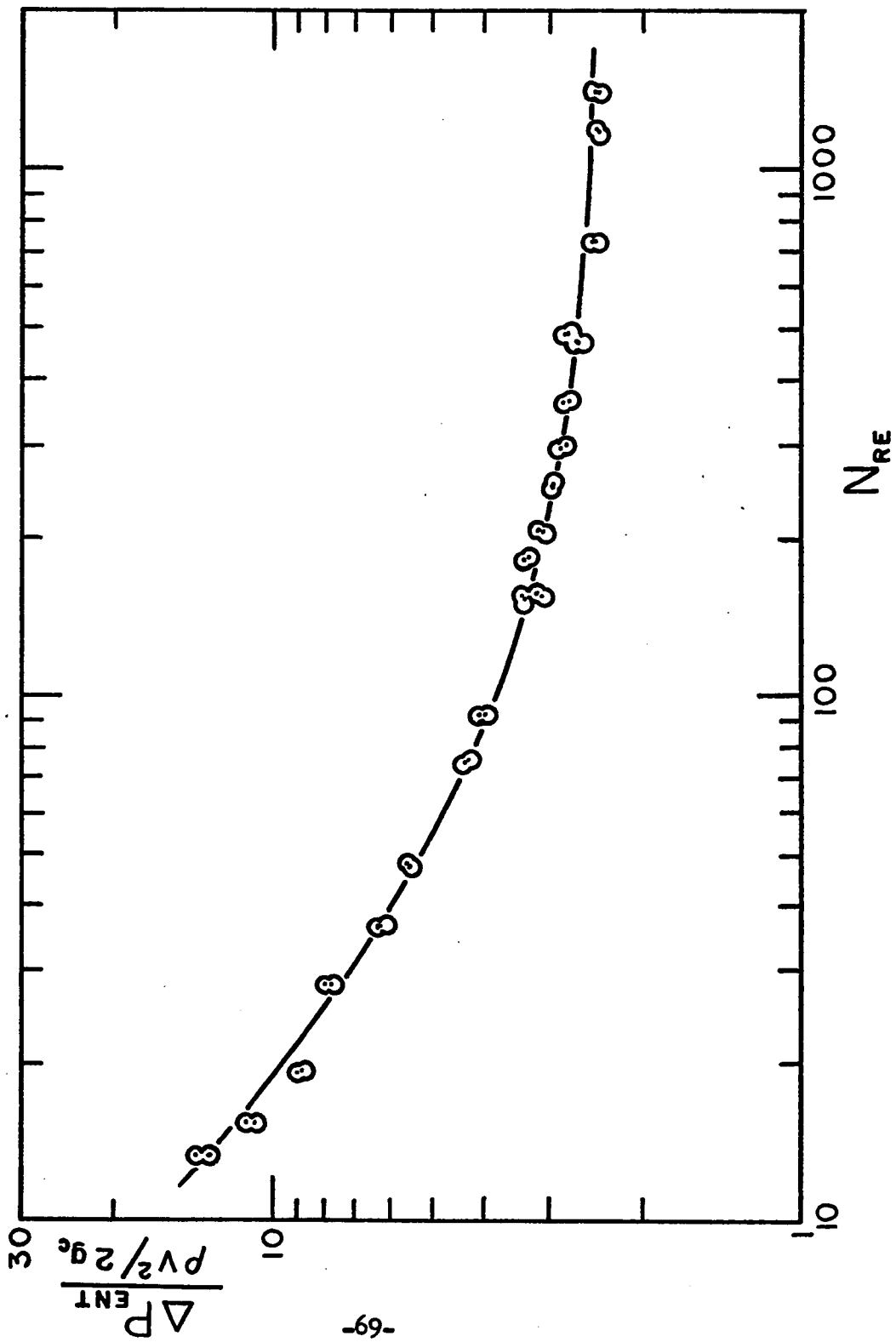

Fig. 3.12. Entrance Pressure Loss for Newtonian Flow through a Conical Contraction, $\alpha = 60^\circ$

Fig. 3.13. K and K' vs. Contraction Angle

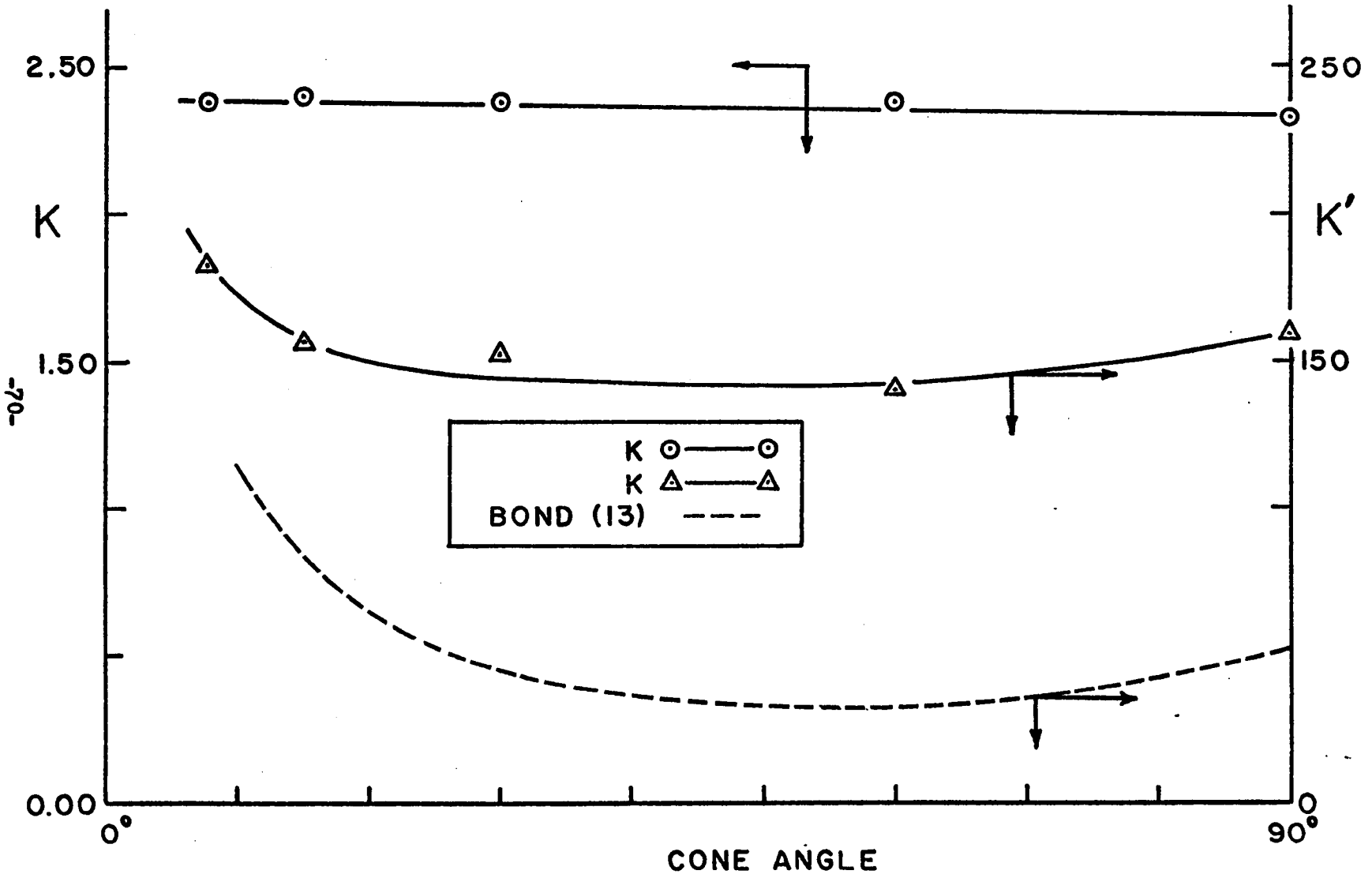

Table 3.2. K and K' vs. Cone Angle for Gradual Contractions

Cone Angle	K	K'
7 1/2°	2.38 ± .05	180 ± 20
15°	2.41 ± .05	156 ± 20
30°	2.36 ± .05	153 ± 20
60°	2.37 ± .05	142 ± 20
90° [1]	2.32 ± .05	159 ± 20

achieved. The parameter K' accounts for viscous losses which should vary with boundary shape and size. For contraction angles decreasing from 90° to 30°, K' shows a slight decrease and then as the angle decreases further, an accelerating increase.

Theoretical predictions of pressure drops for fast (58) and slow (13) flow through a slightly tapered tube suggest similar variations with cone angle. The fast flow solution

$$\frac{\Delta P_{cone}}{\rho v^2/2g_c} = (1-\beta^2) \qquad (1.18)$$

is independent of cone angle. However, the slow flow solution

$$\frac{\Delta P_{cone}}{\rho v^2/2g_c} = \frac{1}{N_{Re}} \left[\frac{32 \frac{\pi \alpha}{180}}{(1-\cos\alpha)(1+2\cos\alpha)} \right] (1-\beta^{3/2}) \qquad (1.19)$$

1. Values for K and K' at $\alpha = 90^\circ$ were taken from the curves $K = K(\beta)$ and $K' = K'(\beta)$ in Fig. 3.8.

depends on angle as shown in Fig. 3.13. Interestingly, the predicted variation with angle has the same form as that suggested by data. Differences in magnitude are probably a result of simplifications made in deriving the theoretical solution.

As the contraction angle becomes very small viscous losses would be expected to increase, since the diameter of the entrance region is effectively narrowing to that of the downstream tube. The additional pressure drop due to this can exceed any reduction in ΔP_{ent} achieved from a gradual transition of flow. In Fig. 3.13, the K' data suggest this occurs for angles less than 15°. Regarding the slight influence of angle on K', Hung (37) suggests that gradual entrances are reducing viscous losses, but for large angles the difference between flow over the cone and flow over the sharp-edged contraction is probably small compared to the entire viscous loss. According to Fig. 3.13 the minimum entrance loss can be obtained for cone angles of 65° to 45°. At low Reynolds numbers this will offer a reduction in entrance loss of almost 11%.

Inelastic Non-Newtonian Fluids through a Sudden Contraction--Dependence on Flow Index

The compositions of the non-Newtonian fluids are listed in Table 3.3. In some cases the same formulation was run for different contraction ratios or fluid temperatures. Flow curves for these fluids as determined while measuring ΔP_{ent} are presented in Fig. 3.14-3.20. These data demonstrate close agreement with the

Table 3.3. Non-Newtonian Fluids

Series	Composition	Flow Index	Consistency$_{2-n}$ ($lb_f/ft.sec^{2-n}$)
Elastic (β=0.041)			
S-1	0.67% Separan AP-30 Recoil = 0.5 cm.	0.42±2%	1.032
Inelastic (β=0.041)			
M-1	0.65% Methocel 90HG	0.63±1%	0.452
M-2	0.55% Methocel 90HG	0.71±5%	0.165
P-1	90%: 1 1/4% Polyox--33 hr. 10%: 1 3/4% Polyox--58 hr.	0.67±5%	0.282
P-2	59%: 1 3/4% Polyox--146 hr. 6%: water 35%: glycerine	0.83±3%	0.117
P-3	59%: 1 3/4% Polyox--146 hr. 6%: water 35%: glycerine	0.84±3%	0.099
P-4	1 1/3% Polyox--32 hr.	0.67±6%	0.256
P-5	63%: 1 1/3% Polyox--32 hr. 16%: 1 3/4% Polyox--146 hr. 1.6%: water 9.4% glycerine	0.75±3%	0.151

Table 3.3. Non-Newtonian Fluids (Continued)

Series	Composition	Flow Index	Consistency ($lb_f/ft.sec^{2-n}$)
Inelastic (β=0.636)			
P-6	80%: 1 1/4% Polyox--33 hr. 20%: 1 3/4% Polyox--146 hr.	0.67±4%	0.342
P-7	63%: 1 1/3% Polyox--32 hr. 16%: 1 3/4% Polyox--146 hr. 1.6%: water 9.4%: glycerine	0.75±3%	0.143

Fig. 3.14. Flow Curve for Separan

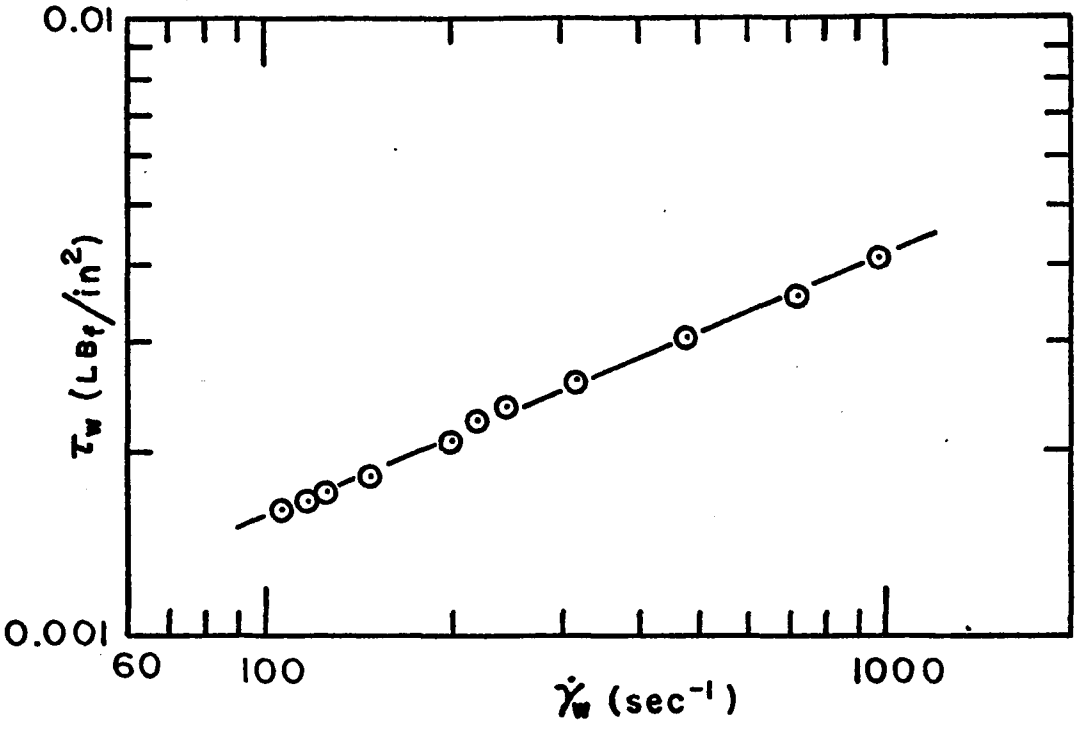

Fig. 3.15. Flow Curve for Methocel

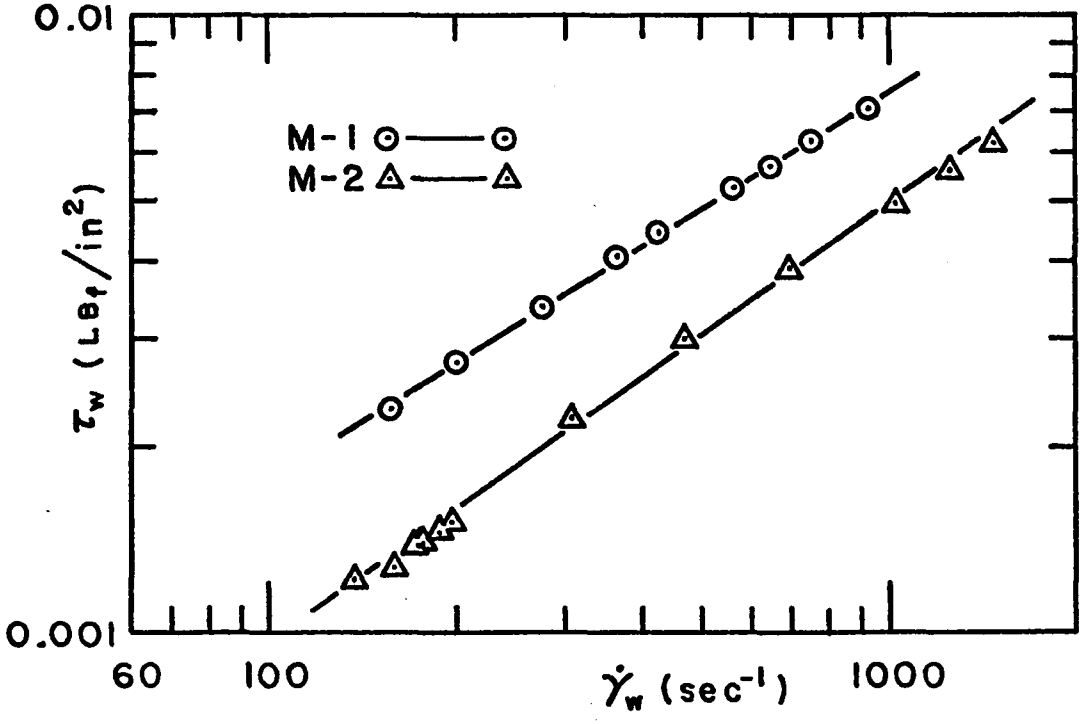

Fig. 3.16. Flow Curve for Polyox

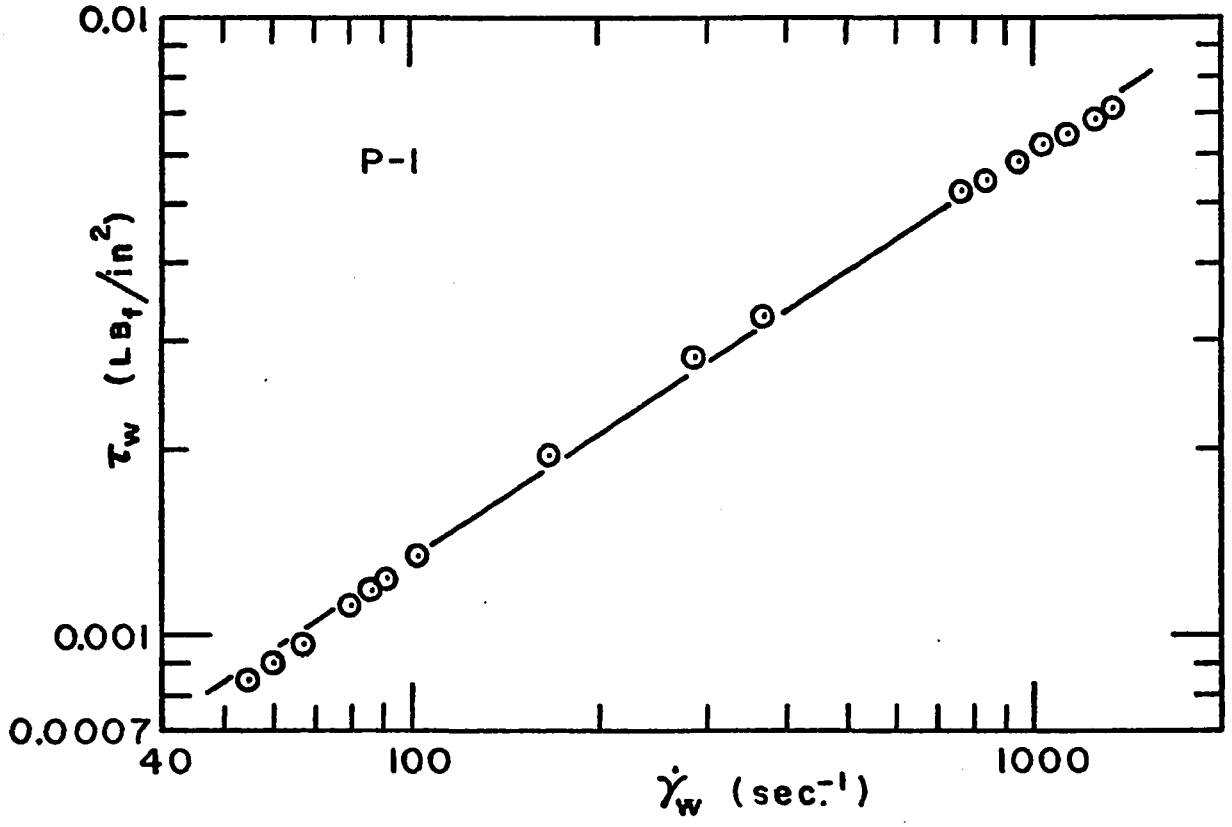

Fig. 3.17. Flow Curve for Polyox

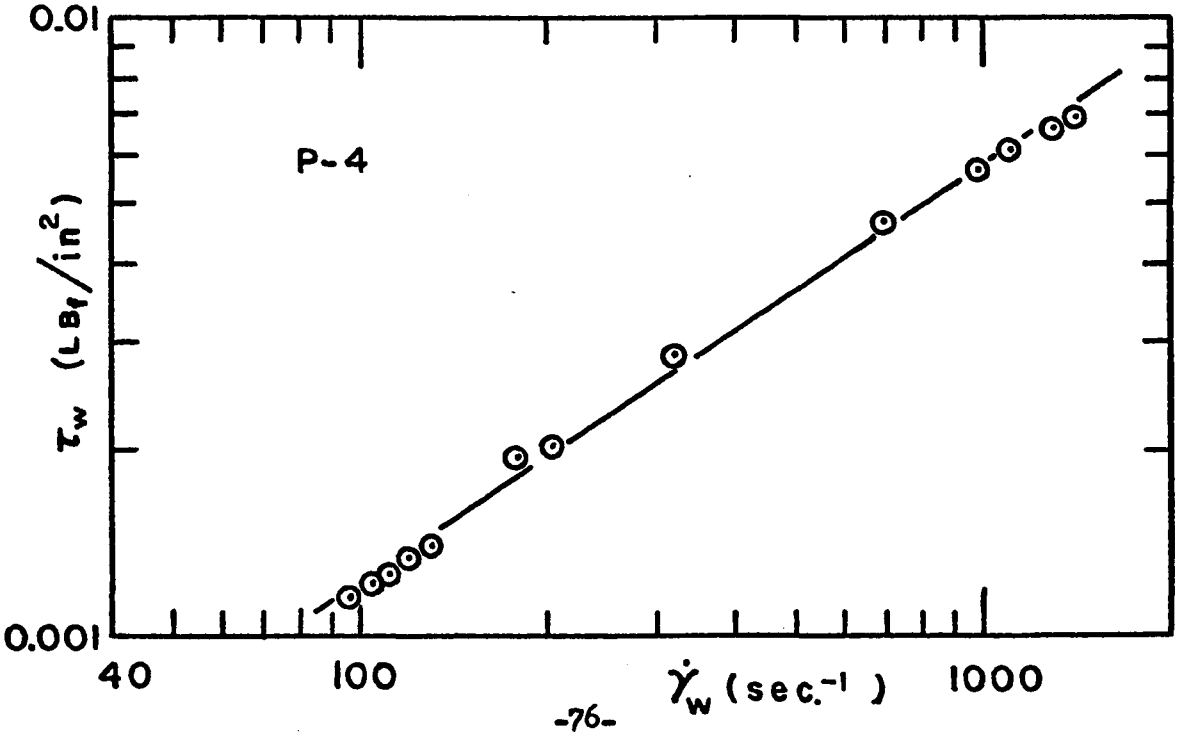

Fig. 3.18. Flow Curve for Polyox

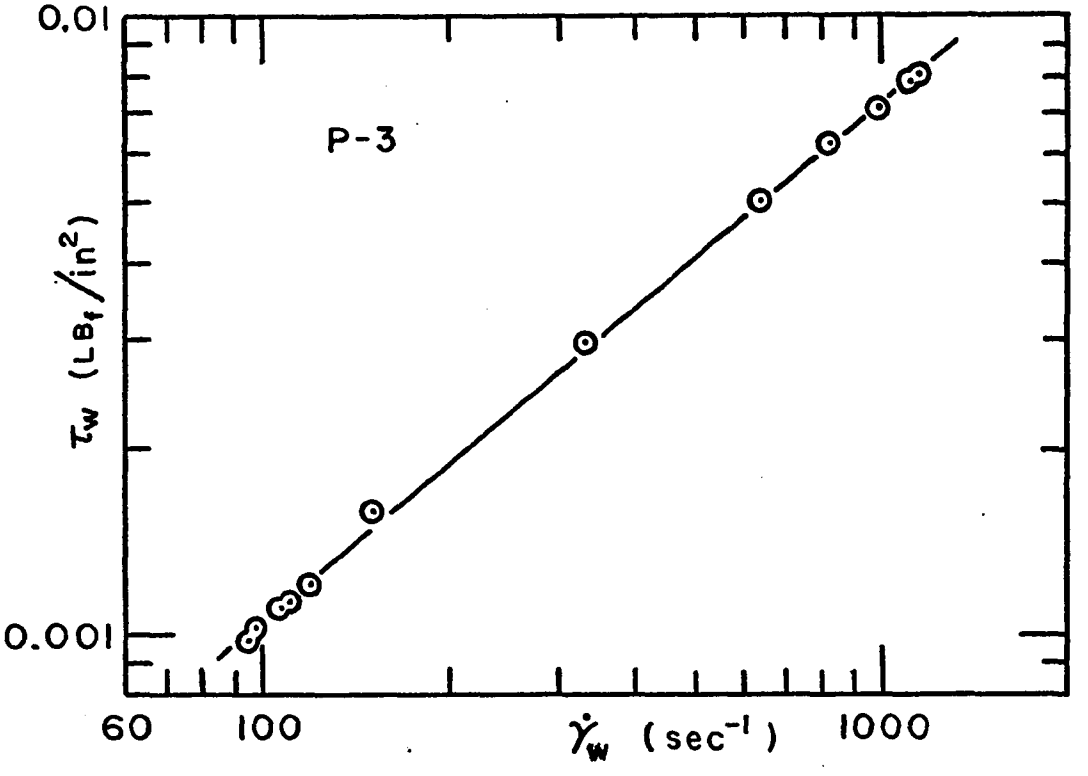

Fig. 3.19. Flow Curves for Polyox

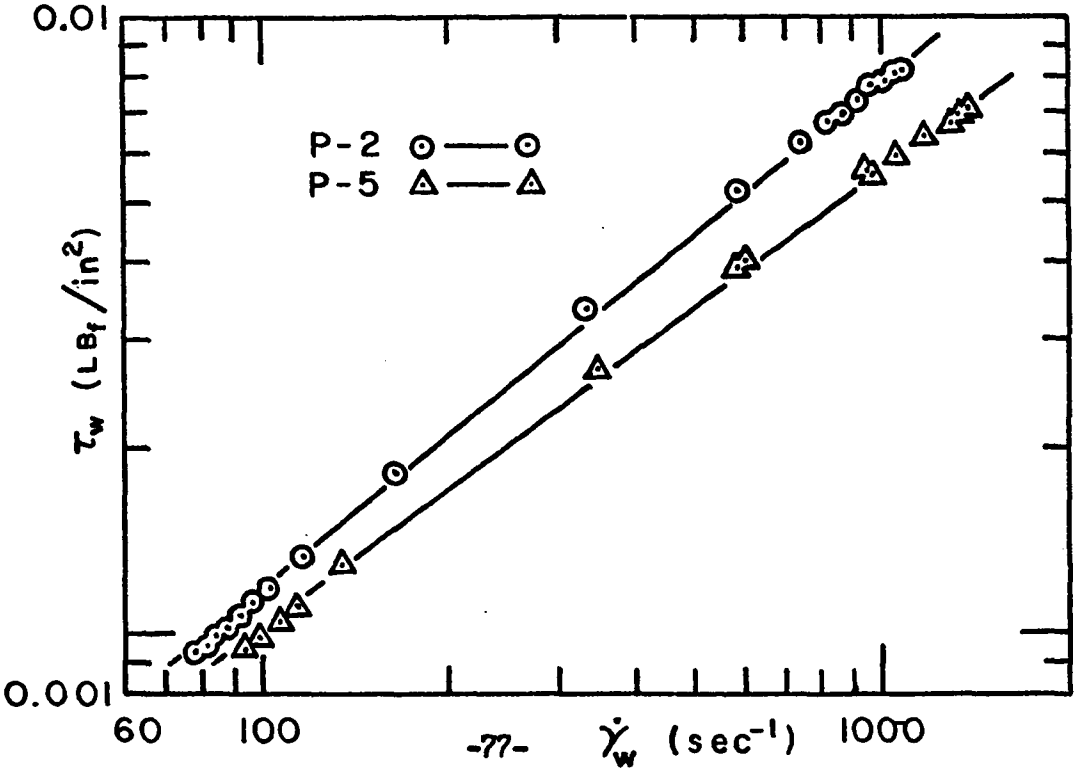

Fig. 3.20. Flow Curves for Polyox

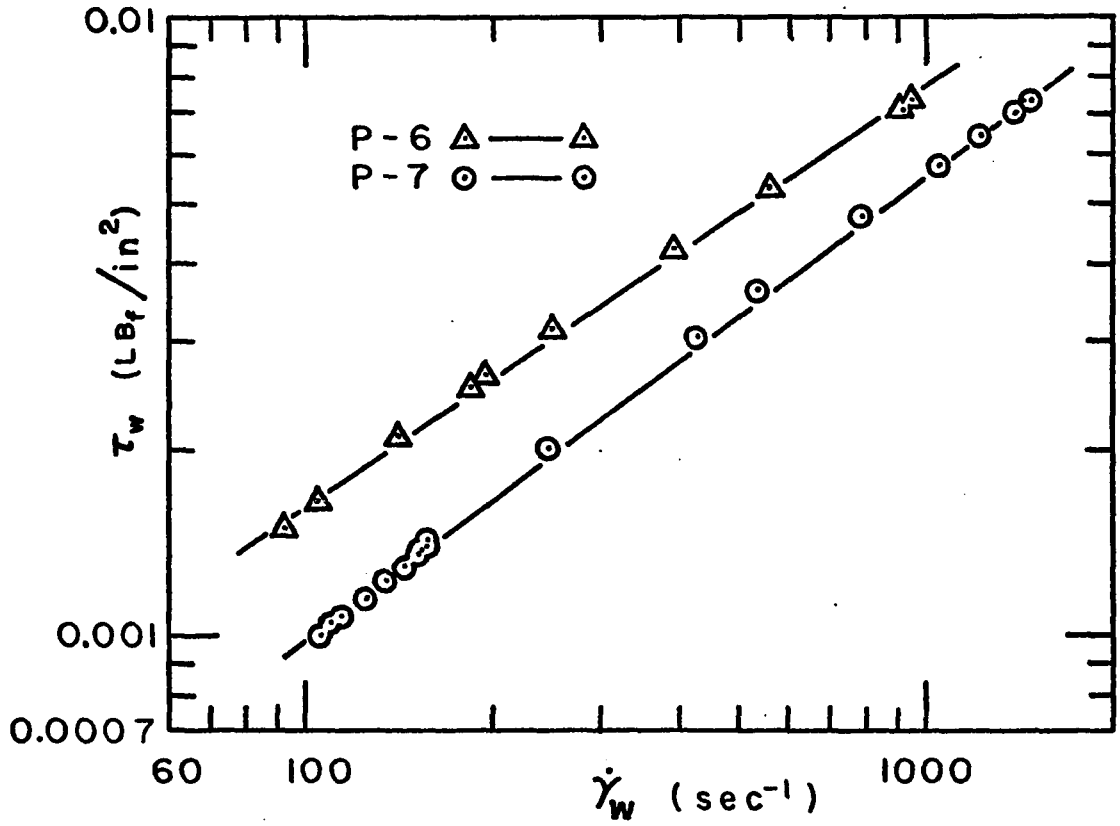

power-law approximation for fluid flow behavior with a maximum deviation of ±6%.

Many systems were evaluated as possible inelastic non-Newtonian fluids. Suspensions of spray-dried polyvinyl chloride with various water-ethylene glycol-glycerine solutions demonstrated Bingham fluid behavior which would have introduced large random errors in manometer readings. Mixtures of corn starch and ethylene glycol were shear thickening ($n>1.0$) but adsorption of moisture from the air led to particle swelling and thus unstable fluid properties. A high solids polystyrene latex (DL-860 from Dow Chemical) was found insufficiently non-Newtonian ($n = 0.88$). Also, this latex was unsuitable for testing in the apparatus of this study because of its toxicity and a tendency to coat surfaces, such as manometer tubes. Most polymer-water solutions (Polyox, Separan, Carbopol, and high molecular weight grades of Methocel) were unacceptable because of elasticity. Exceptions to this are solutions of low molecular weight grades of Methocel that form inelastic non-Newtonian aqueous solutions. Also Polyox solutions, which are very shear sensitive, may be rendered inelastic by shear degradation.

Entrance loss measurements for non-Newtonian fluids are limited by the extent of applicability (about an order of magnitude of shear rate) of the power-law approximation. This restricts the range of N_{Re} that can be studied. Other forms of the viscosity function, $\mu=\mu(\dot{\gamma})$, are available, but these

introduce additional parameters which complicate correlations with ΔP_{ent}. It is also noteworthy that the linear flow curves in Fig. 3.14-3.20 represent average flow indices over the shear rates studied. This will be a source of additional (slight) error in correlating K and K' with n.

A plot of friction factor vs. Reynolds number appears in Fig. 3.21. N_{Re} is a generalized Reynolds number,

$$N_{Re} = \frac{2\rho D^n (2v)^{2-n}}{\kappa (3 + 1/n)^n}$$

The excellent agreement of data with $f = 16/N_{Re}$ substantiates the experimental technique employed and indicates that the average n obtained from each flow curve was a good approximation.

Elasticity of a polymer solution results from having sufficient molecular entanglement so that rearrangement cannot occur within the time scale of deformations. This will depend on a combined level of molecular weight and concentration. Although it is doubtful if elasticity can be entirely eliminated, it can be reduced to a level undetectable and hopefully uninfluential, by lowering polymer concentration and/or molecular weight. In this study, Polyox-water solutions were subjected to high shear which effected a degradation of molecular weight. Methocel-water solutions of moderate molecular weight were diluted until elasticity disappeared.

All fluids were evaluated for elasticity in terms of their ability to recoil after an applied stress was suddenly released

Filmed as received

without page(s) 81 .

UNIVERSITY MICROFILMS.

Fig. 3.21. Representative Friction Factor-Reynolds Number Data

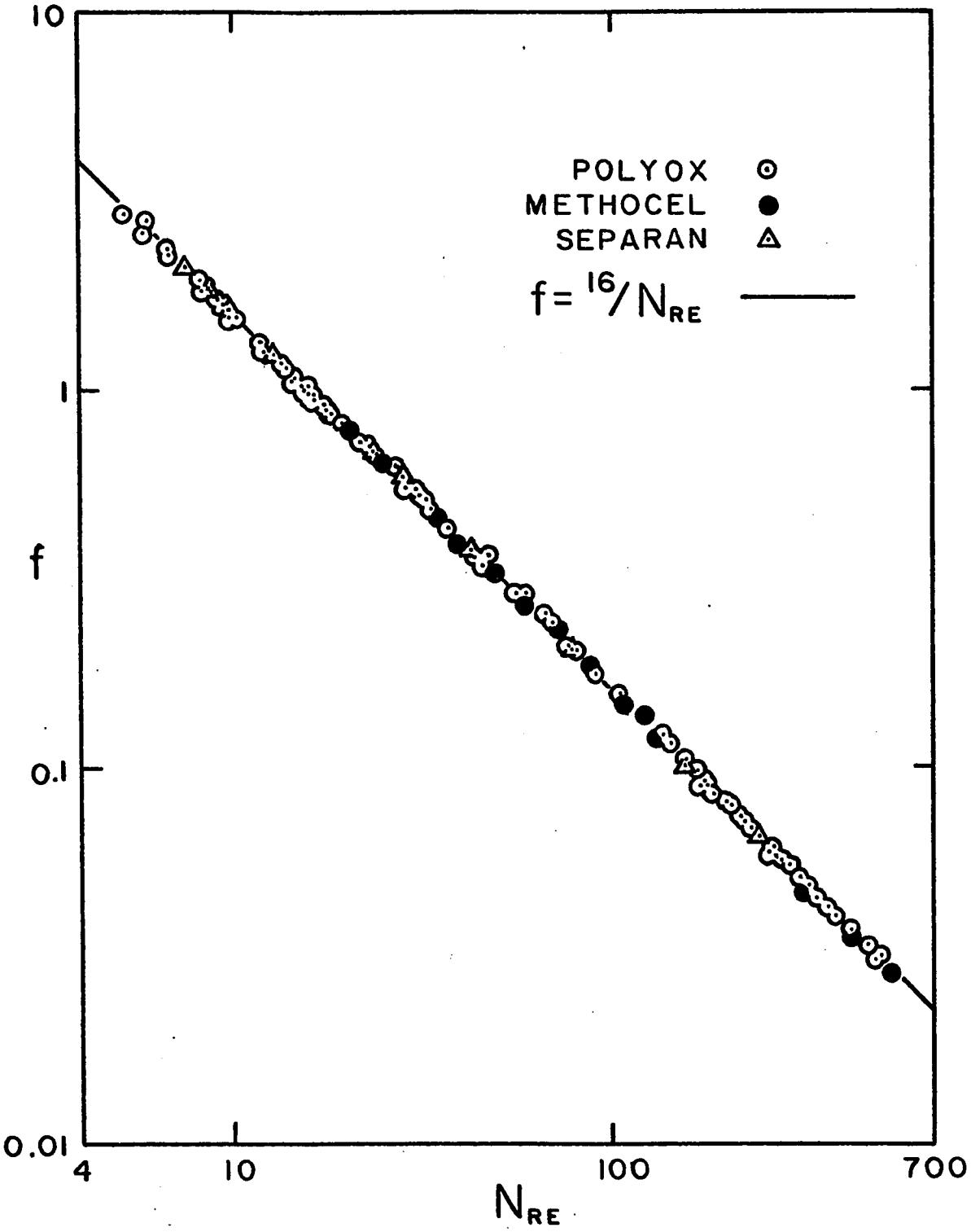

This method provided a qualitative means of comparing and determining levels of fluid elasticity. Loss of elasticity with respect to shear degradation time (Polyox) or concentration (Methocel) is presented in Fig. 3.22. Arrows on the plots indicate the times or concentrations at which fluids were used for testing. For the Polyox solutions, attempts to model loss of elasticity failed because degradation was caused by both continuous operation of a pump and random operation of a high speed mixer. Thus, no curves were drawn through the points in Fig. 3.22, and the times refer only to hours of pumping.

Both shear degraded Polyox (40) and dilute solutions of Methocel (9) have been found to be inelastic by other workers who determined this by observing zero normal stress differences with a rheogoniometer. Kobayashi and Tomita (40) have shown that a 2% Polyox 10N (molecular weight = 10^5) solution can be shear degraded to a level of undetectable elasticity. A grade of Polyox with a larger molecular weight (4×10^6 as used in this work) would require more shearing, perhaps even to a lower average molecular weight than in the inelastic Polyox 10N solution, to achieve inelasticity. It is noteworthy that pituitousness[1] had disappeared, indicating loss of elasticity (68), from all Polyox solutions before shearing was terminated. Bodger and Rama Murthy (9) ceased to observe normal stresses, and thus elasticity, when they diluted a Methocel 90HG solution such that the flow index was larger than 0.58. Although

---

1. Tendency of a material to form strings or filaments as an immersed object is withdrawn from it.

Fig. 3.22. Recoil vs. Shear Degradation Time for Polyox and Recoil vs. Concentration for Methocel

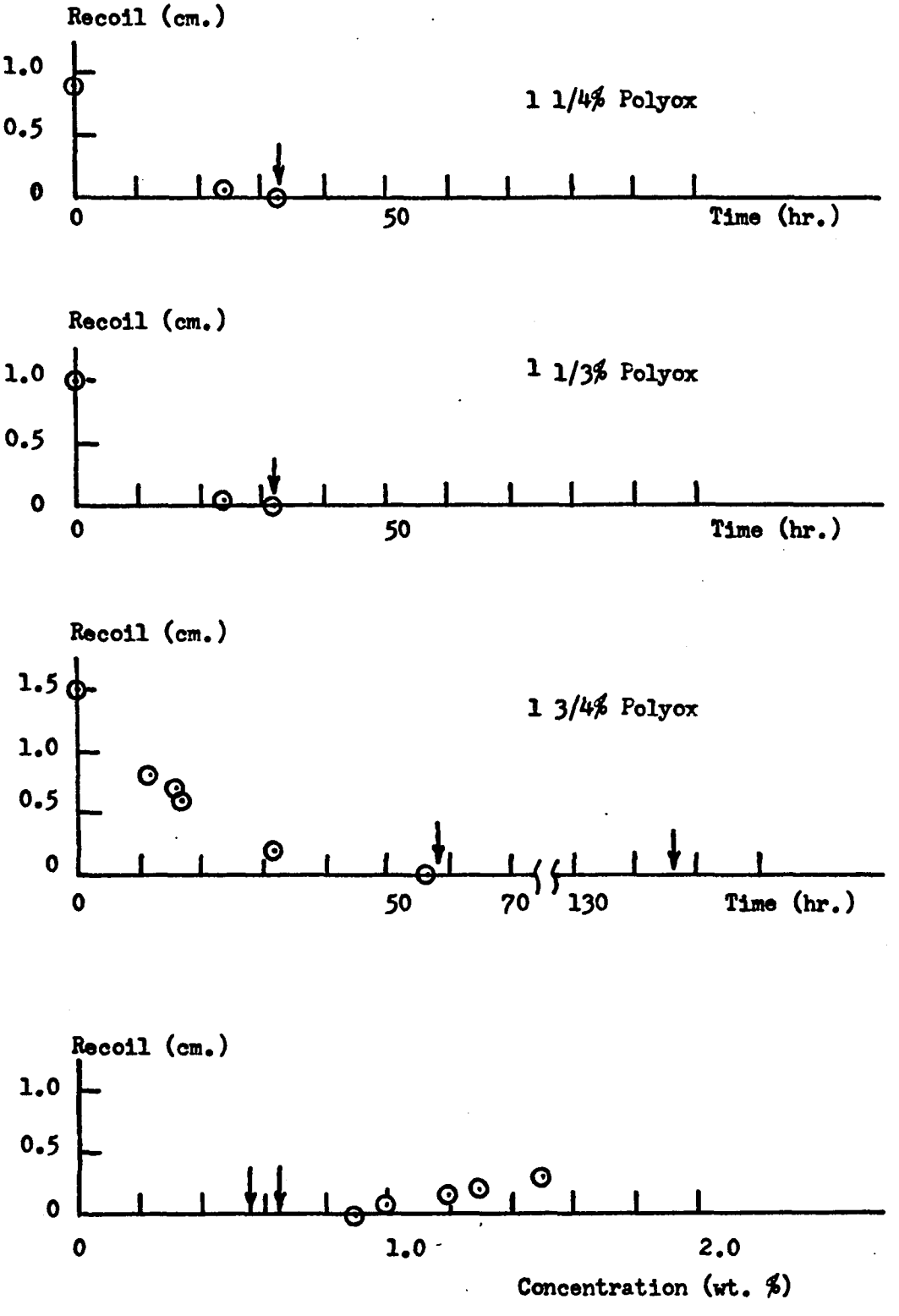

recoil tests stopped detecting elasticity at about n = 0.55, the lowest flow index for Methocel in this study is n = 0.62.

It is possible that this recoil test is less sensitive than a rheogoniometer in determining qualitative levels of elasticity. Consequently, most fluids were diluted or degraded beyond where elasticity became undetectable. That the test fluids were effectively inelastic is demonstrated in Fig. 3.32 and 3.33 showing good agreement of data describing K = K(n) and K' = K'(n). Still, the recoil test should be studied to determine comparisons with rheogoniometer data. Perhaps a theoretical description of recoil may lead to quantitative measurements of elasticity in dilute polymer solutions. This test has merit in being simple and quick.

Correlation of ΔP_{ent} with the contraction ratio, β, for Newtonian fluids indicated that with 4% error a geometry having $\beta = 0.25$ could be approximated by an infinite contraction. Assuming this applicable to inelastic non-Newtonian fluids, data collected at $\beta = 0.041$ were assumed representative of $\beta = 0$. To gain insight to the relationship between β and n, ΔP_{ent} was also measured at $\beta = 0.636$.

Plots of $\frac{\Delta P_{ent}}{\rho v^2/2g_c}$ vs. N_{Re} for $\beta = 0.041$ appear in Fig. 3.23-3.29 and for $\beta = 0.636$ in Fig. 3.30 and 3.31. The close correlation between data and the line drawn from

$$\frac{\Delta P_{ent}}{\rho v^2/2g_c} = K + K'/N_{Re} \qquad (1.18)$$

Fig. 3.23. Entrance Pressure Loss for Inelastic Non-Newtonian Methocel Flowing through a Sudden Contraction with $\beta = 0.041$

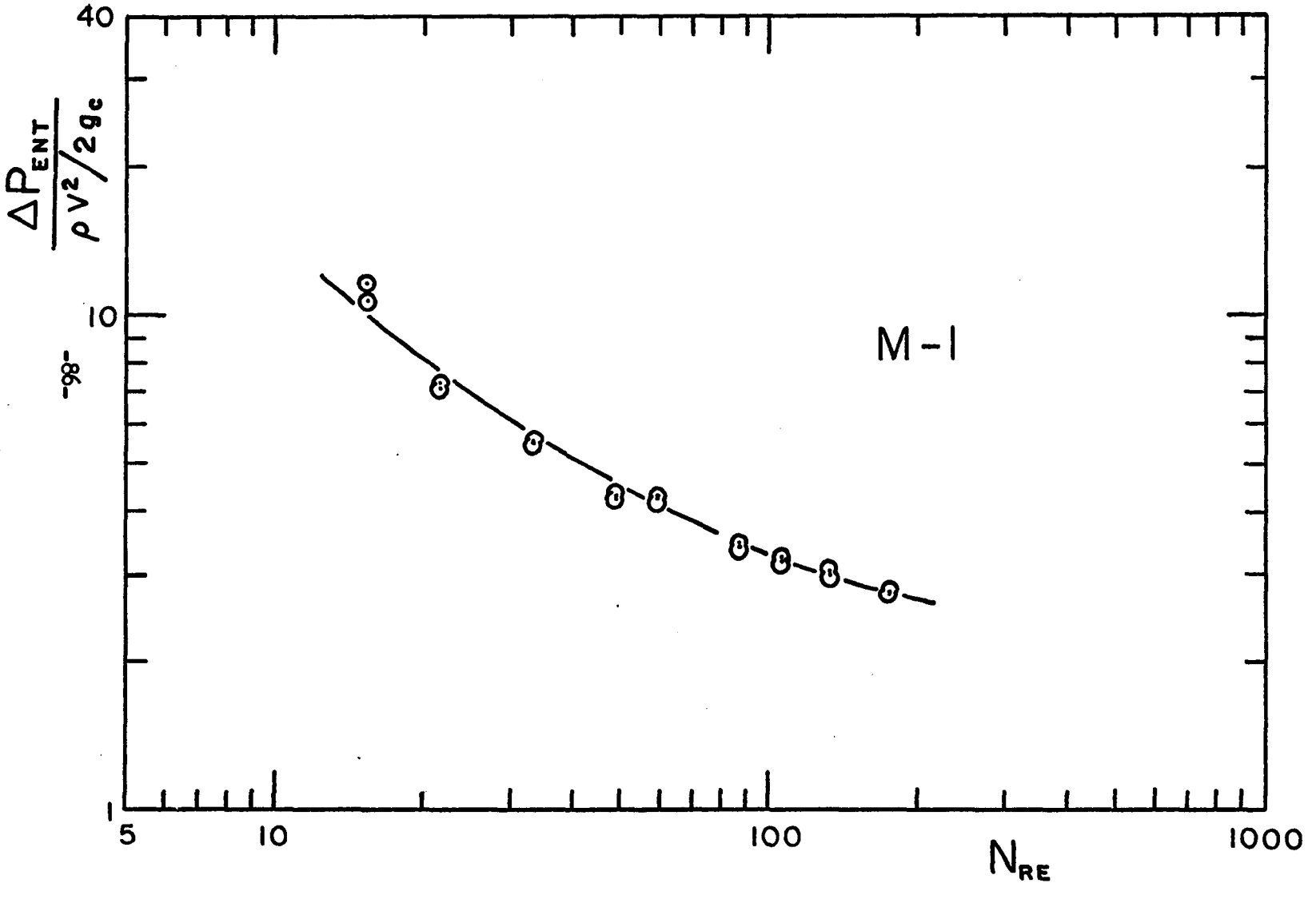

Fig. 3.24. Entrance Pressure Loss for Inelastic Non-Newtonian Methocel Flowing through a Sudden Contraction with $\beta = 0.041$

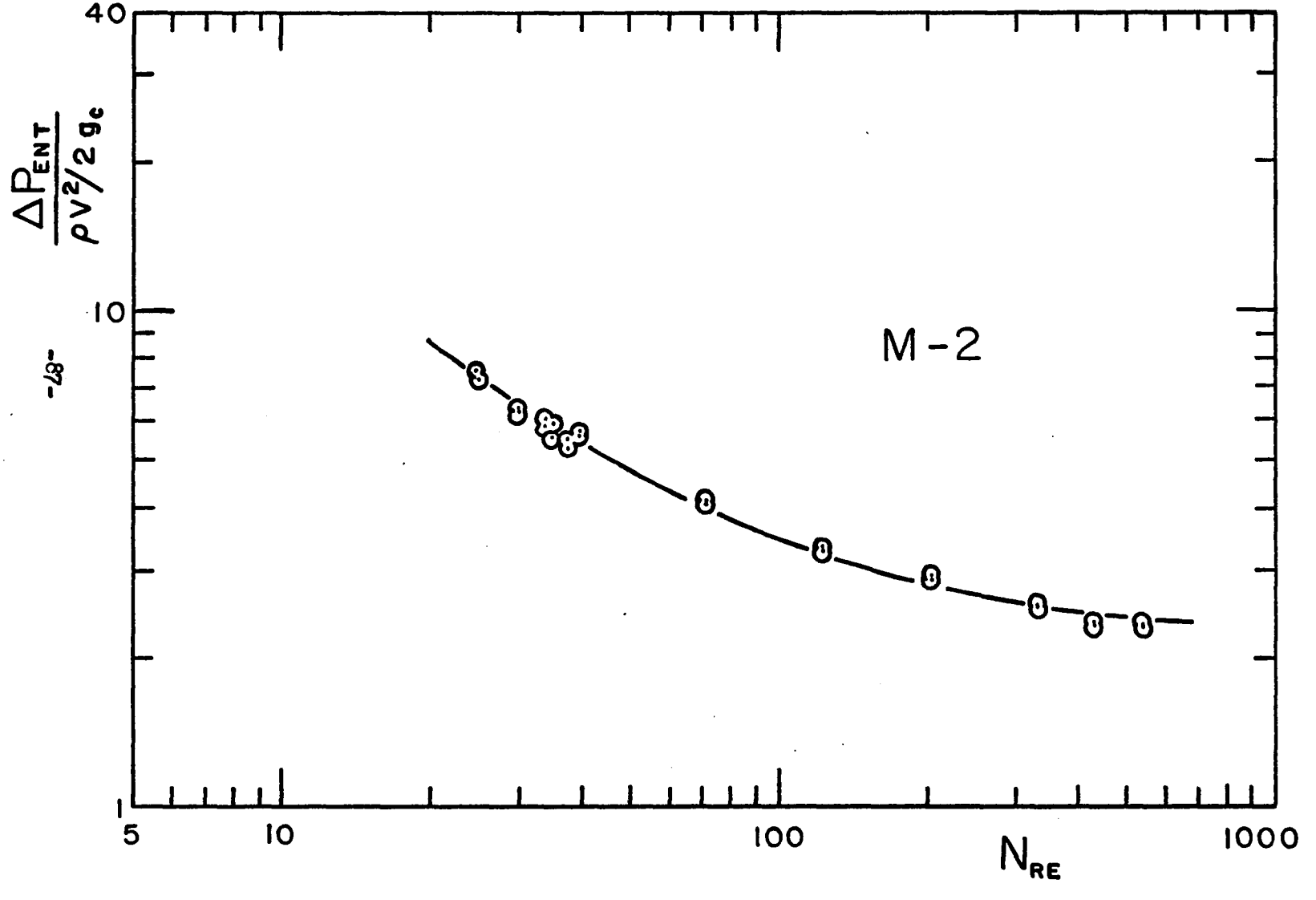

Fig. 3.25. Entrance Pressure Loss for Inelastic Non-Newtonian Polyox Flowing through a Sudden Contraction with $\beta = 0.041$

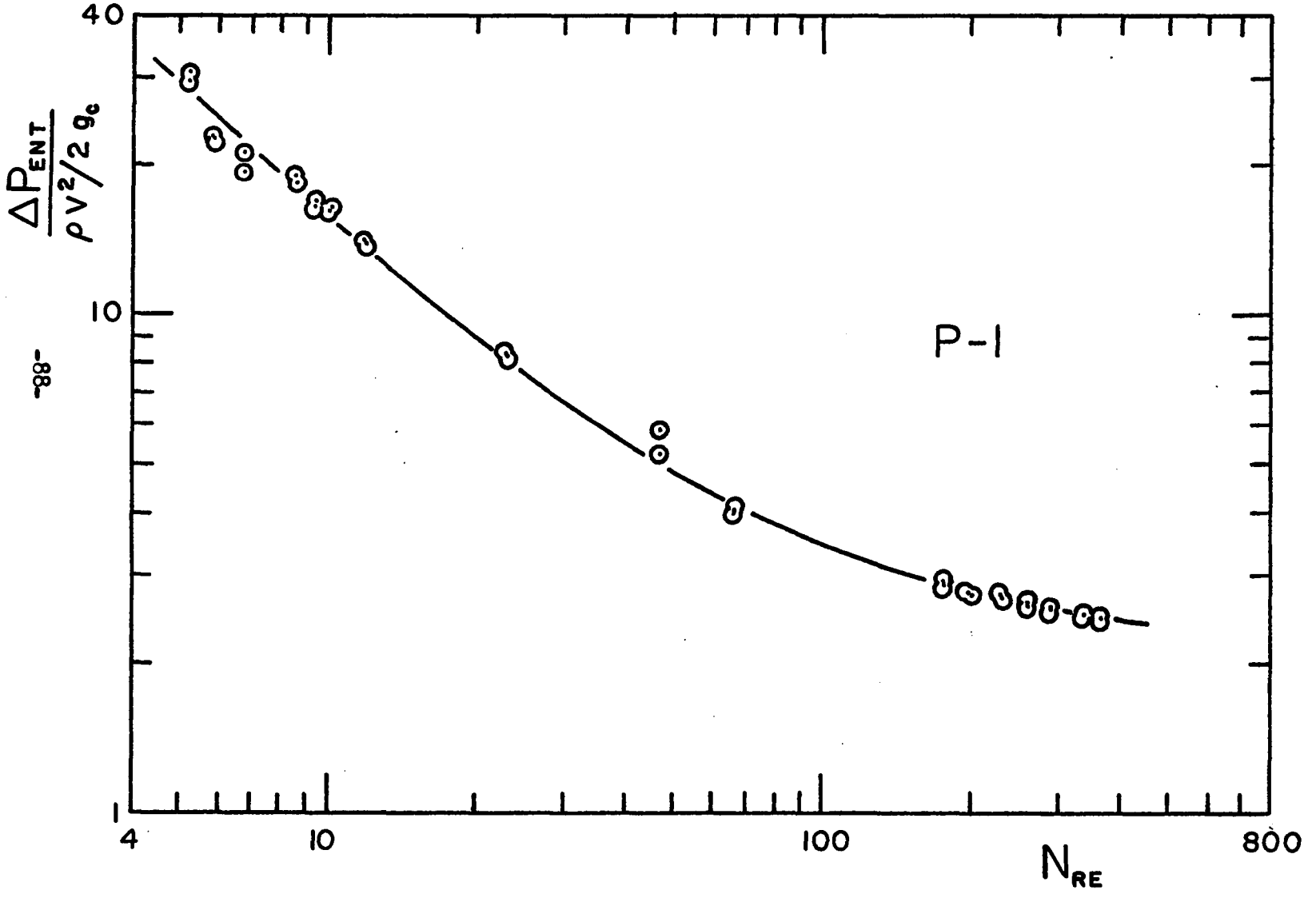

Fig. 3.26. Entrance Pressure Loss for Inelastic Non-Newtonian Polyox Flowing through a Sudden Contraction with β =0.041

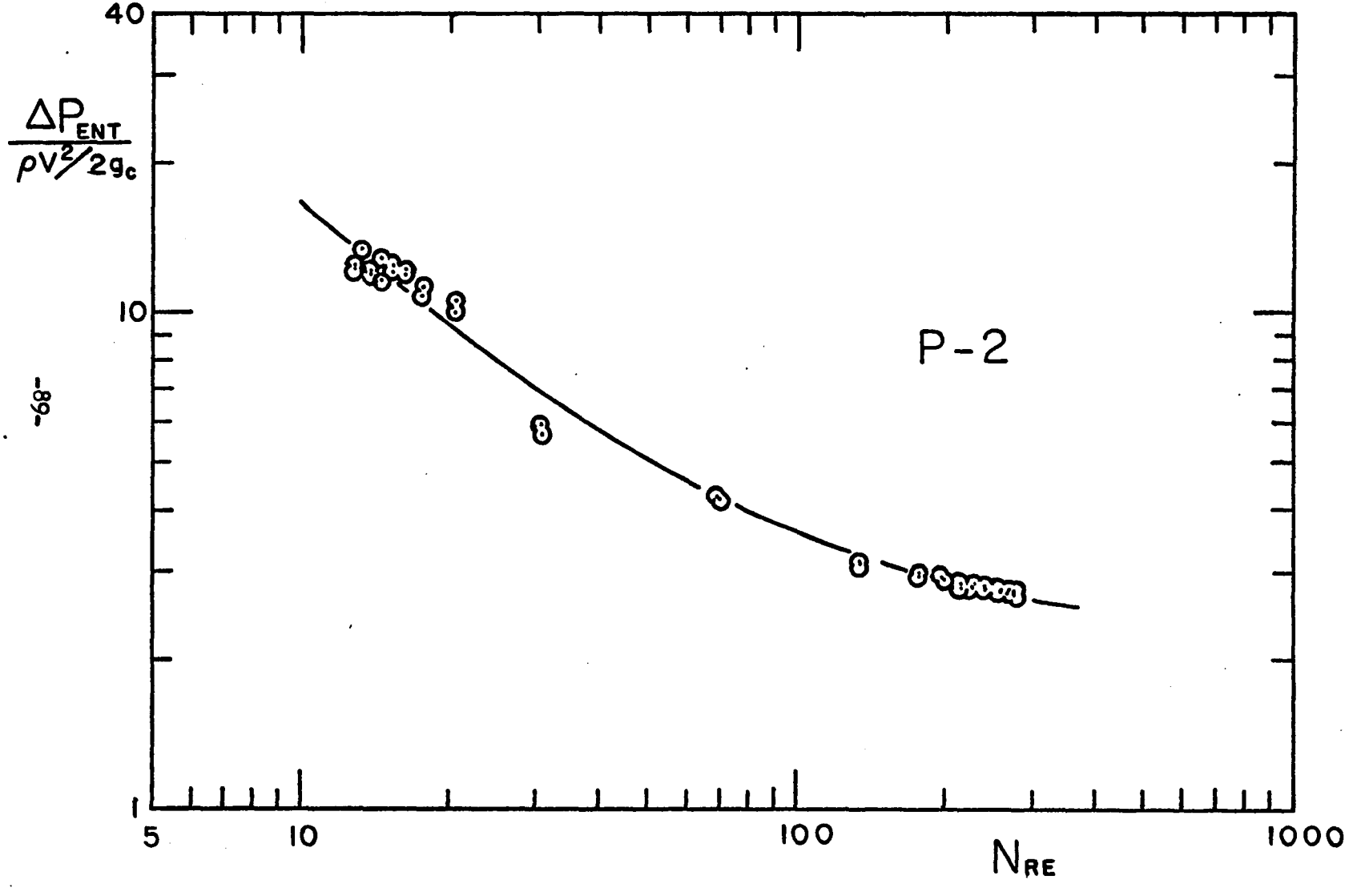

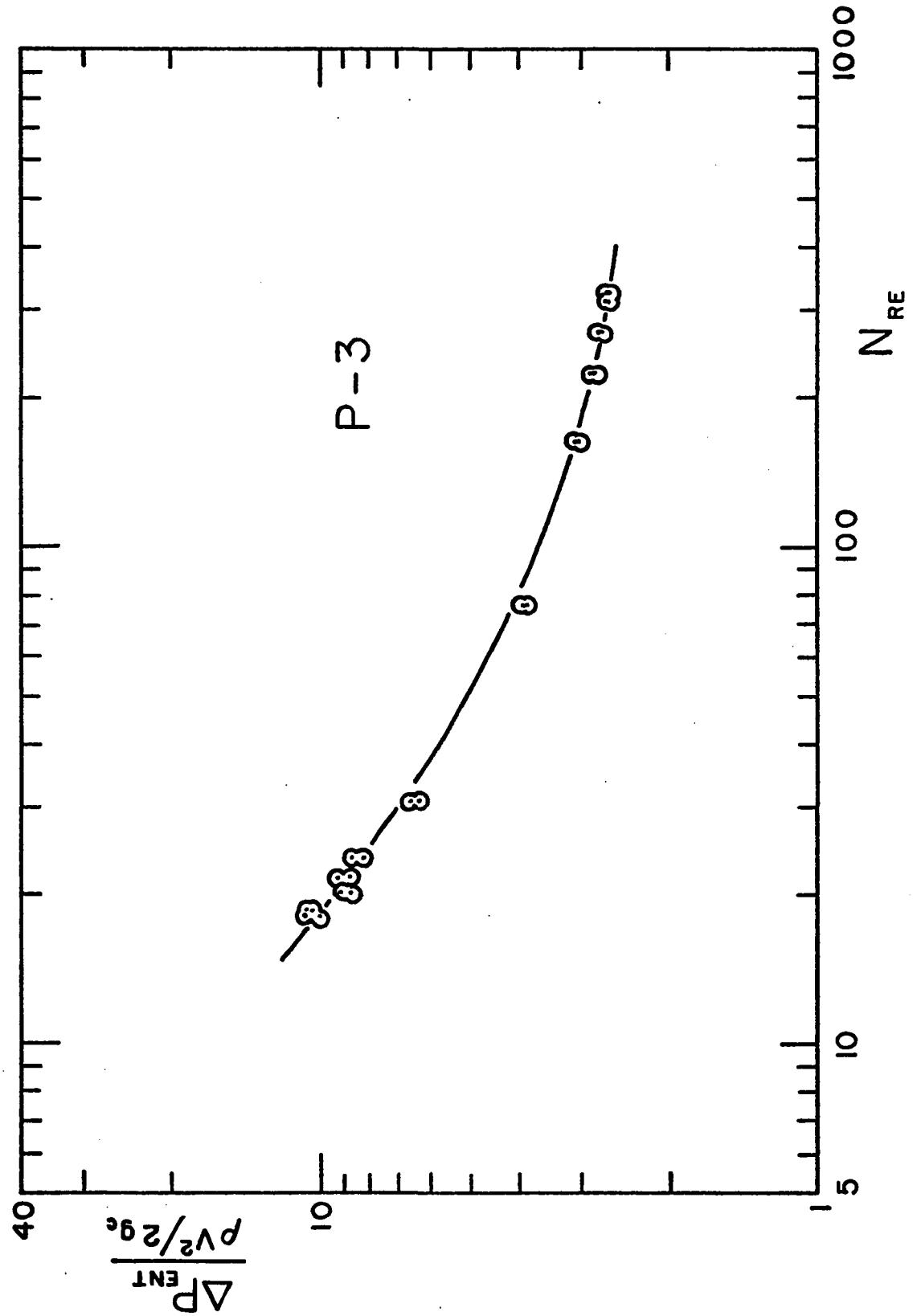

Fig. 3.27. Entrance Pressure Loss for Inelastic Non-Newtonian Polyox Flowing through a Sudden Contraction with $\beta = 0.041$

Fig. 3.28. Entrance Pressure Loss for Inelastic Non-Newtonian Polyox Flowing through a Sudden Contraction with β=0.041

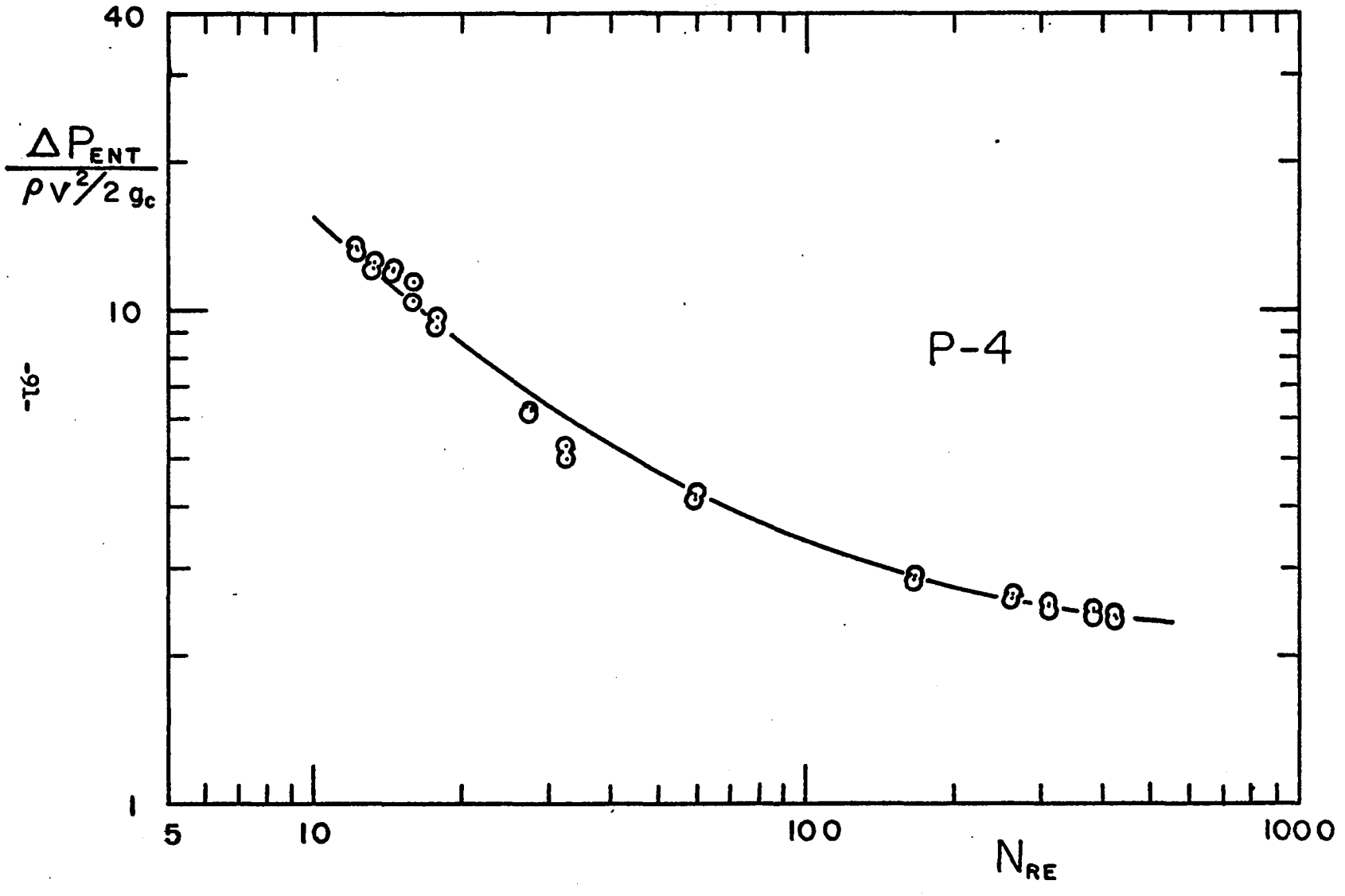

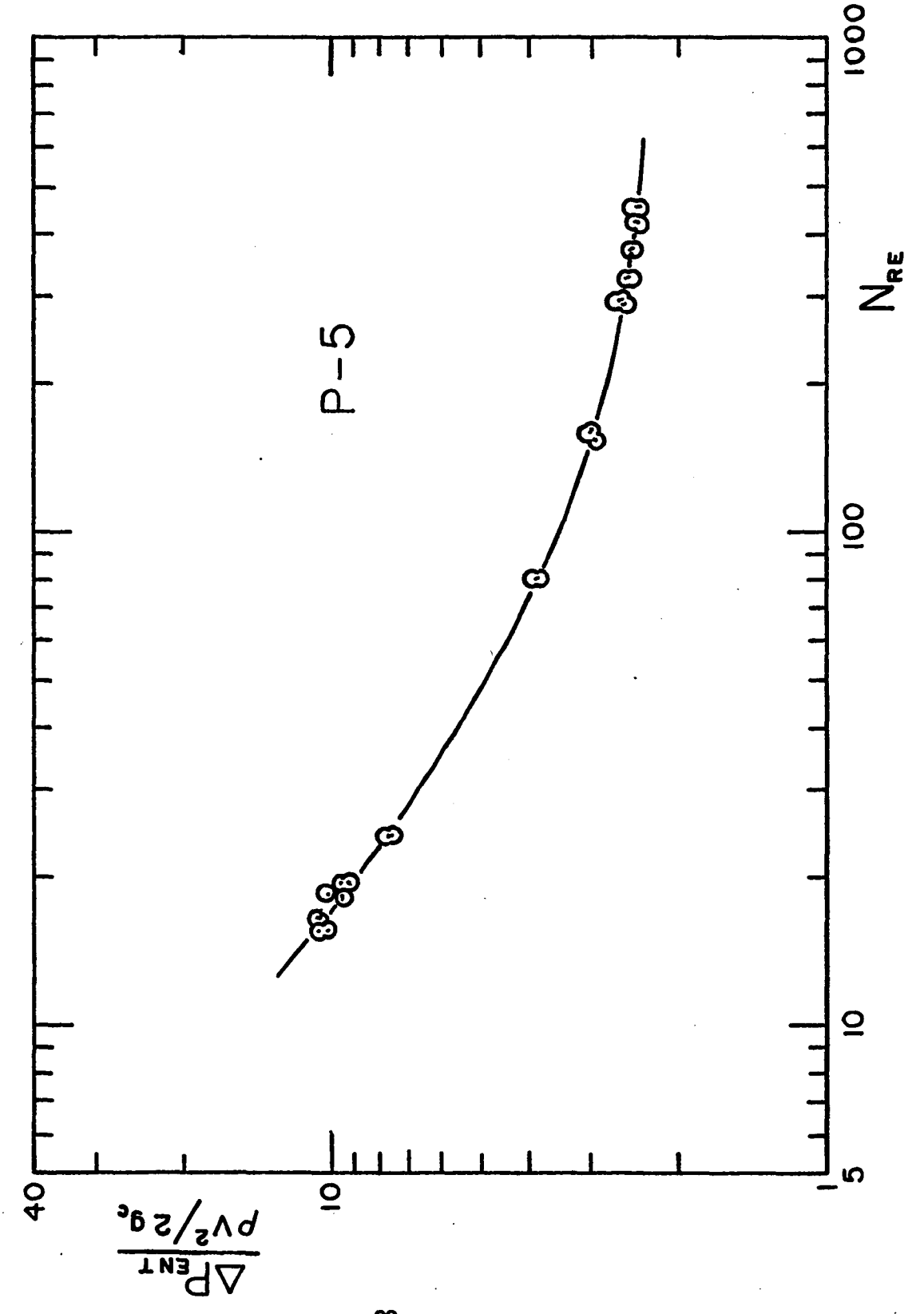

Fig. 3.29. Entrance Pressure Loss for Inelastic Non-Newtonian Polyox Flowing through a Sudden Contraction with β=0.041

Fig. 3.30. Entrance Pressure Loss for Inelastic Non-Newtonian Polyox Flowing through a Sudden Contraction with β=0.636

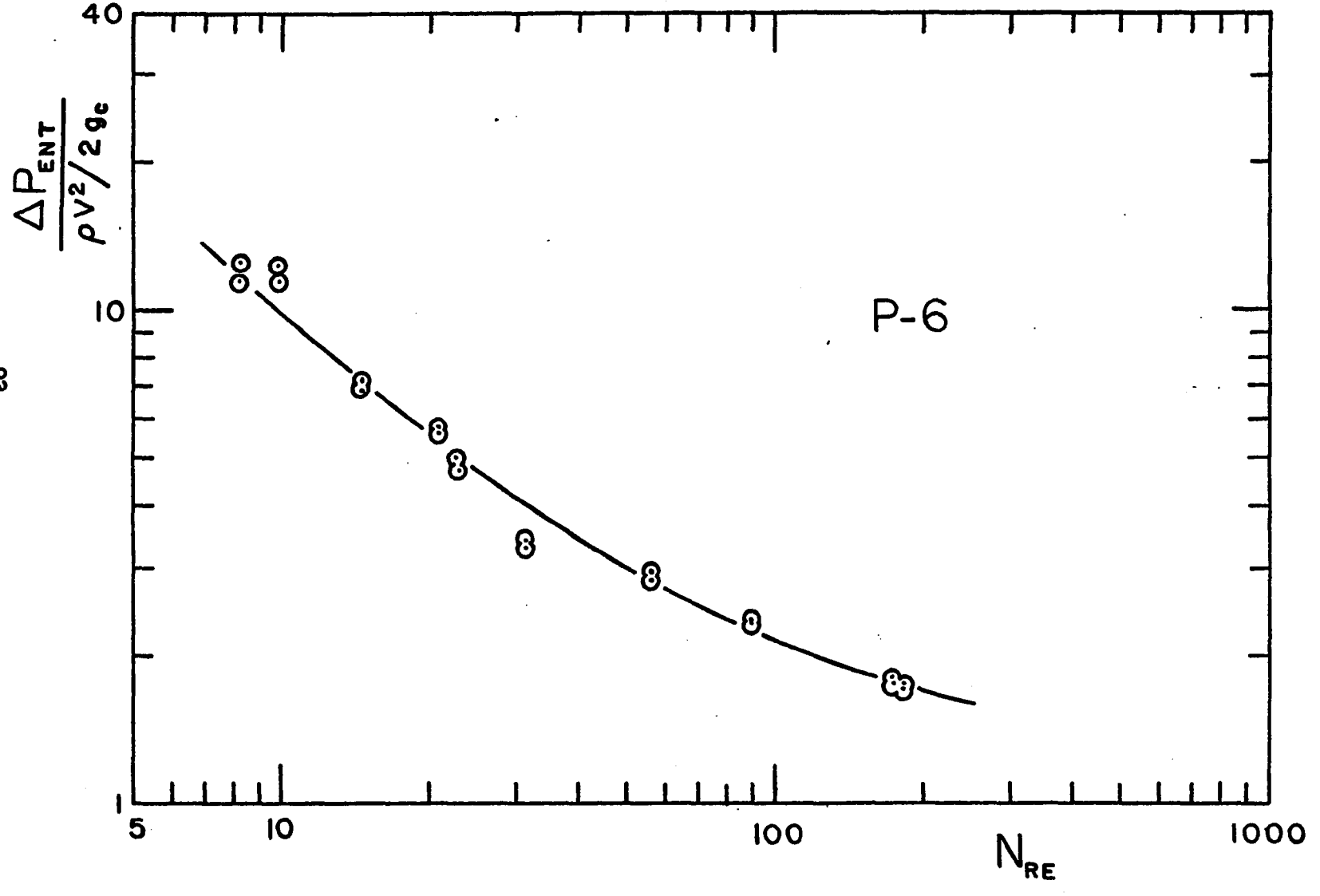

Fig. 3.31. Entrance Pressure Loss for Inelastic Non-Newtonian Polyox Flowing through a Sudden Contraction with $\beta = 0.636$

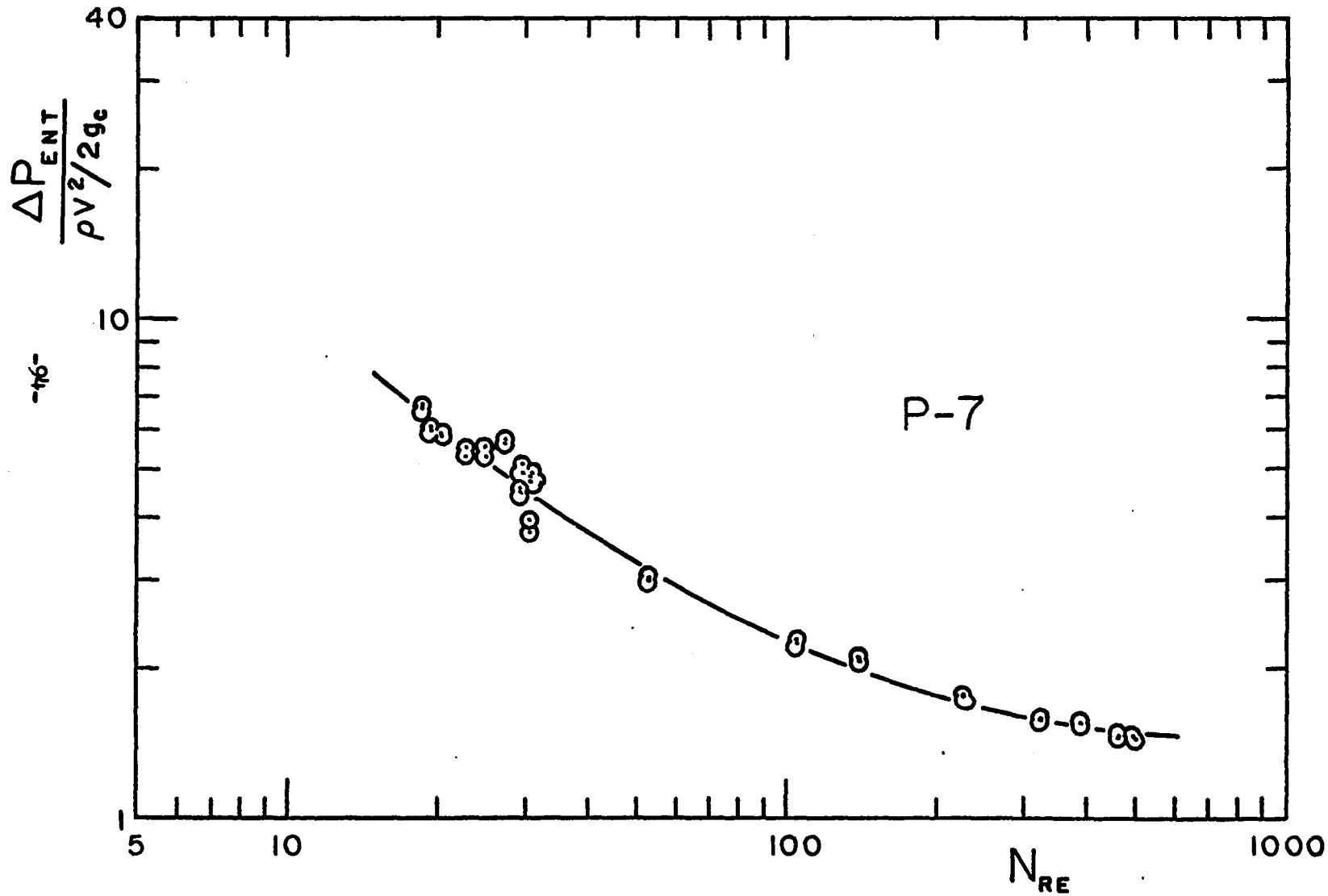

supports the validity of this expression for describing purely viscous entrance losses. Values of K and K' from these curves appear in Table 3.4 and are plotted vs. the power-law index, n, in Fig. 3.32 and 3.33. The data for the kinetic energy correction, K, at $\beta = 0.041$ agree very well with the predictions of Collins and Schowalter (20) and Sestak and Charles (57), but are larger (by about 7%) than Bogue (10) and Tomita (66). These data, although uniformly larger by about 4%, agree with the data of Bodger and Rama Murthy (9) within experimental error. The only comparison with the K' data is the work of Astarita et al. (4) which agrees neither in magnitude nor in variation with n. Reasons for this are not clear, but it is noteworthy that Astarita et al. (4) and Astarita and Greco (3) have published results that greatly disagree with all others.

Within experimental error, the data for K and K' vs. n can be represented by straight lines. For $\beta = 0.041$ which should be comparable to $\beta=0$

$$K = 0.70n + 1.62 \tag{3.5}$$

$$K' = 97n + 64 \tag{3.6}$$

and for $\beta = 0.636$

$$K = 0.25n + 1.13 \tag{3.7}$$

$$K' = 7n + 88 \tag{3.8}$$

Table 3.4. Entrance Loss Parameters for Non-Newtonian Fluids

Series	n	K	K'
M-1	0.63	2.04 ± .05	123 ± 20
M-2	0.71	2.14 ± .05	132 ± 20
P-1	0.67	2.13 ± .05	136 ± 20
P-2	0.83	2.18 ± .05	144 ± 20
P-3	0.84	2.20 ± .05	145 ± 20
P-4	0.67	2.08 ± .05	130 ± 20
P-5	0.75	2.13 ± .05	138 ± 20
P-6	0.67	1.26 ± .05	87 ± 20
P-7	0.75	1.29 ± .05	98 ± 20
S-1	0.42	2.57 ± .05	105 ± 20

Fig. 3.32. K vs. Power-Law Index

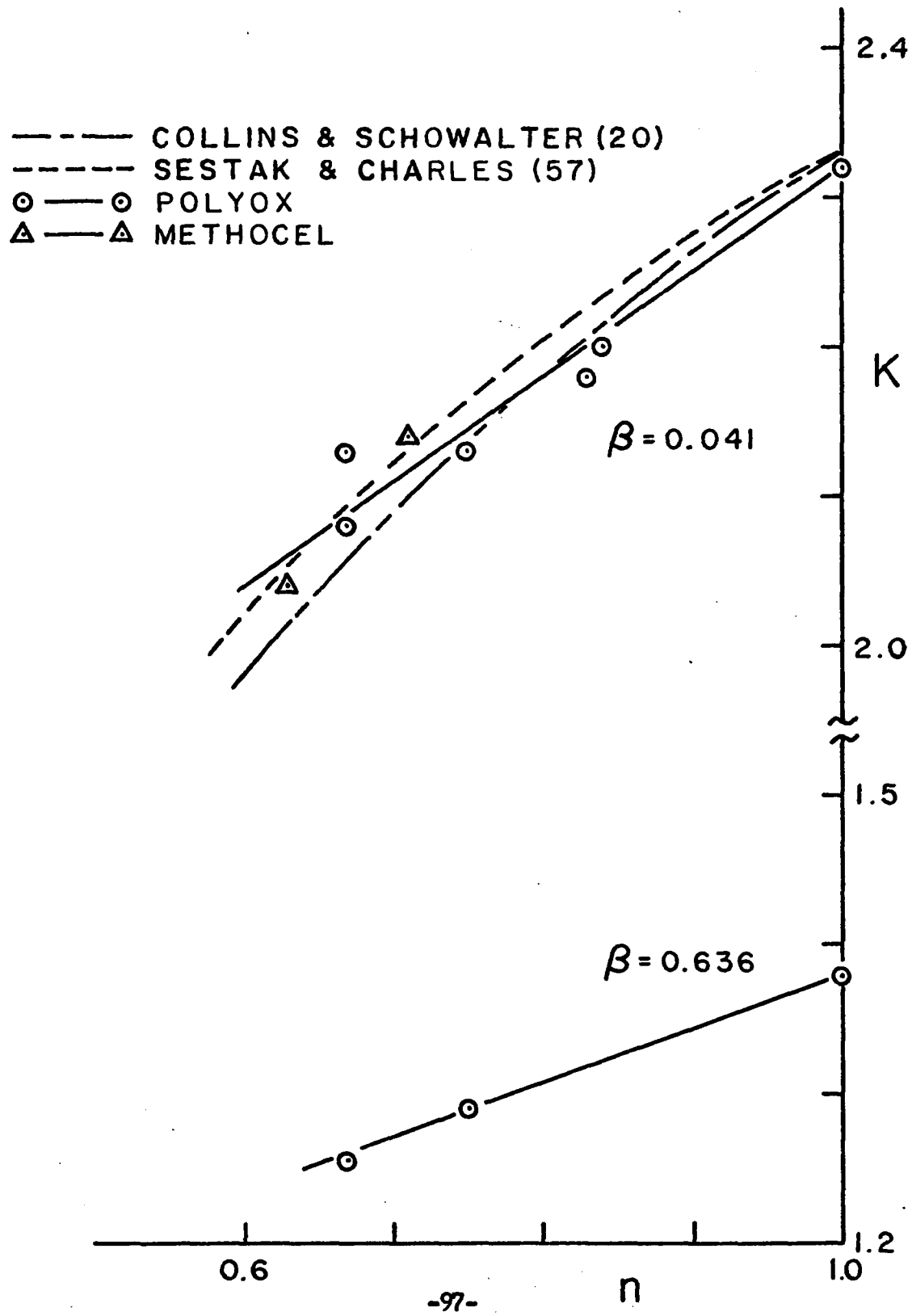

Fig. 3.33. K' vs. Power-Law Index

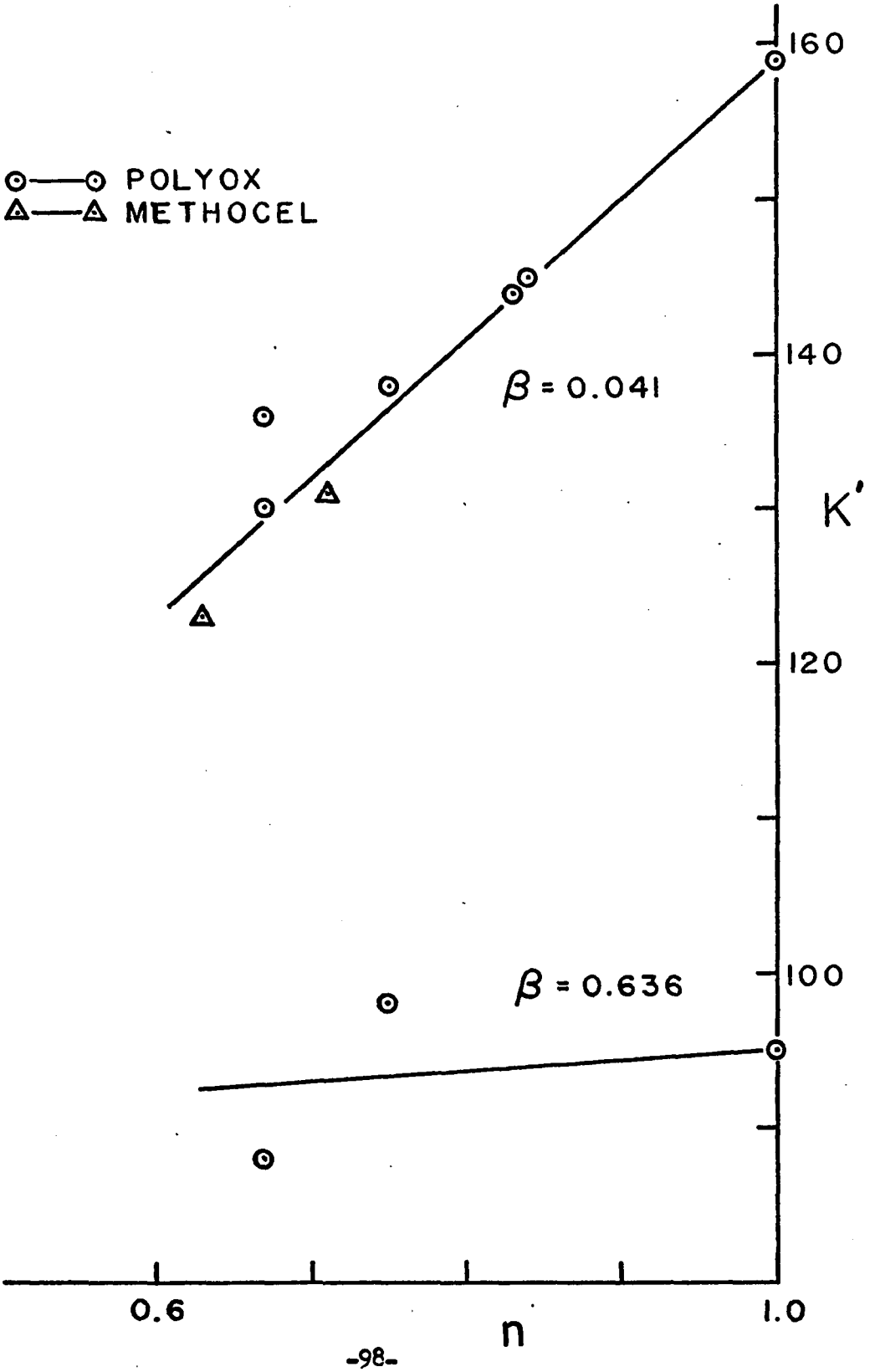

Taking the $(1-\beta^2)$ dependence at n = 1 gives equations of K(n) and K'(n)

$$K = 0.28n + 0.65$$

$$K' = 39n + 26$$

that disagree with those measured at $\beta = 0.636$. For $n > 0.6$ this suggests a form of K and K'

$$K = 0.70n\, f_{11}(\beta,n) + 1.62\, f_{12}(\beta,n) \qquad (3.11)$$

$$K' = 97n\, f_{21}(\beta,n) + 64\, f_{22}(\beta,n) \qquad (3.12)$$

such that at n = 1 the functions $f_{ij}(\beta,n)$ simplify to

$$f_{ij}(\beta,1) = 1 - \beta^2 \qquad (3.13)$$

Data at two values of β do not provide enough information to predict the $f_{ij}(\beta,n)$. However, these data offer a beginning and a comparison for future work. Descriptions of ΔP_{ent} over wider ranges of n, as indicated by Bogue (10) and others (20, 57, 66) will require K(n) and K'(n) nonlinear in n. Unless as part of describing the viscous component of ΔP_{ent} for an elastic fluid, determination of K(n) and K'(n) for $n < 0.6$ may be of little practical interest, because as this study, Bodger and Rama Murthy (9) and Kobayashi and Tomita (40) indicate, $n \approx 0.6$ may be close to the minimum for inelastic fluids. As an intermediate step in obtaining the complete $K(\beta,n)$ and $K'(\beta, n)$, research on ΔP_{ent} could attempt determining the $f_{ij}(\beta,n)$.

One elastic fluid, a Separan-water solution with recoil = 0.5 cm., was tested yielding values of K = 2.56 and K' = 102 at n = 0.42. These data appear in Fig. 3.34. At n = 0.42, Sestak and Charles (57) predict K = 1.78[1] and extrapolating the K' data yields K' = 105, showing that an elastic contribution is appearing in K. Assuming the empirical correlation in (3.6) to be valid at n = 0.42, elasticity had no effect on K'. This appears unusual. Sylvester (62) has observed elasticity contributing to both K and K' and others (25, 40, 46, 48, 50) have demonstrated it should increase ΔP_{ent}. However, elasticity has also been shown to have a negative (9) and a mixed (40, 42) influence on ΔP_{ent} which suggests the Separan data are possible. Collectively, past work well establishes that ΔP_{ent} has a complex dependence on fluid elasticity. This is further complicated by lack of a means to determine fluid elasticity accurately in dilute polymer solutions. The recoil test offers a qualitative measure which could answer this if given quantitative significance. But regardless of method employed, until ΔP_{ent} can be quantitatively related to fluid elasticity, additional data on elastic fluids will only serve to demonstrate differences.

---

1. Extrapolating the K data to n = 0.42 yields K = 1.91.

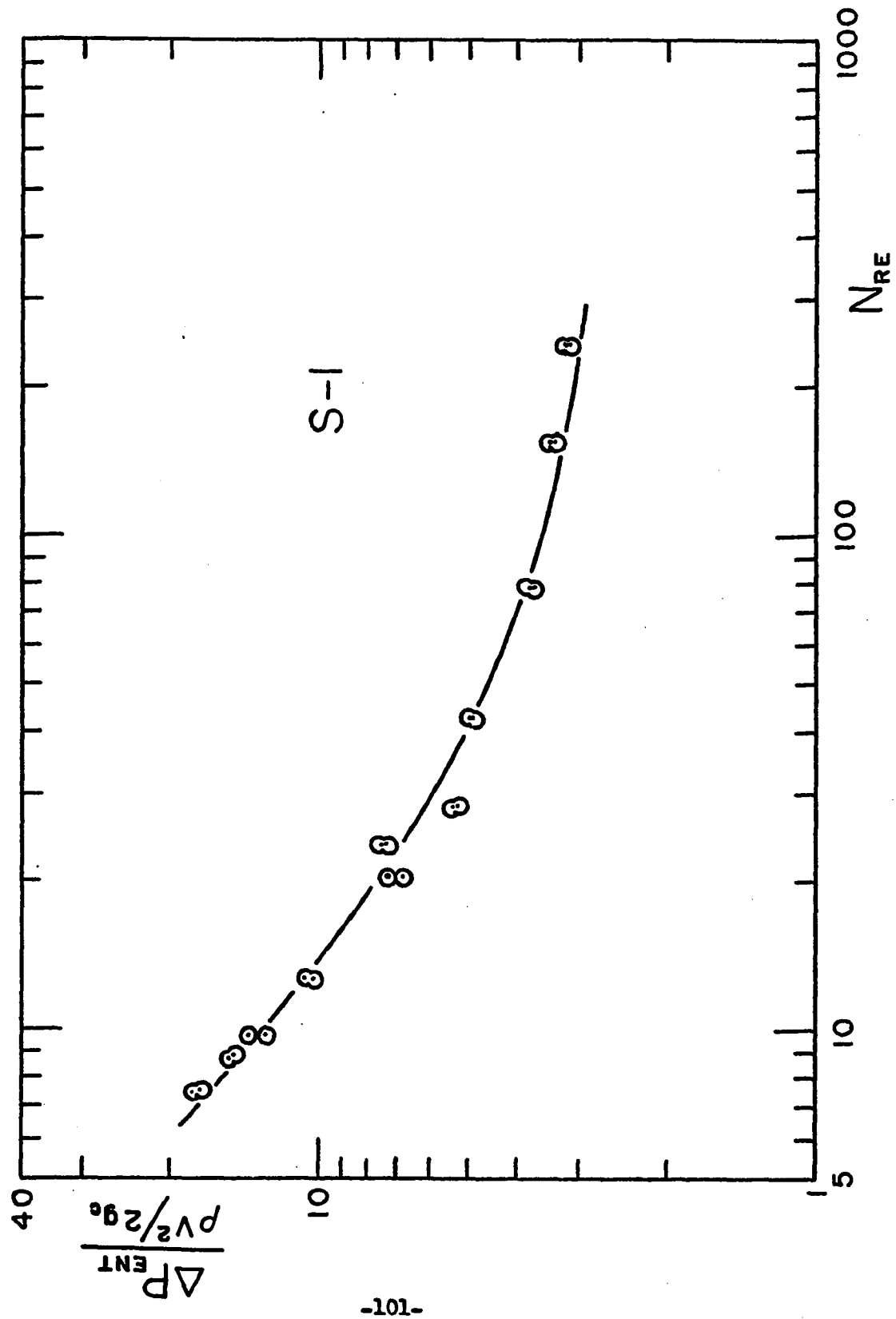

Fig. 3.34. Entrance Pressure Loss for Separan Flowing through a Sudden Contraction with $\beta = 0.041$

CONCLUSIONS

1. Entrance pressure losses for inelastic fluids flowing through a sudden contraction can be described by

$$\frac{\Delta P_{ent}}{\rho v^2/2g_c} = K(n,\beta) + \frac{K'(n,\beta)}{N_{Re}}$$

2. For Newtonian fluids flowing through a sudden contraction, K and K' have been correlated with the contraction ratio, β, according to:

$$K = 2.32 \pm 0.05(1-\beta^2)$$

$$K' = 159 \pm 20(1-\beta^2)$$

3. When Newtonian fluids flow through a gradual ($\beta \approx 0$) contraction with angle α the kinetic energy parameter K remains unchanged within experimental error and the viscous loss correction attains a minimum at $\alpha = 65^\circ$ to 45°.

4. Inelastic fluids described by the power-law approximation yield ΔP_{ent} such that at $\beta = 0.041$ $(0.63 \leq n \leq 1)$

$$K = 0.70n + 1.62$$

$$K' = 97n + 64$$

and at $\beta = 0.636$

$$K = 0.25n + 1.13$$

$$K' = 7n + 88$$

5. There is a non-linear interdependence between n and β on the parameters K and K'.

RECOMMENDATIONS

1. Investigate the sensitivity of the viscous loss correction K' to variations in velocity profile development.

2. Obtain a comparison between the recoil test and normal stress differences as measured on a rheogoniometer.

3. Investigate the recoil test as a means of obtaining quantitative information about fluid elasticity.

4. Determine the relationship between ΔP_{ent} and elasticity.

5. Extend the data on inelastic fluids to obtain K and K' for $n < 0.6$ and for $n > 1.0$.

BIBLIOGRAPHY

1. Ackerberg, R. C., "The Viscous Incompressible Flow Inside a Cone," J. Fluid Mech., 21, 47 (1965).

2. Ashino, I., "On the Theory of the Additional Loss at the Pipe Entrance in Viscous Fluid (2nd Report, When An Entrance is Taper Type," Bul. J.S.M.E., 12, 522 (1969).

3. Astarita, G. and G. Greco, "Excess Pressure Drop in Laminar Flow through Sudden Contraction--Newtonian Liquids," I.E.C.Fund., 7, 27 (1968).

4. Astarita, G., G. Greco, and L. Peluso, "Excess Pressure Drop in Laminar Flow through Sudden Contraction--Non-Newtonian Liquids," I.E.C. Fund., 7, 595 (1968).

5. Bailey, F. D., J. L. Kucera, and L.G. Imhof, "Molecular Weight Relations of Poly(ethylene oxide)," J. Poly. Sci., 32, 517 (1958).

6. Ballenger, T. F., and J. L. White, "The Development of the Viscosity Field in Polymer Melts in a Reservoir Approaching a Capillary Die," J. Appl. Poly. Sci., 15, 1949 (1971).

7. Bennett, C. O., and J. E. Myers, Momentum, Heat, and Mass Transfer, pp. 166-168, McGraw Hill, New York (1962).

8. Bodger, D. V., private communication.

9. Bodger, D. B., and A. V. Rama Murthy, "Experimental Measurements of Loss Coefficients in the Entrance Region of a Pipe for Viscous Power-Law and Viscoelastic Fluids," AIChE J., 16, 1088 (1970).

10. Bogue, D. C., "Entrance Effects and Prediction of Turbulence in Non-Newtonian Flow," I.E.C., 51, 874 (1959).

11. Boles, R. L., H. L. Davis, and D. C. Bogue, "Entrance Flows of Polymeric Materials: Pressure Drop and Flow Patterns," Polymer Eng. Sci., 10, 24 (1970).

12. Bond, W. N., "Viscosity Determination by Means of Orifices and Short Tubes," Proc. Physical Soc. (London), 34, 139 (1922).

13. _____, "Theory of Liquid Flow through Cones," Phil. Mag., 50, 1058 (1925).

14. Campbell, W. D., and J.D. Slattery, "Flow in the Entrance of a Tube," Trans. A.S.M.E. J. of Basic Eng., 85, 41 (1963).

15. Caw, W. A. and R. G. Wylie, "Capillary Viscometers of Negligible Kinetic Energy Effect," Brit. J. Appl. Physics, 12, 94 (1961).

16. Chen, F. C., "Effect of Entrance Geometry on the Capillary Flow of Cellulose Acetate Solutions," J. Appl. Poly. Sci., 16, 2175 (1972).

17. Christiansen, E. B., and H. E. Lemmon, "Entrance Region Flow," AIChE J., 11, 995 (1965).

18. Christiansen, E. B., S. J. Kelsey, and T. R. Carter, "Laminar Flow through an Abrupt Contraction," AIChE J., 18, 372 (1972).

19. Collins, M. and W. R. Schowalter, "Laminar Flow in the Inlet Region of a Straight Channel," Phys. Fluids, 5, 1122 (1962).

20. _____, "Behavior of Non-Newtonian Fluids in the Entry Region of a Pipe," AIChE J., 9, 804 (1963).

21. Dodge, D. W., "Turbulent Flow of Non-Newtonian Fluids in Smooth Round Tubes," PhD thesis, Univ. Delaware, Newark (1957).

22. Dorsey, N. E., "The Flow of Liquids through Capillaries," Phys.Review, 28, 833 (1926).

23. Dow Chemical, "Methocel" Product Information, Midland, Michigan (1968).

24. Dryden, H. L., F. D. Murnaghan, and H. Bateman, Hydrodynamics, p. 469, Dover, New York (1956).

25. Feig, J. E., "Laminar Viscoelastic Flow in the Capillary Tube," M.Ch.E. thesis, Univ. Delaware (1966).

26. Fields, Jr., T. R., and Bogue, D. C., "Stress Birefringent Patterns of a Viscoelastic Fluid at a Sharp-Edged Entrance," Trans. Soc. Rheol., 12, 39 (1968).

27. Freeman, J. R., Experiments upon the Flow of Water in Pipes and Pipe Fittings, published by ASME, Plimpton Press, Norwood, Mass. (1941).

28. Gibson, A. H., "On the Steady Flow of an Incompressible Viscous Fluid through a Circular Tube with Uniformly Converging Boundaries," Phil. Mag. (6) 18, 35 (1909).

29. Goldstein, S., Modern Developments in Fluid Mechanics, Oxford Press, London (1938).

30. Han, D. C., letter to the editor, AIChE J., 17, 258 (1971).

31. Harrison, W. J., "The Pressure in a Viscous Liquid Moving through a Channel with Diverging Boundaries," Proc. Camb. Phil. Soc., 19, 307 (1919).

32. Holmes, D. B., "Experimental Studies on Laminar Flows in Ducts," dissertation, Delft (1967).

33. Hornbeck, R. A., "Laminar Flow in the Entrance Region of a Pipe," Appl. Sci. Res., A13, 224 (1964).

34. Hosking, R., "The Viscosity of Water," Phil. Mag., 17, 502 (1909).

35. _____, "The Electrical Conductivity and Fluidity of Solutions," Phil. Mag., 7 (1904).

36. _____, and T. R. Lyle, "The Temperature Variations of the Specific Molecular Conductivity and of the Fluidity of Sodium Chloride Solutions," Phil. Mag., 3, 487 (1902).

37. Hung, Tin-Kan, private communication (1972).

38. Kaye, S. E., and S. L. Rosen, "The Dependence of Laminar Entrance Loss Coefficients on Contraction Ratio for Newtonian Fluids," AIChE J., 17, 1269 (1971).

39. Knibbs, G. S., "The History, Theory, and the Determination of the Viscosity of Water by the Efflux Method," Proc. Roy. Soc. N.S. Wales, 29, 77 (1895).

40. Kobayashi, T., and Y. Tomita, "Pressure Drop of Viscoelastic Fluids in the Inlet Region of a Circular Tube," Bul. J.S.M.E., 14, 208 (1971).

41. LaNieve, H. L., "Entrance Effects in Non-Newtonian Pipe Flow," MS thesis, Univ. Tenn. (1963).

42. _____, and D. C. Bogue, "Correlation of Capillary Entrance Pressure Drops with Normal Stress Data," J. Appl. Poly. Sci., 12, 353 (1968).

43. Langhaar, H. D., "Steady Flow in the Transition Length of a Straight Tube," Trans. A.S.M.E. J. Appl. Mech, 64, A-55 (1942).

44. Lundgren, T. S., E. M. Sparrow, and J. B. Starr, "Pressure Drop Due to the Entrance Region in Ducts of Arbitrary Cross Section," J. Basic Eng., 86, 620 (1964).

45. Markovitz, H., "Nonlinear Steady Flow Behavior," Rheology, Vol. 4, p. 347, F. R. Erich, ed., Academic Press, New York (1967).

46. Metzner, A. B., E. A. Vebler, and C. F. Chan Man Fong., "Converging Flows of Viscoelastic Materials," AIChE J., 15, 750 (1969).

47. Oka, S., "The Steady Slow Motion of a Viscous Fluid through a Tapered Tube," J. Physical Soc. Japan, 19, 1481 (1964).

48. Philippoff, W., and F. H. Gaskins, "The Capillary Experiment in Rheology," Trans. Soc. Rheol., 2, 263 (1958).

49. Poiseuille, J. L., "Experimental Investigations upon the Flow of Liquids in Tubes of Very Small Diameter," translated by W. H. Herschel from Mem. Savants Etrangers, 9, 433 (1846), Easton, Pa. (1940).

50. Pruitt, G. T., and H. R. Crawford, "Effect of Molecular Weight and Segmental Constitution on the Drag Reduction of Water Soluble Polymers," David Taylor Model Basin Report No. DTMB-1, Contract nonr-4306(00), AD625 801, April 1965.

51. Rama Murthy, A. V., and D. V. Bodger, "Developing Velocity Profiles on the Downstream Side of a Contraction for Inelastic Polymer Solutions," Trans. Soc. Rheol.,15, 709 (1971).

52. Rieman II, W., "The Value of the Hagenbach Factor in the Determination of Viscosity by the Efflux Method," J.A.C.S., 50, 46 (1928).

53. Schiller, L., "Die Entwicklung der laminarin Geschwindigkeits-verteilung und ihre Bedeutung fur Zahigkeitsmessungen," Z. angew. Math. Mech., 2, 96 (1922).

54. Schmidt, F. W., and K. Wimmer, "Laminar Flows in Tubes with Step Changes in Cross Section," AIChE J., 17, 1248 (1971).

55. _____, and B. Zeldin, "Laminar Flows in Inlet Sections of Tubes and Ducts," AIChE J., 15, 612 (1969).

56. Schott, H., "Elastic Effects and Extrudate Distortions in Capillary Flow of Molten Polyethylene Resins," J. Poly. Sci., A, 2, 3791 (1964).

57. Sestak, J., and M. E. Charles, "Hagenbach Factor Prediction for Flow of Non-Newtonian Fluids in Pipes," Acta Technica CSAV, 14, 25 (1969).

58. Sutterby, J. L., "Laminar Newtonian and Non-Newtonian Converging Flow in Conical Sections," PhD thesis, Univ. Wisc. (1964).

59. _____, "Finite Difference Analysis of Viscous Laminar Converging Flow in Conical Tubes," Appl. Sci. Res, A15, 241 (1965).

60. _____, "Laminar Converging Flow of Dilute Polymer Solutions in Conical Sections, Part II," Trans. Soc. Rheol., 9, No. 2, 227 (1965).

61. _____, "Laminar Converging Flow of Dilute Polymer Solutions in Conical Sections, Part I," AIChE J., 12, 63 (1966).

62. Sylvester, N.S., "Entrance and Equilibrium Flow of Viscoelastic Fluids through a Cylindrical Tube," PhD thesis, Carnegie-Mellon Univ., Pittsburgh, Pa. (1968).

63. Sylvester, N.S. and S. L. Rosen, "Laminar Flow in the Entrance Region of a Cylindrical Tube, Part 1, Newtonian Fluids," AIChE J., 16, 964 (1970).

64. _____, ibid, 967.

65. Tanner, R. I., "Non-Newtonian Fluid Parameter Estimation Using Conical Flows," I.E.C. Fund., 5, 55 (1966).

66. Tomita, Y., "Analytical Treatments of Non-Newtonian Fluid Flow by Introducing the Conception of Boundary Layer," Bul. J.S.M.E., 4, 77 (1961).

67. _____, and R. Yamane, "A Study of Viscoelastic Fluid Flow," Bul. J.S.M.E., 9, 739 (1966).

68. Union Carbide, "Polyox Water-Soluble Resins," Union Carbide Corporation, New York (1968).

69. Weissberg, H. L., "End Correction for Slow Viscous Flow through Long Tubes," Phys. Fluids, 5, 1033 (1962).

APPENDICES

APPENDIX A-1

Calculation of Least Squares for the Relative Error

Given the general form

$$y = mx + b$$

in the case of widely varying values of y, it may be more effective to minimize the relative errors

$$\sum_i \left[\left(\frac{y_i - mx_i - b}{y_i}\right)^2\right]$$

with respect to the parameters m and b. Differentiating with respect to m and b, and setting equal to zero gives:

$$\sum_i \frac{x_i}{y_i} - m\sum_i \frac{x_i^2}{y_i^2} - b\sum_i \frac{x_i}{y_i^2} = 0$$

$$\sum_i \frac{1}{y_i} - m\sum_i \frac{x_i}{y_i^2} - b\sum_i \frac{1}{y_i^2} = 0$$

Solving for m and b

$$m = \frac{\sum_i \frac{x_i}{y_i}\sum_i \frac{1}{y_i^2} - \sum_i \frac{x_i}{y_i^2}\sum_i \frac{1}{y_i}}{\sum_i \frac{x_i^2}{y_i^2}\sum_i \frac{1}{y_i^2} - \sum_i\left(\frac{x_i}{y_i^2}\right)^2}$$

$$b = \frac{\sum_i \frac{x_i^2}{y_i^2}\sum_i \frac{1}{y_i} - \sum_i \frac{x_i}{y_i}\sum_i \frac{x_i}{y_i^2}}{\sum_i \frac{x_i^2}{y_i^2}\sum_i \frac{1}{y_i^2} - \sum_i\left(\frac{x_i}{y_i^2}\right)^2}$$

APPENDIX A-2

Computer Program for Treating Data

Computer Program Flowchart

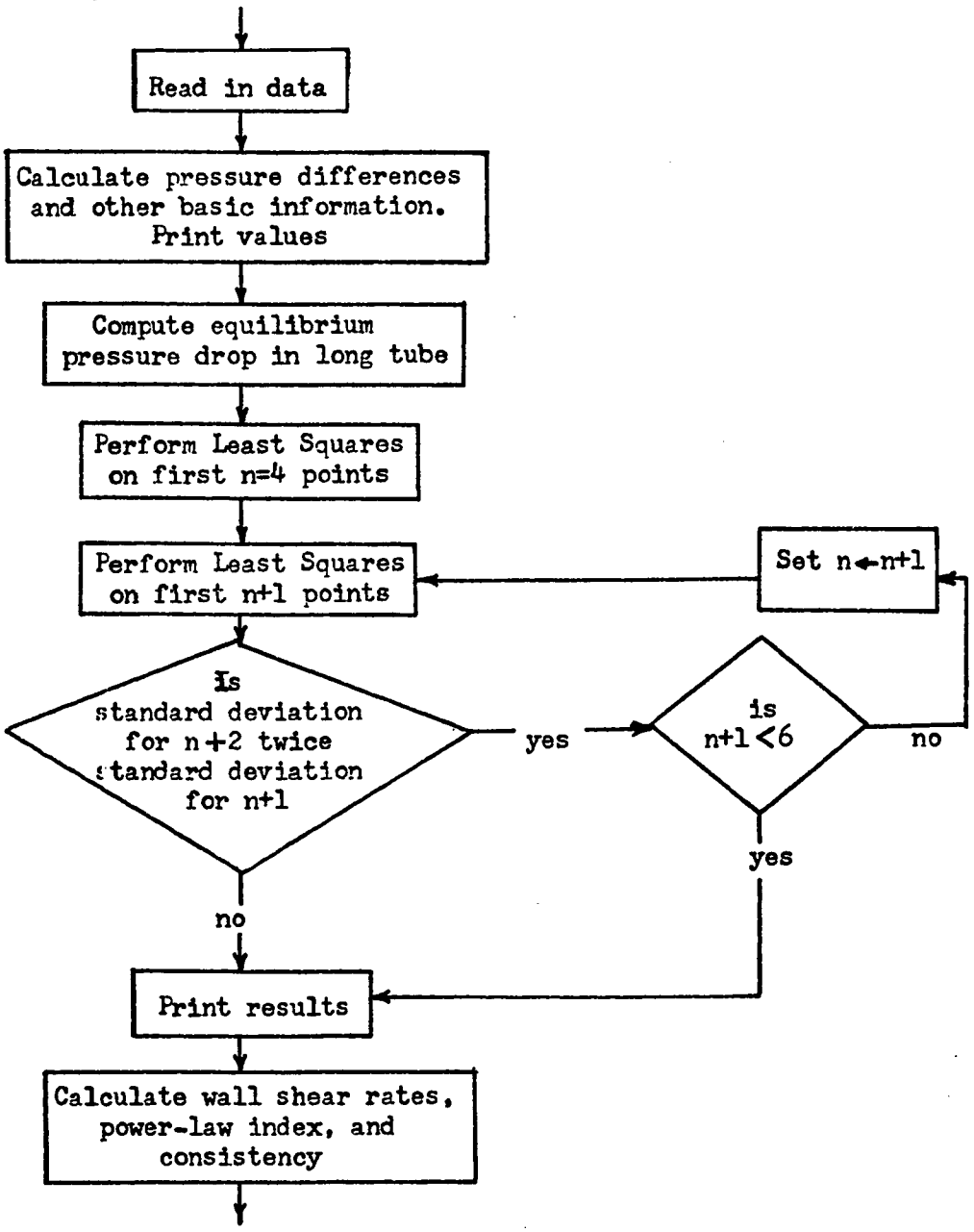

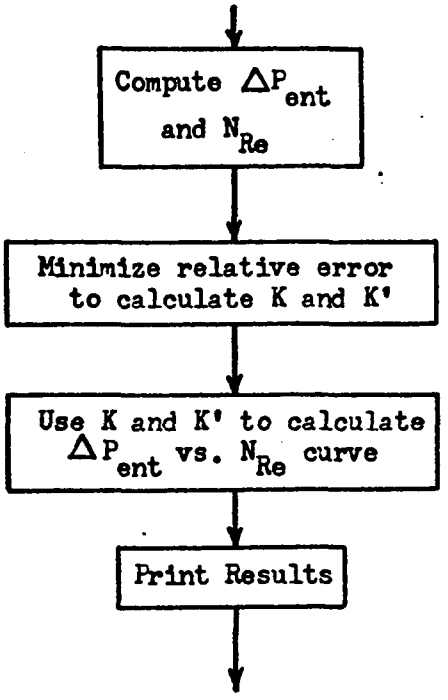
Compute ΔP_{ent} and N_{Re}
Minimize relative error to calculate K and K'
Use K and K' to calculate ΔP_{ent} vs. N_{Re} curve
Print Results

```
C          ****************************************************************
C          PROGRAM TO COMPUTE ENTRANCE PRESSURE DROP
C          COMPUTE K AND K PRIME
C          BY MINIMIZING THE RELATIVE ERROR
C          ****************************************************************
      DIMENSION V(60),DPL(60),TW(60),PF(60),VLG(60),TLG(60),SSW(60)
      DIMENSION P(9),Z(9),PP(9),STD(9),AB(9),CD(9),BP(9),GLG(60)
      DIMENSION R(60),PE(60),RI(60),RHO(60),FFF(60)
  100 FORMAT (5X,67HPROGRAM TO COMPUTE ENTRANCE PRESSURE DROPS FOR A SUD
     1DEN CONTRACTION)
  101 FORMAT (1H1)
  102 FORMAT (10X,2HRE,7X,11HTHEO E.P.D.)
  103 FORMAT (1X)
  104 FORMAT (7X,F8.3,6X,F7.3)
  106 FORMAT (5X,2HK=,F7.4)
  107 FORMAT (5X,3HKP=,F7.2)
  110 FORMAT (9X,13HTUBE DIAM: L=,F6.3,3H-IN,5X,2HS=,F6.3,3H-IN,5X,6HBET
     1A =,F6.3)
  130 FORMAT (I3,2X,20HPRES DATA (IN-FLUID),F4.2,3(F6.2),4(F7.2))
  160 FORMAT (5X,15HPRES INCR (PSI),F4.2,7(F7.4))
  180 FORMAT (5X,10HVOL FLOW =,F6.3,8H-CIN/SEC,5X,10HBULK VEL =,F7.4,7H-
     1FT/SEC)
  190 FORMAT (5X,9HDENSITY =,F6.3,9H-LB/CFT =,F7.5,7H-LB/CIN)
  200 FORMAT (5X,30HEQUIL PRES DROP IN LONG TUBE =,F7.5,7H-PSI/IN)
  210 FORMAT (5X,10HLOOP AT K=,I2,5H & E=,F8.5,5X,9HSTD DEV =,F8.5)
  220 FORMAT (5X,19HPRES AT TUBE EXIT =,F8.5,4H-PSI)
  250 FORMAT (2X,I3)
  280 FORMAT (2X,7F6.2,F5.2)
```

```
2900     300 FORMAT (2X,7F6.2,F7.1,F6.3)
3000     310 FORMAT (2X,F5.3,2X,F5.3)
3100     320 FORMAT (5X,6H1/NP =,F6.3,14HWITH STD DEV =,F8.5,5X,4HNP =,F6.3)
3200     325 FORMAT (5X,28HFROM RABINOWITSCH MOONEY EQN)
3300     330 FORMAT (9X,2HTW,13X,3HGDW,11X,3HDPS,12X,5HDPENT,8X,8HDPENT/KE,10X,
3400        12HRE,12X,4H1/RE,14X,1HF)
3500     331 FORMAT (9X,3HPSI,11X,5HSEC-1,10X,3HPCI,13X3HPSI)
3600     335 FORMAT (I3,2X,F10.6,4X,F10.3,5X,F10.8,5X,2(F10.6,5X),F10.5,5X,
3700        1F10.6,5X,F10.6)
3800     340 FORMAT (5X,17HPOWER LAW INDEX =,F6.4,5X,13HCONSISTANCY =,F8.6,14HL
3900        1B/FT SEC**2-N,5X,9HSTD DEV =,F8.6)
4000          WRITE (6,101)
4100          WRITE (6,100)
4200          PI=3.14159
4300          GC=32.1740
4400          Z(1)=0.0
4500          Z(2)=1.0
4600          Z(3)=2.0
4700          Z(4)=3.0
4800          Z(5)=4.0
4900          Z(6)=5.0
5000          Z(7)=7.0
5100          Z(8)=96.5/12.0
5200          DL=0.406
5300          READ (5,250) NNN
```

```
5400          READ (5,310) DS,ZE
5500          RNN=FLOAT(NNN)
5600          BETA=(DL*DL)/(DS*DS)
5700          WRITE (6,110) DL,DS,BETA
5800          WRITE (6,103)
5900          WRITE (6,103)
6000          WRITE (6,103)
6100          ZE=ZE/12.0
6200          RS=DS/24.0
6300          RL=DL/24.0
6400          DL=DL/12.0
6500          DO 10 NM=1,NNN
6600    C        ************************************************************
6700    C        READING IN OF DATA
6800    C        ************************************************************
6900          READ (5,300) (AB(I),I=2,8),T,RHO(NM)
7000          READ (5,280) (CD(I),I=2,8),DPEND
7100          P(1)=0.0
7200          DO 8 I=2,8
7300          P(I)=AB(I)-CD(I)
7400        8 CONTINUE
7500          SUP=0.0
7600          DO 9 J=2,8
7700          SUP=SUP+P(J)
7800          P(J)=SUP
7900        9 CONTINUE
8000          Q=100000.0/T
8100          RHO(NM)=RHO(NM)*62.261
```

```
 8200          WRITE (6,103)
 8300          WRITE (6,130) NM,(P(I),I=1,8)
 8400          PP(1)=P(1)
 8500          DO 1 I=2,8
 8600          P(I)=P(I)/12.0
 8700          PP(I)=(P(I)-P(I-1))*RHO(NM)/144.0
 8800        1 CONTINUE
 8900          WRITE (6,160) (PP(I),I=1,8)
 9000          PF(NM)=P(8)
 9100          QQ=Q/16.387
 9200          Q=Q/28320.0
 9300          V(NM)=Q/(PI*RL*RL)
 9400          RO=RHO(NM)/1728.0
 9500          WRITE (6,180) QQ,V(NM)
 9600          WRITE (6,190) RHO(NM),RO
 9700          DO 2 K=4,6
 9800  C       ************************************************************
 9900  C       CALCULATION OF EQUILIBRIUM PRESSURE DROP IN LONG TUBE
10000  C       FORMATION OF SUMS FOR LEAST SQUARES
10100  C       ************************************************************
10200          SP=0.0
10300          SZ=0.0
10400          SPZ=0.0
10500          SZSQ=0.0
10600          DO 3 J=1,K
```

```
10700          SP=SP+P(J)
10800          SZ=SZ+Z(J)
10900          SPZ=SPZ+P(J)*Z(J)
11000          SZSQ=SZSQ+Z(J)*Z(J)
11100        3 CONTINUE
11200          RN=FLOAT(K)
11300          DPL(NM)=(RN*SPZ-SP*SZ)/(RN*SZSQ-SZ*SZ)
11400          E=(SZSQ*SP-SZ*SPZ)/(RN*SZSQ-SZ*SZ)
11500  C       ************************************************************
11600  C          COMPUTATION OF STANDARD DEVIATION
11700  C       ************************************************************
11800          SUM=0.0
11900          DO 4 N=1,K
12000          PT=DPL(NM)*Z(N)+E
12100          SUM=SUM+(P(N)-PT)*(P(N)-PT)
12200        4 CONTINUE
12300          STD(K)=SQRT(SUM/(RN-1.0))
12400          IF (K-4) 5,2,5
12500        5 IF (STD(K)-2.0*STD(K-1)) 7,6,6
12600        7 IF (K-6) 2,6,2
12700        2 CONTINUE
12800        6 DPSIL=DPL(NM)*RO
12900          STD(K)=STD(K)*RO
13000          E=E*RO
13100          WRITE (6,200) DPSIL
13200          WRITE (6,210) K,E,STD(K)
13300          PEX=(DPEND-6.10)*RO-0.43*DPSIL
13400          WRITE (6,220) PEX
```

```
13500          TW(NM)=RL*DPL(NM)*RHO(NM)/2.0
13600          FFF(NM)=2.0*TW(NM)*GC/(RHO(NM)*V(NM)*V(NM))
13700       10 CONTINUE
13800    C     ************************************************************
13900    C     USE OF RABINOWITSCH MOONEY EQN. TO GET WALL SHEAR RATE
14000    C     BEGIN WITH LEAST SQUARES CALCULATION OF SLOPE
14100    C     DLOG(V)/DLOG(TW) =1/N'          N' = PN
14200    C     ************************************************************
14300          SV=0.0
14400          ST=0.0
14500          SVT=0.0
14600          STT=0.0
14700          DO 11 I=1,NNN
14800          VLG(I)=ALOG(V(I))
14900          TLG(I)=ALOG(TW(I))
15000          SV=SV+VLG(I)
15100          ST=ST+TLG(I)
15200          SVT=SVT+VLG(I)*TLG(I)
15300          STT=STT+TLG(I)*TLG(I)
15400       11 CONTINUE
15500          PNI=(RNN*SVT-SV*ST)/(RNN*STT-ST*ST)
15600          C2=(STT*SV-ST*SVT)/(RNN*STT-ST*ST)
15700          PN=1.0/PNI
15800    C     ************************************************************
15900    C     COMPUTATION OF STD. DEV. AND OF WALL SHEAR RATE
16000    C     ************************************************************
```

```
16100          SUM=0.0
16200          DO 12 N=1,NNN
16300          CV=PNI*TLG(N)+C2
16400          SUM=SUM+(VLG(N)-CV)*(VLG(N)-CV)
16500          SSW(N)=-V(N)*(3.0*PN+1.0)/(RL*PN)
16600       12 CONTINUE
16700          STDN=SQRT(SUM/(RNN-1.0))
16800          WRITE (6,103)
16900          WRITE (6,103)
17000          WRITE (6,103)
17100          WRITE (6,320) PNI,STDN,PN
17200          WRITE (6,325)
17300    C     ************************************************************
17400    C     CALCULATION OF POWER LAW INDEX AND CONSISTANCY
17500    C     ************************************************************
17600          ST=0.0
17700          SG=0.0
17800          SGT=0.0
17900          SGG=0.0
18000          DO 13 N=1,NNN
18100          GLG(N)=ALOG(-SSW(N))
18200          ST=ST+TLG(N)
18300          SG=SG+GLG(N)
18400          SGT=SGT+TLG(N)*GLG(N)
18500          SGG=SGG+GLG(N)*GLG(N)
18600       13 CONTINUE
18700          PLI=(PNN*SGT-ST*SG)/(RNN*SGG-SG*SG)
18800          CLG=(SGG*ST-SG*SGT)/(RNN*SGG-SG*SG)
18900          CON=GC*EXP(CLG)
19000    C     ************************************************************
19100    C     PLI = POWER LAW INDEX      CON = CONSISTANCY
19200    C     ************************************************************
19300          SUM=0.0
19400          DO 14 N=1,NNN
19500          CV=PLI*GLG(N)+CLG
19600          SUM=SUM+(TLG(N)-CV)*(TLG(N)-CV)
```

```
19700      14 CONTINUE
19800         STDN=SQRT(SUM/(RNN-1.0))
19900         WRITE (6,101)
20000         WRITE (6,330)
20100         WRITE (6,331)
20200         WRITE (6,103)
20300         WRITE (6,103)
20400         DO 15 N=1,NNN
20500         DPS=DPL(N)*((RL/RS)**(3.0*PLI+1.0))
20600         DPSIS=DPS*RHO(N)/1728.0
20700   C        ************************************************************
20800   C        COMPUTATION OF ENTRANCE PRESSURE LOSS
20900   C        ************************************************************
21000         DPENT=(PF(N)-DPS*ZE-DPL(N)*Z(8))*RHO(N)
21100         DPE=DPENT/144.0
21200         PE(N) =GC*DPENT/(0.5*RHO(N)*V(N)*V(N))
21300         R(N)=2.0*RHO(N)*(DL**PLI)*((2.0*V(N))**(2.0-PLI))/
21400        1  (CON*((3.0+(1.0/PLI))**PLI))
21500         TWIS=TW(N)/144.0
21600         RI(N)=1.0/R(N)
21700         WRITE (6,335) N,TWIS,SSW(N),DPSIS,DPE,PE(N),R(N),RI(N),FFF(N)
21800         WRITE (6,103)
21900      15 CONTINUE
22000         WRITE (6,103)
22100         WRITE (6,103)
22200         WRITE (6,340) PLI,CON,STDN
22300   C        ************************************************************
22400   C        FORMATION OF SUMS
22500   C        R IMPLIES REYNOLDS NUMBER      P IMPLIES ENT PRES DROP
22600   C        ************************************************************
22700         SPP=0.0
22800         SPPR=0.0
22900         SP=0.0
23000         SPR=0.0
23100         SPPRR=0.0
```

```
23200           DO 21 N=1,NNN
23300           SPP=SPP+(1.0/(PE(N)*PE(N)))
23400           SPPR=SPPR+1.0/(PE(N)*PE(N)*R(N))
23500           SP=SP+1.0/PE(N)
23600           PR=PE(N)*R(N)
23700           SPPRR=SPPRR+1.0/(PR*PR)
23800           SPR=SPR+1.0/PR
23900        21 CONTINUE
24000           DENOM=SPP*SPPRR-SPPR*SPPR
24100     C        ************************************************************
24200     C        COMPUTATION OF K AND K PRIME
24300     C        ************************************************************
24400           C=(SPPRR*SP-SPPR*SPR)/DENOM
24500           CP=(SPP*SPR-SPPR*SP)/DENOM
24600           RT=1.0
24700           WRITE (6,101)
24800           WRITE (6,102)
24900           WRITE (6,103)
25000     C        ************************************************************
25100     C        THEORETICAL CURVE FOR ENT PRESS DROP VS. REYNOLDS NUMBER
25200     C        ************************************************************
25300           DO 22 N=1,10
25400           RT=RT+RT
25500           PT=C+CP/RT
25600           WRITE (6,104) RT,PT
25700        22 CONTINUE
25800           WRITE (6,103)
25900           WRITE (6,103)
26000           WRITE (6,103)
26100           WRITE (6,106) C
26200           WRITE (6,103)
26300           WRITE (6,107) CP
26400           STOP
26500           END
```

APPENDIX A-3

Data

The following pages contain the data for this study. Presented are incremental pressures (P_1 to P_8) in terms of test fluid head, volumetric flow rate (Q) in terms of $in.^3/sec.$, and the specific gravity (SG) of the test fluid. The notation (P_1, P_2,.... P_8) represents the pressure tap having that pressure. Taps were located as shown below.

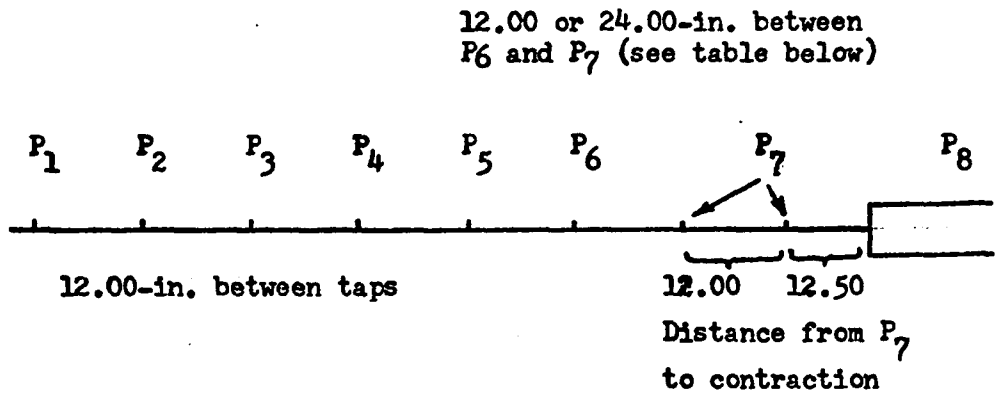

Placement of P_8 depended on the entrance section. Table 2.1, page 38, is a listing of placement distances from the contraction for P_8. One exception is the data for the 7 1/2° conical entrance where P_8 was located 10.63-in. from the contraction. Since equilibrium pressure gradients were obtained from P_1-P_6, choice of location for P_7 did not affect calculation of ΔP_{ent}.

Table A1. Newtonian Data for 1/2" Entrance Section

RUN	P1	P2	P3	P4	P5	P6	P7	P8	Q	SG
1	0.00	15.93	31.76	47.15	63.28	79.48	111.62	129.86	1.3104	1.239
2	0.00	15.99	31.84	47.25	63.39	79.60	111.76	130.02	1.3138	1.239
3	0.00	21.33	42.50	63.08	84.63	106.31	149.35	173.81	1.7843	1.239
4	0.00	21.29	42.44	63.00	84.54	106.23	149.19	173.63	1.7838	1.239
5	0.00	5.97	11.91	17.66	23.72	29.75	41.73	48.54	0.4007	1.244
6	0.00	5.99	11.93	17.69	23.74	29.79	41.77	48.58	0.4004	1.244
7	0.00	7.16	14.25	21.14	28.40	35.68	50.07	58.22	0.4961	1.245
8	0.00	7.14	14.23	21.13	28.38	35.65	50.03	58.18	0.4961	1.245
9	0.00	9.46	18.83	27.93	37.51	47.07	66.00	76.77	0.7909	1.241
10	0.00	9.47	18.86	27.99	37.59	47.17	66.13	76.90	0.7909	1.241
11	0.00	10.63	21.17	31.46	42.25	53.07	74.46	86.59	0.8354	1.240
12	0.00	10.63	21.17	31.47	42.26	53.08	74.48	86.61	0.8356	1.240
13	0.00	5.32	10.63	15.80	21.24	26.65	37.34	43.44	0.4092	1.240
14	0.00	5.33	10.65	15.82	21.25	26.65	37.35	43.45	0.4090	1.240
15	0.00	6.54	12.94	19.25	25.91	32.53	45.64	53.06	0.5135	1.241
16	0.00	6.52	13.00	19.29	25.89	32.50	45.61	53.03	0.5104	1.241
17	0.00	8.73	17.39	25.81	34.63	43.45	60.94	70.84	0.6938	1.240
18	0.00	8.72	17.39	25.79	34.59	43.41	60.89	70.79	0.6916	1.240
19	0.00	4.92	9.79	14.53	19.48	24.43	34.23	39.83	0.3813	1.241
20	0.00	4.89	9.73	14.45	19.41	24.36	34.17	39.77	0.3803	1.241
21	0.00	13.31	26.52	39.36	52.83	66.32	93.08	108.22	1.0789	1.240
22	0.00	13.27	26.54	39.34	52.78	66.26	92.98	108.12	1.0785	1.240
23	0.00	1.29	2.57	3.84	5.13	6.43	9.10	11.00	2.0150	1.164
24	0.00	1.29	2.57	3.84	5.14	6.44	9.11	11.01	2.0162	1.164
25	0.00	1.80	3.65	5.43	7.34	9.14	12.98	15.96	2.8850	1.164

Table A1. Newtonian Data for 1/2" Entrance Section

RUN	P1	P2	P3	P4	P5	P6	P7	P8	Q	SG
26	0.00	1.82	3.66	5.45	7.35	9.18	13.03	16.00	2.8831	1.164
27	0.00	2.24	4.58	6.81	9.16	11.51	16.29	20.20	3.5690	1.164
28	0.00	2.22	4.58	6.80	9.16	11.50	16.29	20.20	3.5695	1.164
29	0.00	3.01	6.22	9.16	12.40	15.47	20.06	27.80	4.7884	1.164
30	0.00	3.04	6.24	9.19	12.43	15.49	22.08	27.83	4.8001	1.164
31	0.00	3.74	7.80	11.48	15.47	19.39	27.78	35.57	5.9570	1.163
32	0.00	3.74	7.81	11.48	15.48	19.39	27.77	35.56	5.9588	1.163
33	0.00	1.73	3.48	5.11	6.93	8.63	12.15	14.18	0.6719	1.208
34	0.00	1.74	3.48	5.13	6.93	8.66	12.16	14.19	0.6713	1.208
35	0.00	3.08	6.11	9.10	12.17	15.31	21.49	25.10	1.1442	1.210
36	0.00	3.09	6.12	9.11	12.19	15.32	21.51	25.12	1.1436	1.210
37	0.00	5.45	11.00	16.32	21.92	27.53	38.70	45.31	1.9956	1.210
38	0.00	5.44	10.99	16.30	21.91	27.50	38.68	45.30	1.9923	1.210
39	0.00	7.45	15.03	22.28	29.95	37.57	52.87	62.22	2.7954	1.212
40	0.00	7.45	15.02	22.28	29.94	37.57	52.87	62.21	2.7929	1.212

Table A2. Newtonian Data for 5/8" Entrance Section

RUN	P1	P2	P3	P4	P5	P6	P7	P8	Q	SG
1	0.00	5.25	10.43	15.48	20.76	26.07	36.60	42.37	0.3087	1.246
2	0.00	5.21	10.39	15.43	20.73	26.06	36.58	42.35	0.3072	1.246
3	0.00	8.15	16.22	24.04	32.24	40.49	56.80	65.73	0.5060	1.246
4	0.00	8.11	16.15	23.96	32.25	40.51	56.84	65.77	0.5056	1.246
5	0.00	10.19	20.26	30.03	40.31	50.64	71.06	82.23	0.6520	1.246
6	0.00	10.18	20.28	30.08	40.35	50.69	71.12	82.29	0.6513	1.246
7	0.00	8.67	17.26	25.60	34.33	43.10	60.43	69.92	0.5851	1.246
8	0.00	8.66	17.25	25.59	34.31	43.08	60.42	69.91	0.5834	1.246
9	0.00	8.01	15.94	23.65	31.73	39.94	55.96	64.72	0.5377	1.245
10	0.00	8.03	15.97	23.69	31.77	39.90	55.93	64.69	0.5377	1.245
11	0.00	11.67	23.25	34.53	46.35	58.24	81.75	94.65	0.8061	1.245
12	0.00	11.68	23.27	34.55	46.38	58.26	81.78	94.68	0.8072	1.246
13	0.00	13.34	26.62	39.53	53.06	66.65	93.49	108.30	1.1347	1.244
14	0.00	13.35	26.63	39.54	53.08	66.66	93.51	108.31	1.1294	1.244
15	0.00	19.83	39.53	58.68	78.72	98.90	138.89	161.02	1.6682	1.243
16	0.00	19.86	39.58	58.77	78.82	99.01	139.03	161.18	1.6678	1.243
17	0.00	26.47	52.72	78.27	105.01	131.93	185.32	214.77	1.8627	1.244
18	0.00	26.44	52.67	78.21	104.93	131.81	185.17	214.61	1.8650	1.244
19	0.00	15.41	30.65	45.51	61.08	76.71	107.74	124.77	1.1404	1.244
20	0.00	15.40	30.60	45.41	60.96	76.58	107.57	124.59	1.1364	1.244
21	0.00	1.46	2.82	4.20	5.64	7.07	9.92	11.53	0.5216	1.212
22	0.00	1.47	2.82	4.21	5.65	7.11	9.96	11.57	0.5217	1.212
23	0.00	1.74	3.42	5.06	6.82	8.55	11.99	13.98	0.6373	1.212
24	0.00	1.73	3.41	5.06	6.81	8.55	11.99	13.97	0.6371	1.212
25	0.00	3.02	5.97	8.86	11.90	14.98	21.05	24.58	1.1253	1.212

Table A2. Newtonian Data for 5/8" Entrance Section

RUN	P1	P2	P3	P4	P5	P6	P7	P8	Q	SG
26	0.00	3.04	5.99	8.87	11.94	14.99	21.06	24.58	1.1234	1.212
27	0.00	4.97	10.04	14.91	20.02	25.23	35.51	41.62	1.8940	1.212
28	0.00	5.04	10.09	14.99	20.14	25.31	35.57	41.69	1.8899	1.212
29	0.00	7.62	15.35	22.77	30.62	38.41	54.08	63.75	2.8596	1.212
30	0.00	7.63	15.40	22.81	30.71	38.48	54.17	68.86	2.8577	1.212
31	0.00	1.23	2.47	3.66	4.93	6.17	8.69	10.68	2.0441	1.161
32	0.00	1.27	2.48	3.71	4.95	6.21	8.75	10.73	2.0408	1.161
33	0.00	1.74	3.53	5.24	7.09	8.87	12.60	15.82	2.9836	1.158
34	0.00	1.74	3.54	5.25	7.11	8.87	12.61	15.84	2.9829	1.158
35	0.00	2.41	5.04	7.44	10.04	12.57	17.94	23.15	4.1955	1.158
36	0.00	2.50	5.04	7.52	10.13	12.64	18.01	23.23	4.1950	1.158
37	0.00	2.80	5.86	8.61	11.65	14.57	20.85	27.22	4.8020	1.161
38	0.00	2.81	5.88	8.63	11.68	14.59	20.88	27.26	4.8043	1.161
39	0.00	3.64	7.70	11.28	15.23	19.07	27.47	36.87	6.2454	1.160
40	0.00	3.65	7.71	11.30	15.25	19.11	27.52	36.92	6.2480	1.160
41	0.00	0.72	1.34	2.01	2.67	3.39	4.69	5.63	1.0143	1.160
42	0.00	0.73	1.35	2.02	2.68	3.40	4.71	5.65	1.0141	1.160

Table A3. Newtonian Data for 7/8" Entrance Section

RUN	P1	P2	P3	P4	P5	P6	P7	P8	Q	SG
1	0.00	4.50	9.06	13.48	18.14	22.90	32.14	37.09	0.2794	1.248
2	0.00	4.46	8.98	13.38	22.64	31.81	31.81	36.72	0.2770	1.248
3	0.00	5.28	10.65	15.87	21.33	26.82	37.69	43.54	0.3309	1.248
4	0.00	5.26	10.62	15.83	21.28	26.77	37.67	43.52	0.3295	1.248
5	0.00	7.20	14.49	21.54	28.90	36.32	51.04	58.98	0.4551	1.248
6	0.00	7.20	14.47	21.53	28.89	36.32	51.04	58.98	0.4544	1.248
7	0.00	3.78	7.61	11.32	15.25	19.18	26.97	31.18	0.2337	1.248
8	0.00	3.79	7.62	11.35	15.26	19.18	26.97	31.18	0.2331	1.248
9	0.00	10.45	20.92	31.11	41.78	52.51	73.73	85.20	0.6841	1.247
10	0.00	10.47	20.97	31.14	41.81	52.54	73.75	85.22	0.6834	1.247
11	0.00	17.16	34.33	51.02	68.49	86.06	120.91	139.81	1.1471	1.247
12	0.00	17.12	34.34	51.08	68.57	86.17	121.05	139.95	1.1460	1.247
13	0.00	24.48	48.90	72.64	97.52	122.56	172.15	199.07	1.6273	1.247
14	0.00	24.47	48.89	72.62	97.44	122.47	172.05	198.95	1.6059	1.247
15	0.00	2.77	5.48	8.14	10.92	13.71	19.21	22.37	1.1071	1.207
16	0.00	2.77	5.48	8.14	10.91	13.70	19.21	22.36	1.1067	1.207
17	0.00	1.36	2.77	4.08	5.49	6.89	9.69	11.27	0.5752	1.208
18	0.00	1.36	2.77	4.09	5.49	6.90	9.70	11.28	0.5754	1.208
19	0.00	4.46	9.06	13.40	18.07	22.64	31.86	37.38	1.8667	1.208
20	0.00	4.46	9.05	13.40	18.05	22.64	31.86	37.38	1.8645	1.208
21	0.00	1.29	2.55	3.63	5.09	6.20	8.81	10.91	2.0924	1.159
22	0.00	1.28	2.54	3.62	5.07	6.20	8.80	10.90	2.0904	1.159
23	0.00	1.66	3.37	4.79	6.72	8.18	11.68	14.77	2.7740	1.160
24	0.00	1.68	3.38	4.85	6.73	8.25	11.74	14.83	2.7781	1.160
25	0.00	2.45	4.90	7.16	9.56	11.96	16.94	21.95	3.8958	1.160

Table A3. Newtonian Data for 7/8" Entrance Section

RUN	P1	P2	P3	P4	P5	P6	P7	P8	Q	SG
26	0.00	2.45	4.90	7.16	9.57	11.95	16.93	21.94	3.9040	1.160
27	0.00	3.15	6.36	9.27	12.42	15.51	22.14	29.49	5.0693	1.160
28	0.00	3.14	6.37	9.27	12.42	15.51	22.14	29.49	5.0697	1.160
29	0.00	3.90	8.02	11.66	15.67	19.58	28.23	38.82	6.4358	1.161
30	0.00	3.90	8.04	11.67	15.68	19.59	28.25	38.84	6.4425	1.161
31	0.00	0.95	1.61	2.35	3.04	3.77	5.20	6.21	1.1549	1.161
32	0.00	0.94	1.61	2.33	3.04	3.76	5.19	6.20	1.1571	1.161

Table A4. Newtonian Data for 1 1/4" Entrance Section

RUN	P1	P2	P3	P4	P5	P6	P7	P8	Q	SG
1	0.00	4.90	9.87	14.73	19.81	24.90	35.01	40.43	0.2823	1.246
2	0.00	9.77	19.67	29.19	39.28	49.42	69.46	80.15	0.6006	1.246
3	0.00	5.24	10.54	15.69	21.07	26.50	37.25	43.03	0.3274	1.247
4	0.00	5.21	10.49	15.62	20.98	26.37	37.07	42.81	0.3249	1.247
5	0.00	7.04	14.14	21.03	28.16	35.44	49.78	57.50	0.4460	1.247
6	0.00	7.01	14.08	20.96	28.18	35.45	49.82	57.48	0.4454	1.247
7	0.00	10.13	20.30	30.16	40.50	50.89	71.43	82143	0.6890	1.247
8	0.00	10.11	20.26	30.13	40.45	50.82	71.36	82.36	0.6383	1.247
9	0.00	12.67	25.34	37.69	50.62	62.58	88.26	102.07	0.8008	1.247
10	0.00	20.72	41.40	61.50	82.53	103.69	145.63	168.26	1.3209	1.247
11	0.00	0.95	1.76	2.64	3.49	4.40	6.14	7.11	0.3639	1.209
12	0.00	0.95	1.76	2.65	3.49	4.41	6.15	7.12	0.3607	1.209
13	0.00	2.22	4.43	6.51	8.77	10.96	15.37	17.86	0.9367	1.208
14	0.00	2.23	4.43	6.52	8.77	10.97	15.39	17.88	0.9375	1.208
15	0.00	1.48	2.83	4.20	5.59	7.04	9.86	11.41	0.5894	1.207
16	0.00	1.48	2.82	4.20	5.59	7.04	9.86	11.41	0.5889	1.207
17	0.00	4.02	8.09	11.95	16.06	20.14	28.31	33.16	1.6979	1.206
18	0.00	4.02	8.10	11.95	16.08	20.14	28.33	33.17	1.6979	1.206
19	0.00	5.91	11.89	17.61	23.61	29.63	41.67	49.12	2.5144	1.206
20	0.00	5.92	11.89	17.60	23.60	29.63	41.67	49.12	2.5144	1.206
21	0.00	1.48	2.46	3.99	4.94	6.55	9.13	11.23	2.1148	1.155
22	0.00	1.50	2.46	4.01	4.95	6.55	9.12	11.22	2.1133	1.155
23	0.00	1.60	3.45	5.15	6.88	8.68	12.27	15.61	2.9282	1.160
24	0.00	1.62	3.46	5.16	6.90	8.70	12.30	15.64	2.9323	1.160
25	0.00	2.30	4.80	7.08	9.52	11.94	17.03	22.35	4.0510	1.159

Table A4. Newtonian Data for 1 1/4" Entrance Section

RUN	P1	P2	P3	P4	P5	P6	P7	P8	Q	SG
26	0.00	2.30	4.80	7.08	9.52	11.94	17.03	22.35	4.0520	1.159
27	0.00	3.30	6.90	10.13	13.61	17.07	24.57	33.72	5.8446	1.157
28	0.00	3.28	6.90	10.12	13.61	17.06	24.57	33.73	5.8463	1.157
29	0.00	0.83	1.66	2.50	3.30	4.19	5.88	7.09	1.3801	1.158
30	0.00	0.83	1.65	2.50	3.29	4.18	5.87	7.08	1.3817	1.158

Table A5. Newtonian Data for 1 5/8" Entrance Section

RUN	P1	P2	P3	P4	P5	P6	P7	P8	G	SG
1	0.00	4.43	8.82	13.07	17.54	22.06	30.99	35.79	0.4994	1.234
2	0.00	4.43	8.82	13.07	17.53	22.05	30.98	35.78	0.4998	1.234
3	0.00	5.16	10.29	15.26	20.46	25.70	36.10	41.68	0.6175	1.234
4	0.00	5.14	10.26	15.22	20.42	25.65	36.03	41.60	1.6177	1.234
5	0.00	1.40	2.80	4.14	5.57	6.98	9.81	11.33	0.1828	1.232
6	0.00	1.42	2.81	4.15	5.58	6.98	9.81	11.33	0.1829	1.232
7	0.00	9.35	18.67	27.71	37.19	46.73	65.61	75.92	1.2183	1.234
8	0.00	9.34	18.65	27.69	37.16	46.70	65.58	75.89	1.2041	1.234
9	0.00	9.83	19.64	29.16	39.12	49.16	69.03	79.89	1.3163	1.233
10	0.00	9.82	19.61	29.12	39.07	49.10	68.96	79.83	1.3132	1.233
11	0.00	12.22	24.38	36.23	48.64	61.14	85.90	99.54	1.6497	1.232
12	0.00	12.22	24.38	36.23	48.64	61.14	85.91	99.54	1.6497	1.232
13	0.00	1.88	3.73	5.53	7.44	9.34	13.17	15.22	0.2605	1.232
14	0.00	1.88	3.74	5.54	7.44	9.34	13.17	15.22	0.2605	1.232
15	0.00	3.68	7.36	10.92	14.65	18.40	25.87	29.88	0.5030	1.232
16	0.00	3.68	7.36	10.92	14.65	18.40	25.87	29.88	0.5033	1.232
17	0.00	6.13	12.27	18.18	24.37	30.65	43.09	49.81	0.7768	1.234
18	0.00	6.13	12.27	18.20	24.39	30.67	43.11	49.84	0.7750	1.234
19	0.00	1.69	3.40	5.04	6.77	8.52	11.96	13.95	0.8532	1.203
20	0.00	1.69	3.40	5.05	6.77	8.52	11.98	13.97	0.8530	1.203
21	0.00	2.03	4.09	5.96	8.05	10.15	14.26	16.67	1.0320	1.201
22	0.00	2.03	4.09	5.96	8.05	10.16	14.28	16.69	1.0326	1.201
23	0.00	2.56	5.14	7.64	10.27	12.92	18.12	21.22	1.2995	1.203
24	0.00	2.56	5.15	7.64	10.26	12.92	18.12	21.22	1.2995	1.203
25	0.00	3.06	6.15	9.17	12.38	15.60	21.90	25.71	1.5643	1.202

Table A5. Newtonian Data for 1 5/8" Entrance Section

RUN	P1	P2	P3	P4	P5	P6	P7	P8	Q	SG
26	0.00	3.06	6.17	9.20	12.41	15.63	21.93	25.75	1.5667	1.202
27	0.00	3.22	6.49	9.68	13.06	16.45	23.10	27.13	1.6369	1.201
28	0.00	3.21	6.48	9.68	13.05	16.44	23.08	27.12	1.6365	1.201
29	0.00	3.29	6.63	9.89	13.33	16.79	23.57	27.72	1.6673	1.200
30	0.00	3.28	6.63	9.89	13.33	16.78	23.56	27.71	1.6660	1.200
31	0.00	3.85	7.75	11.54	15.53	19.54	27.52	32.46	1.9534	1.200
32	0.00	3.85	7.75	11.54	15.53	19.55	27.52	32.46	1.9559	1.200
33	0.00	5.76	11.61	17.25	23.16	29.09	40.94	48.66	2.8344	1.200
34	0.00	5.76	11.61	17.25	23.16	29.10	40.97	48.69	2.8291	1.200
35	0.00	2.55	5.25	7.81	10.50	13.17	18.60	22.34	2.4120	1.186
36	0.00	2.56	5.25	7.82	10.51	13.18	18.16	22.35	2.4187	1.186
37	0.00	9.14	18.46	27.40	36.81	46.18	65.12	78.49	4.3997	1.203
38	0.00	9.15	18.49	27.44	36.86	46.25	65.22	78.57	4.3934	1.203
39	0.00	3.99	8.23	12.18	16.39	20.53	28.97	35.42	3.5397	1.187
40	0.00	3.99	8.22	12.17	16.38	20.52	28.96	35.40	3.5233	1.187
41	0.00	6.57	13.55	20.06	26.94	33.78	47.84	60.49	5.6872	1.187
42	0.00	6.59	13.56	20.07	26.96	33.78	47.84	60.50	5.6973	1.187
43	0.00	10.36	21.51	31.66	42.55	53.28	76.00	100.61	8.8415	1.189
44	0.00	10.48	21.63	31.80	42.69	53.45	76.19	100.82	8.8351	1.189

Table A6. Newtonian Data for 2" Entrance Section

RUN	P1	P2	P3	P4	P5	P6	P7	P8	Q	SG
1	0.00	2.35	4.67	6.92	9.32	11.81	14.16	19.13	0.2437	1.236
2	0.00	2.36	4.69	6.94	9.35	11.84	14.20	19.16	0.2438	1.236
3	0.00	3.05	6.08	9.01	12.09	15.21	18.27	24.71	0.3234	1.234
4	0.00	3.06	6.09	9.03	12.12	15.24	18.29	24.73	0.3297	1.234
5	0.00	3.77	7.50	11.12	14.94	18.78	22.56	30.50	0.4220	1.234
6	0.00	3.77	7.50	11.11	14.93	18.77	22.54	30.49	0.4217	1.234
7	0.00	4.25	8.46	12.54	16.85	21.19	25.45	34.41	0.4582	1.234
8	0.00	4.25	8.46	12.56	16.86	21.21	25.48	34.44	0.4583	1.234
9	0.00	4.93	9.82	14.57	19.58	24.60	29.48	39.85	0.5484	1.233
10	0.00	4.92	9.80	14.54	19.55	24.58	29.49	39.86	0.5481	1.233
11	0.00	8.43	16.79	24.89	33.41	41.98	50.38	68.14	0.9803	1.233
12	0.00	8.39	16.73	24.84	33.36	41.93	50.32	68.08	0.9803	1.233
13	0.00	13.43	26.76	39.76	53.37	67.05	80.49	109.08	1.6503	1.232
14	0.00	13.41	26.75	39.74	53.32	66.98	80.43	109.00	1.6497	1.232
15	0.00	2.36	4.75	7.01	9.43	11.82	16.58	19.27	0.9784	1.207
16	0.00	2.36	4.75	7102	9.43	11.83	16.59	19.29	0.9787	1.207
17	0.00	3.72	7.51	11.07	14.90	18.68	26.26	30.72	1.5480	1.207
18	0.00	3.72	7.51	11.07	14.90	18.68	26.26	30.71	1.5469	1.207
19	0.00	6.20	12.51	18.55	24.91	31.26	43.98	51.84	2.5662	1.207
20	0.00	6.20	12.52	18.56	24.91	31.28	44.01	51.87	2.5608	1.207
21	0.00	2.40	4.87	7.24	9.78	12.24	17.27	20.73	2.1191	1.181
22	0.00	2.41	4.88	7.26	9.80	12.26	17.29	20.75	2.1228	1.181
23	0.00	3.18	6.47	9.59	12.96	16.21	22.85	27.74	2.8057	1.181
24	0.00	3.19	6.48	9.60	12.98	16.23	22.88	27.77	2.8032	1.181
25	0.00	4.74	9.79	14.46	19.56	24.42	34.55	42.95	4.2322	1.181

Table A6. Newtonian Data for 2" Entrance Section

RUN	P1	P2	P3	P4	P5	P6	P7	P8	Q	SG
26	0.00	4.73	9.79	14.47	19.59	24.44	34.58	42.98	4.2263	1.181
27	0.00	6.92	14.25	21.04	28.37	35.44	50.29	64.51	6.1972	1.180
28	0.00	6.96	14.29	21.16	28.48	35.61	50.48	64.71	6.1934	1.180
29	0.00	7.67	15.76	23.29	31.35	39.19	55.60	71.62	6.6330	1.184
30	0.00	7.66	15.75	23.28	31.35	39.19	55.60	71.63	6.6323	1.184
31	0.00	9.91	20.55	30.24	40.73	50.90	72.64	96.34	8.6867	1.184
32	0.00	9.93	20.55	30.23	40.75	50.89	72.61	96.30	8.6780	1.184

Table A7. Newtonian Data for 2 1/2" Entrance Section

RUN	P1	P2	P3	P4	P5	P6	P7	P8	Q	SG
1	0.00	2.17	4.27	6.38	8.61	10.82	15.20	17.63	0.7755	1.212
2	0.00	2.18	4.27	6.38	8.61	10.81	15.20	17.63	0.7755	1.212
3	0.00	3.17	6.24	9.29	12.53	15.72	22.12	25.75	1.1396	1.212
4	0.00	3.16	6.24	9.28	12.52	15.70	22.09	25.71	1.1377	1.212
5	0.00	4.85	9178	14.50	19.56	24.54	34.56	40.45	1.8238	1.212
6	0.00	4.85	9.79	14.51	19.58	24.56	34.58	40.47	1.8360	1.212
7	0.00	8.32	16.72	24.86	33.42	41.93	59.05	69.81	3.1209	1.212
8	0.00	8.33	16.73	24.88	33.44	41.94	59.06	69.83	3.1173	1.212
9	0.00	3.66	7.21	10.66	14.34	17.86	25.12	30.72	3.2322	1.180
10	0.00	3.67	7.23	10.68	14.38	17.90	25.18	30.79	3.2329	1.180
11	0.00	2.52	4.82	7.12	9.55	11.86	16.64	19.95	2.1101	1.180
12	0.00	2.51	4.83	7.11	9.55	11.86	16.63	19.93	2.1109	1.180
13	0.00	4.49	9.08	13.38	18.02	22.47	31.70	39.38	4.0813	1.180
14	0.00	4.49	9.08	13.39	18.03	22.48	31.71	39.38	4.0824	1.180
15	0.00	6.53	13.26	19.55	26.28	32.84	46.54	59.72	5.9945	1.178
16	0.00	6.57	13.32	19.64	26.40	32.95	46.68	59.90	6.0016	1.178
17	0.00	10.06	20.80	30.65	41.26	51.58	73.80	99.05	9.1917	1.180
18	0.00	10.20	20.95	30.88	41.53	51.88	74.16	99.37	9.1945	1.180
19	0.00	1.31	2.56	3.79	5.07	6.37	8.94	10.31	0.1237	1.236
20	0.00	1.30	2.55	3.77	5.06	6.37	8.95	10.32	0.1235	1.236
21	0.00	1.80	3.57	5.29	7.08	8.92	12.51	14.44	0.1796	1.236
22	0.00	1.79	3.56	5.28	7.06	8.90	12.50	14.43	0.1797	1.236
23	0.00	2.59	5.18	7.68	10.28	12.95	18.19	21.00	0.2650	1.235
24	0.00	2.60	5.19	7.69	10.29	12.96	18.20	21.01	0.2650	1.235
25	0.00	3.45	6.87	10.19	13.67	17.22	24.17	27.88	0.3362	1.234

Table A7. Newtonian Data for 2 1/2" Entrance Section

RUN	P1	P2	P3	P4	P5	P6	P7	P8	Q	SG
26	0.00	3.45	6.87	10.19	13.68	17.23	24.19	27.89	0.3365	1.234
27	0.00	2.63	5.22	7.75	10.41	13.10	18.40	21.23	0.2777	1.233
28	0.00	2.62	5.21	7.74	10.39	13.09	18.40	21.23	0.2777	1.233
29	0.00	6.13	12.22	18.13	24.32	30.58	42.91	49.51	0.5692	1.234
30	0.00	6.13	12.21	18.11	24.29	30.55	42.89	49.49	0.5689	1.234
31	0.00	11.06	22.05	32.72	43.88	55.14	77.43	89.44	1.0424	1.234
32	0.00	11.04	22.02	32.68	43.83	55.08	77.37	89.38	1.0404	1.234
33	0.00	18.84	37.58	55.79	74.85	94.09	132.18	152.90	1.7770	1.234
34	0.00	18.86	37.61	55.80	74.84	94.09	132.16	152.89	1.7791	1.234

Table A8. Newtonian Data for 7 1/2° Conical Entrance Section

RUN	P1	P2	P3	P4	P5	P6	P7	P8	Q	SG
1	0.00	3.13	6.25	9.27	12.40	15.59	21.88	25.33	C.4005	1.230
2	0.00	3.13	6.25	9.26	12.38	15.57	21.85	25.30	0.4011	1.230
3	0.00	5.10	10.16	15.08	20.20	25.39	35.64	41.29	0.6811	1.230
4	0.00	5.08	10.15	15.06	20.17	25.35	35.61	41.26	C.6820	1.230
5	0.00	4.30	8.58	12.74	17.07	21.45	30.14	34.90	0.5865	1.230
6	0.00	4.29	8.57	12.73	17.05	21.42	30.11	34.87	C.5862	1.230
7	0.00	5.97	11.90	17.68	23.66	29.72	41.67	48.28	0.8061	1.230
8	0.00	5.99	11.94	17.74	23.73	29.80	41.78	48.41	C.8061	1.230
9	0.00	7.96	15.85	23.54	31.54	39.59	55.55	64.43	1.0496	1.230
10	0.00	8.00	15.92	23.62	31.62	39.69	55.67	64.55	1.0476	1.230
11	0.00	10.72	21.36	31.72	42.5C	53.35	74.89	86.91	1.3814	1.230
12	0.00	10.73	21.39	31.77	42.56	53.42	74.95	86.97	1.3814	1.230
13	0.00	13.70	27.34	40.64	54.45	68.44	96.05	111.53	1.7326	1.230
14	0.00	13.72	27.36	40.65	54.46	68.44	96.05	111.53	1.7361	1.230
15	0.00	7.08	14.11	20.95	28.07	35.27	49.55	57.42	0.8620	1.230
16	0.00	7.05	14.04	20.85	27.94	35.09	49.33	57.17	C.8619	1.230
17	0.00	18.01	35.96	53.46	71.65	89.98	126.56	147.27	2.3707	1.230
18	0.00	18.17	36.29	53.86	72.21	90.71	127.61	148.51	2.3689	1.230
19	0.00	17.93	35.80	53.25	71.33	89.56	125.91	146.50	2.3956	1.230
20	0.00	17.88	35.70	53.11	71.17	89.38	125.69	146.26	2.3984	1.230
21	0.00	2.66	5.30	7.88	10.52	13.21	18.52	21.54	C.9289	1.210
22	0.00	2.65	5.28	7.84	10.48	13.16	18.47	21.50	0.9314	1.210
23	0.00	3.05	6.05	8.99	12.02	15.09	21.20	24.72	1.1113	1.210
24	0.00	3.02	6.00	8.92	11.94	14.98	21.08	24.59	1.1086	1.210
25	0.00	4.28	8.57	12.73	17.04	21.40	30.06	35.17	1.5949	1.210

Table A8. Newtonian Data for 7 1/2° Conical Entrance Section

RUN	P1	P2	P3	P4	P5	P6	P7	P8	Q	SG
26	0.00	4.27	8.54	12.70	17.00	21.35	30.02	35.13	1.5878	1.210
27	0.00	5.38	10.77	16.01	21.45	26.94	37.91	44.45	1.9238	1.210
28	0.00	5.38	10.77	16.01	21.45	26.92	37.89	44.43	1.9399	1.210
29	0.00	6.45	12.92	19.21	25.73	32.28	45.49	53.53	2.3155	1.211
30	0.00	6.47	12.96	19.28	25.82	32.40	45.64	53.69	2.3419	1.211
31	0.00	8.20	16.45	24.48	32.78	41.12	57.87	68.39	3.0155	1.211
32	0.00	8.15	16.35	24.32	32.57	40.86	57.56	68.03	2.9720	1.211
33	0.00	9.03	18.15	27.01	36.17	45.37	63.91	75.75	3.3447	1.211
34	0.00	8.96	17.98	26.74	35.82	44.93	63.33	75.03	3.2872	1.211
35	0.00	11.59	23.31	34.66	46.44	58.23	82.16	98.27	4.3931	1.211
36	0.00	11.65	23.45	34.88	46.71	58.57	82.64	98.87	4.4023	1.211
37	0.00	16.10	32.51	48.34	64.75	81.15	114.57	138.95	6.1690	1.211
38	0.00	16.13	32.59	48.46	64.90	81.33	114.81	139.26	6.2073	1.211
39	0.00	2.40	4.88	7.26	9.70	12.18	17.19	20.81	2.3175	1.182
40	0.00	2.41	4.90	7.27	9.71	12.18	17.19	20.79	2.3170	1.182
41	0.00	3.92	7.97	11.83	15.87	19.89	28.13	34.97	3.7751	1.182
42	0.00	3.94	8.00	11.90	15.95	19.99	28.26	35.11	3.7753	1.182
43	0.00	6.38	13.07	19.38	25.93	32.43	46.18	59.72	6.1516	1.183
44	0.00	6.38	13.08	19.39	25.95	32.47	46.22	59.76	6.1479	1.183
45	0.00	8.62	17.77	26.29	35.22	44.05	63.14	84.40	8.3003	1.184
46	0.00	8.63	17.81	26.34	35.29	44.13	63.23	84.51	8.3400	1.184

Table A9. Newtonian Data for 15° Conical Entrance Section

RUN	P1	P2	P3	P4	P5	P6	P7	P8	Q	SG
1	0.00	4.90	9.76	14.48	19.38	24.34	34.15	39.55	0.5930	1.230
2	0.00	4.90	9.76	14.48	19.38	24.35	34.15	39.55	0.5936	1.230
3	0.00	6.02	12.01	17.83	23.86	29.98	42.10	48.72	0.6777	1.231
4	0.00	5.97	11.93	17.74	23.77	29.88	42.00	48.62	0.6784	1.231
5	0.00	6.30	12.56	18.68	25.01	31.40	44.06	51.03	0.8159	1.230
6	0.00	6.29	12.55	18.65	24.97	31.34	43.99	50.96	0.8163	1.230
7	0.00	7.31	14.59	21.71	29.09	36.53	51.26	59.39	1.0077	1.228
8	0.00	7.30	14.57	21.66	29.02	36.45	51.17	59.30	1.0068	1.228
9	0.00	9.73	19.41	28.86	38.65	48.54	68.15	79.11	1.4090	1.228
10	0.00	9.74	19.42	28.87	38.67	48.55	68.17	79.13	1.4116	1.228
11	0.00	11.31	22.65	33.65	45.06	56.53	79.36	92.19	1.6715	1.228
12	0.00	11.31	22.58	33.59	45.02	56.50	79.37	92.21	1.6754	1.228
13	0.00	14.09	28.17	41.90	56.13	70.45	98.97	115.12	2.0975	1.228
14	0.00	14.13	28.23	42.00	56.28	70.67	99.32	115.55	2.1024	1.228
15	0.00	3.49	6.92	10.42	13.96	17.56	24.68	28.79	1.2145	1.212
16	0.00	3.48	6.88	10.38	13.91	17.49	24.60	28.71	1.2116	1.212
17	0.00	4.24	8.50	12.63	16.90	21.25	29.86	34.94	1.5452	1.212
18	0.00	4.24	8.50	12.62	16.90	21.24	29.85	34.92	1.5444	1.212
19	0.00	5.37	10.75	15.97	21.38	26.81	37.73	44.31	1.9793	1.214
20	0.00	5.38	10.77	15.99	21.39	26.84	37.76	44.34	1.9813	1.214
21	0.00	6.75	13.54	20.13	26.93	33.80	47.63	56.16	2.5229	1.214
22	0.00	6.77	13.59	20.19	27.00	33.87	47.70	56.24	2.5257	1.214
23	0.00	9.48	19.03	28.36	38.00	47.63	67.09	79.70	3.5525	1.212
24	0.00	9.51	19.07	28.37	38.01	47.66	67.13	79.74	3.5500	1.212
25	0.00	13.47	27.15	40.33	54.00	67.70	95.51	114.71	5.0429	1.212

Table A9. Newtonian Data for 15° Conical Entrance Section

RUN	P1	P2	P3	P4	P5	P6	P7	P8	Q	SG
26	0.00	13.47	27.14	40.33	54.01	67.72	95.53	114.74	5.0433	1.212
27	0.00	19.49	39.41	58.61	78.53	98.39	138.92	168.85	6.9432	1.212
28	0.00	19.50	39.42	58.62	78.51	98.36	138.89	168.81	6.9599	1.212
29	0.00	2.15	4.35	6.48	8.69	10.89	15.34	18.55	2.1792	1.182
30	0.00	2.15	4.36	6.50	8.71	10.89	15.36	18.58	2.1816	1.182
31	0.00	2.32	4.70	6.97	9.34	11.69	16.52	20.02	2.2779	1.182
32	0.00	2.32	4.70	6.99	9.36	11.72	16.55	20.05	2.2667	1.182
33	0.00	4.02	8.16	12.12	16.23	20.32	28.78	35.91	3.9284	1.182
34	0.00	4.02	8.17	12.13	16.25	20.36	28.84	35.99	3.9365	1.182
35	0.00	6.14	12.59	18.66	24.99	31.27	44.51	57.44	5.9149	1.182
36	0.00	6.17	12.63	18.71	25.05	31.33	44.57	57.52	5.9816	1.182
37	0.00	8.17	16.83	24.90	33.34	41.69	59.63	79.18	7.8771	1.183
38	0.00	8.17	16.83	24.92	33.40	41.78	59.76	79.32	7.8985	1.183
39	0.00	9.82	20.31	30.02	40.23	50.31	72.33	98.08	9.4552	1.183
40	0.00	9.84	20.36	30.10	40.32	50.41	72.47	98.24	9.4684	1.183

Table A10. Newtonian Data for 30° Conical Entrance Section

RUN	P1	P2	P3	P4	P5	P6	P7	P8	Q	SG
1	0.00	5.02	10.02	14.90	19.96	25.06	35.22	40.73	0.7442	1.229
2	0.00	5.04	10.02	14.89	19.95	25.05	35.21	40.72	0.7446	1.229
3	0.00	9.45	18.84	27.99	37.50	47.10	66.19	76.61	1.2828	1.230
4	0.00	9.42	18.80	27.93	37.42	47.00	66.05	76.45	1.2816	1.230
5	0.00	11.45	22.84	33.95	45.48	57.08	80.16	92.87	1.6095	1.229
6	0.00	11.45	22.83	33.95	45.48	57.08	80.17	92.89	1.6133	1.229
7	0.00	14.11	28.17	41.87	56.09	70.42	98.96	114.70	1.8592	1.230
8	0.00	14.12	28.18	41.90	56.13	70.48	99.04	114.79	1.8607	1.230
9	0.00	13.20	26.33	39.16	52.48	65.91	92.60	107.32	1.7850	1.230
10	0.00	13.19	26.31	39.14	52.46	65.89	92.58	107.30	1.7857	1.230
11	0.00	1.79	3.56	5.27	7.07	8.88	12.46	14.47	0.6183	1.211
12	0.00	1.79	3.57	5.28	7.08	8.90	12.48	14.49	0.6205	1.211
13	0.00	4.37	8.72	12.96	17.37	21.83	30.69	35.86	1.5689	1.211
14	0.00	4.38	8.75	13.01	17.43	21.89	30.76	35.91	1.5727	1.211
15	0.00	6.43	12.88	19.16	25.69	32.27	45.45	53.40	2.3429	1.212
16	0.00	6.46	12.93	19.21	25.74	32.33	45.52	53.48	2.3415	1.212
17	0.00	8.88	17.82	26.53	35.56	44.59	62.82	74.28	3.2380	1.213
18	0.00	8.90	17.84	26.55	35.59	44.64	62.90	74.36	3.2396	1.213
19	0.00	14.77	29.83	44.33	59.36	74.38	104.96	126.09	5.4200	1.214
20	0.00	14.78	29.84	44.34	59.37	74.42	105.01	126.14	5.4142	1.214
21	0.00	19.79	40.07	59.57	79.77	99.95	141.17	171.97	7.2934	1.214
22	0.00	19.79	40.07	59.56	79.76	99.94	141.16	171.97	7.3013	1.214
23	0.00	2.14	4.29	6.37	8.52	10.67	15.02	18.14	2.1788	1.182
24	0.00	2.15	4.30	6.36	8.50	10.65	15.00	18.12	2.1786	1.182
25	0.00	3.34	6.77	10.04	13.41	16.79	23.78	29.43	3.4268	1.182

Table A10. Newtonian Data for 30° Conical Entrance Section

RUN	P1	P2	P3	P4	P5	P6	P7	P8	Q	SG
26	0.00	3.34	6.79	10.07	13.44	16.83	23.81	29.47	3.4407	1.182
27	0.00	4.92	10.04	14.87	19.94	24.94	35.41	45.05	4.9942	1.182
28	0.00	4.92	10.06	14.91	19.99	25.00	35.47	45.10	4.9901	1.182
29	0.00	7.06	14.51	21.48	28.77	35.99	51.37	67.61	7.0736	1.182
30	0.00	7.08	14.57	21.58	28.89	36.12	51.54	67.78	7.0769	1.182

Table All. Newtonian Data for 60° Conical Entrance Section

RUN	P1	P2	P3	P4	P5	P6	P7	P8	Q	SG
1	0.00	4.88	9.73	14.48	19.42	24.42	34.33	39.65	0.6662	1.228
2	0.00	4.90	9.76	14.51	19.46	24.46	34.36	39.68	0.6669	1.228
3	0.00	5.55	11.06	16.43	22.03	27.70	38.88	44.92	0.7611	1.228
4	0.00	5.54	11.05	16.44	22.05	27.71	38.90	44.94	0.7609	1.228
5	0.00	7.16	14.29	21.26	28.49	35.80	50.26	58.09	0.9730	1.228
6	0.00	7.15	14.27	21.26	28.49	35.79	50.26	58.08	0.9735	1.228
7	0.00	10.41	20.74	30.83	41.32	51.90	72.94	84.44	1.4117	1.229
8	0.00	10.40	20.73	30.83	41.31	51.91	72.98	84.50	1.4150	1.229
9	0.00	13.46	26.89	39.97	53.57	67.26	94.53	109.57	1.8367	1.229
10	0.00	13.50	26.95	40.05	53.68	67.41	94.74	109.81	1.8388	1.229
11	0.00	3.08	6.15	9.15	12.25	15.39	21.63	25.12	1.0037	1.214
12	0.00	3.09	6.17	9.16	12.26	15.41	21.66	25.15	1.0056	1.214
13	0.00	4.37	8.76	13.02	17.44	21.91	30.80	35.92	1.5040	1.214
14	0.00	4.38	8.76	13.03	17.46	21.92	30.81	35.92	1.5025	1.214
15	0.00	4.92	9.83	14.60	19.55	24.54	34.50	40.32	1.7566	1.214
16	0.00	4.90	9.79	14.55	19.49	24.48	34.43	40.24	1.7577	1.214
17	0.00	7.89	15.76	23.43	31.42	39.41	55.47	65.38	2.8696	1.213
18	0.00	7.91	15.80	23.48	31.48	39.50	55.61	65.54	2.8675	1.213
19	0.00	14.46	29.17	43.37	58.04	72.72	102.51	122.53	5.0061	1.214
20	0.00	14.50	29.23	43.45	58.15	72.85	102.69	122.75	4.9983	1.214
21	0.00	20.95	42.30	62.93	84.28	105.59	149.19	181.10	7.2372	1.214
22	0.00	21.08	42.59	63.34	84.82	106.24	149.97	182.00	7.2665	1.214
23	0.00	3.00	6.02	8.95	11.98	15.03	21.11	24.89	1.7798	1.198
24	0.00	3.02	6.05	8.97	12.00	15.04	21.14	24.92	1.7860	1.198
25	0.00	3.58	7.19	10.68	14.30	17.93	25.28	29.93	2.1204	1.197

Table All. Newtonian Data for 60° Conical Entrance Section

RUN	P1	P2	P3	P4	P5	P6	P7	P8	Q	SG
26	0.00	3.59	7.20	10.68	14.29	17.93	25.26	29.92	2.1095	1.197
27	0.00	3.72	7.48	11.08	14.82	18.58	26.18	31.08	2.2961	1.197
28	0.00	3.75	7.53	11.15	14.91	18.71	26.35	31.30	2.3047	1.197
29	0.00	5.78	11.66	17.33	23.20	29.07	40.98	49.30	3.4498	1.198
30	0.00	5.80	11.68	17.36	23.23	29.10	41.02	49.34	3.4561	1.198
31	0.00	7.75	15.70	23.32	31.21	39.08	55.24	68.00	5.0007	1.197
32	0.00	7.80	15.77	23.41	31.34	39.22	55.42	68.20	5.0007	1.197
33	0.00	3.13	6.38	9.29	12.69	15.92	22.52	27.80	3.2348	1.181
34	0.00	3.14	6.39	9.30	12.69	15.92	22.52	27.80	3.2360	1.181
35	0.00	4.39	9.58	14.20	19.00	23.78	33.72	42.96	4.8952	1.180
36	0.00	4.38	9.57	14.19	18.96	23.72	33.65	42.88	4.8870	1.180
37	0.00	7.31	15.09	22.33	29.89	37.36	53.50	71.60	7.8116	1.179
38	0.00	7.32	15.09	22.32	29.89	37.36	53.51	71.62	7.7708	1.179
39	0.00	8.67	17.97	26.53	35.53	44.41	63.96	87.63	9.3223	1.179
40	0.00	8.67	17.95	26.50	35.50	44.39	64.03	87.73	9.3039	1.179

Table A12. Data for Methocel M-1 at $\beta = 0.041$

RUN	P1	P2	P3	P4	P5	P6	P7	P8	Q	SG
1	0.00	9.02	17.68	26.85	35.67	45.11	63.24	73.08	1.1578	1.003
2	0.00	9.02	17.71	26.85	35.67	45.11	63.25	73.09	1.1580	1.003
3	0.00	11.09	21.94	33.10	44.00	55.60	77.97	90.25	1.5823	1.003
4	0.00	11.09	21.95	33.10	44.02	55.62	78.00	90.28	1.5808	1.003
5	0.00	13.34	26.46	39.81	53.09	66.89	93.82	108.85	2.1046	1.003
6	0.00	13.33	26.47	39.81	53.11	66.90	93.83	108.86	2.1057	1.003
7	0.00	18.67	37.35	55.88	74.74	93.85	131.81	154.22	3.7054	1.003
8	0.00	18.66	37.35	55.89	74.76	93.86	131.82	154.23	3.7013	1.003
9	0.00	22.86	45.55	68.73	92.11	115.43	162.25	191.73	5.3032	1.003
10	0.00	22.87	45.55	68.73	92.11	115.44	162.26	191.73	5.2954	1.003
11	0.00	14.54	28.99	43.42	58.28	72.93	102.37	118.97	2.4254	1.003
12	0.00	14.53	29.00	43.42	58.28	72.95	102.40	119.00	2.4274	1.003
13	0.00	20.40	40.89	61.18	81.89	102.73	144.37	169.55	4.3313	1.003
14	0.00	20.40	40.90	61.19	81.90	102.75	144.38	169.55	4.3292	1.003
15	0.00	17.15	34.51	51.36	68.76	86.30	121.21	141.41	3.2074	1.003
16	0.00	17.15	34.53	51.39	68.81	86.35	121.25	141.46	3.2055	1.003
17	0.00	7.53	15.09	22.62	30.29	38.03	53.28	61.56	0.9026	1.003
18	0.00	7.55	15.09	22.60	30.27	38.01	53.27	61.55	0.9042	1.003

Table A13. Data for Methocel M-2 at $\beta = 0.041$

RUN	P1	P2	P3	P4	P5	P6	P7	P8	Q	SG
1	0.00	3.99	8.07	11.88	15.82	20.00	27.99	32.39	0.8162	1.002
2	0.00	3.99	8.08	11.87	15.82	19.99	27.98	32.39	0.8137	1.002
3	0.00	7.34	14.49	21.89	29.25	36.77	51.57	60.15	1.8398	1.002
4	0.00	7.33	14.52	21.88	29.25	36.78	51.57	60.15	1.8379	1.002
5	0.00	9.82	19.53	29.34	39.36	49.27	69.22	81.05	2.7929	1.002
6	0.00	9.81	19.54	29.34	39.37	49.28	69.23	81.05	2.7949	1.002
7	0.00	12.73	25.53	38.24	51.23	64.23	90.31	106.87	4.1663	1.002
8	0.00	12.73	25.55	38.26	51.26	64.26	90.34	106.90	4.1726	1.002
9	0.00	16.16	32.54	48.74	65.37	81.83	115.14	138.69	6.1000	1.002
10	0.00	16.16	32.54	48.72	65.35	81.81	115.14	138.68	6.0902	1.002
11	0.00	18.14	36.70	54.90	73.63	92.20	129.90	158.60	7.4748	1.002
12	0.00	18.13	36.69	54.88	73.60	92.17	129.87	158.56	7.4675	1.002
13	0.00	20.09	40.70	60.93	81.65	102.33	144.28	178.92	8.9138	1.002
14	0.00	20.07	40.68	60.90	81.62	102.30	144.26	178.90	8.9203	1.002
15	0.00	4.52	9.00	13.47	18.01	22.66	31.81	36.87	1.0372	1.002
16	0.00	4.52	9.00	13.46	18.02	22.67	31.82	36.88	1.0374	1.002
17	0.00	4.58	9.10	13.63	18.20	22.92	32.16	37.28	1.0561	1.002
18	0.00	4.58	9.11	13.64	18.22	22.94	32.18	37.29	1.0545	1.002
19	0.00	4.77	9.44	14.23	18.93	23.94	33.60	38.91	1.1186	1.002
20	0.00	4.77	9.46	14.25	18.95	23.97	33.63	38.94	1.1195	1.002
21	0.00	4.21	8.32	12.50	16.73	21.03	29.51	34.21	0.9558	1.002
22	0.00	4.20	8.32	12.49	16.72	21.02	29.50	34.20	0.9572	1.002
23	0.00	4.92	9.71	14.69	19.48	24.72	34.70	40.20	1.1696	1.002
24	0.00	4.94	9.75	14.72	19.51	24.75	34.73	40.23	1.1703	1.002

Table A14. Data for Polyox P-1 at $\beta = 0.041$

RUN	P1	P2	P3	P4	P5	P6	P7	P8	Q	SG
1	0.00	3.68	7.35	10.94	14.67	18.46	25.94	29.93	0.4683	0.999
2	0.00	3.68	7.34	10.92	14.66	18.45	25.93	29.92	0.4664	0.999
3	0.00	3.89	7.77	11.56	15.50	19.50	27.41	31.62	0.5027	0.999
4	0.00	3.89	7.77	11.57	15.51	19.51	27.42	31.63	0.5029	0.999
5	0.00	4.07	8.14	12.12	16.25	20.42	28.70	33.14	0.5316	0.999
6	0.00	4.07	8.14	12.12	16.25	20.42	28.69	33.13	0.5265	0.999
7	0.00	4.45	8.89	13.22	17.72	22.27	31.30	36.13	0.6000	0.999
8	0.00	4.45	8.89	13.23	17.72	22.27	31.30	36.13	0.5985	0.999
9	0.00	2.79	5.59	8.35	11.21	14.08	19.74	22.75	0.3227	0.999
10	0.00	2.78	5.58	8.34	11.19	14.06	19.72	22.73	0.3225	0.999
11	0.00	2.95	5.89	8.78	11.78	14.81	20.79	23.99	0.3508	0.999
12	0.00	2.95	5.89	8.77	11.77	14.80	20.78	23.97	0.3501	0.999
13	0.00	3.21	6.40	9.51	12.75	16.05	22.54	25.99	0.3906	0.999
14	0.00	3.22	6.42	9.55	12.79	16.09	22.58	26.04	0.3906	0.999
15	0.00	10.82	21.66	32.28	43.21	54.22	76.17	88.57	2.1646	0.999
16	0.00	10.83	21.68	32.31	43.24	54.24	76.19	88.58	2.1606	0.999
17	0.00	16.85	33.86	50.45	67.59	84.67	119.11	140.65	4.5023	0.999
18	0.00	16.86	33.86	50.44	67.58	84.68	119.14	140.65	4.4887	0.999
19	0.00	17.80	35.84	53.45	71.51	89.59	126.10	149.28	4.9233	0.999
20	0.00	17.81	35.86	53.47	71.56	89.67	126.18	149.38	4.9380	0.999
21	0.00	19.06	38.31	57.05	76.38	95.73	134.79	160.28	5.5155	0.999
22	0.00	19.05	38.32	57.06	76.39	95.73	134.78	160.27	5.5195	0.999
23	0.00	20.06	40.45	60.29	80.76	101.17	142.49	170.14	6.0528	0.999
24	0.00	20.05	40.44	60.28	80.73	101.11	142.40	170.04	6.0636	0.999
25	0.00	21.03	42.51	63.31	84.81	106.20	149.63	179.43	6.5589	0.999

Table A14. Data for Polyox P-1 at $\beta = 0.041$

RUN	P1	P2	P3	P4	P5	P6	P7	P8	Q	SG
26	0.00	21.05	42.52	63.34	84.85	106.24	149.67	179.47	6.5582	0.999
27	0.00	22.50	45.50	67.76	90.79	113.70	160.26	193.46	7.3897	0.999
28	0.00	22.51	45.53	67.82	90.85	113.75	160.32	193.53	7.3763	0.999
29	0.00	23.23	47.01	70.02	93.83	117.49	165.69	200.73	7.8146	0.999
30	0.00	23.25	47.05	70.08	93.89	117.54	165.73	200.76	7.8166	0.999
31	0.00	9.27	18.51	27.61	36.98	46.42	65.27	75.69	1.6738	0.999
32	0.00	9.28	18.54	27.64	37.03	46.46	65.29	75.90	1.6743	0.999
33	0.00	6.48	12.94	19.25	25.78	32.38	45.52	52.59	0.9770	0.999
34	0.00	6.49	12.94	19.25	25.79	32.39	45.53	52.60	0.9787	0.999

Table A15. Data for Polyox P-2 at $\beta = 0.041$

RUN	P1	P2	P3	P4	P5	P6	P7	P8	Q	SG
1	0.00	9.73	19.47	29.00	38.86	48.79	68.58	79.77	2.0932	1.137
2	0.00	9.73	19.46	28.98	38.83	48.76	68.53	79.71	2.0981	1.137
3	0.00	15.08	30.23	45.01	60.29	75.67	106.39	124.84	3.6852	1.137
4	0.00	15.07	30.22	45.00	60.28	75.66	106.37	124.82	3.6824	1.137
5	0.00	18.00	36.17	53.84	72.10	90.45	127.33	150.36	4.6647	1.137
6	0.00	17.99	36.17	53.84	72.10	90.45	127.32	150.35	4.6783	1.137
7	0.00	19.41	39.01	58.09	77.80	97.55	137.31	162.67	5.1337	1.138
8	0.00	19.40	38.99	58.06	77.77	97.51	137.26	162.62	5.1536	1.138
9	0.00	20.18	40.61	60.46	80.96	101.50	142.88	169.59	5.4735	1.138
10	0.00	20.14	40.53	60.35	80.82	101.37	142.69	169.40	5.4544	1.138
11	0.00	21.12	42.51	63.31	84.79	106.32	149.73	178.20	5.7947	1.138
12	0.00	21.11	42.51	63.31	84.77	106.30	149.71	178.17	5.7997	1.138
13	0.00	21.65	43.61	64.94	86.96	109.02	153.58	183.04	6.0223	1.138
14	0.00	21.65	43.62	64.97	87.01	109.09	153.66	183.16	6.0146	1.138
15	0.00	22.54	45.45	67.74	90.74	113.75	160.30	191.58	6.3993	1.138
16	0.00	22.56	45.48	67.77	90.76	113.76	160.31	191.59	6.4000	1.138
17	0.00	23.22	46.80	69.71	93.36	117.02	164.95	197.45	6.6345	1.138
18	0.00	23.22	46.82	69.73	93.39	117.06	165.01	197.53	6.6656	1.138
19	0.00	23.48	47.38	70.55	94.49	118.45	166.95	200.04	6.7647	1.138
20	0.00	23.48	47.37	70.54	94.48	118.43	166.93	200.01	6.7504	1.138
21	0.00	5.25	10.51	15.65	20.97	26.35	36.99	42.77	1.0312	1.138
22	0.00	5.25	10.51	15.65	20.96	26.35	36.99	42.78	1.0307	1.138
23	0.00	2.72	5.42	8.06	10.80	13.56	19.05	21.99	0.4920	1.138
24	0.00	2.72	5.42	8.06	10.80	13.57	19.07	22.00	0.4918	1.138
25	0.00	2.79	5.57	8.28	11.09	13.93	19.59	22.61	0.5081	1.138

Table A15. Data for Polyox P-2 at $\beta = 0.041$

RUN	P1	P2	P3	P4	P5	P6	P7	P8	Q	SG
26	0.00	2.79	5.56	8.27	11.08	13.93	19.59	22.61	0.5069	1.138
27	0.00	2.85	5.70	8.48	11.36	14.28	20.07	23.17	0.5223	1.138
28	0.00	2.85	5.69	8.47	11.35	14.27	20.05	23.15	0.5217	1.138
29	0.00	2.97	5.92	8.80	11.80	14.84	20.86	24.10	0.5461	1.138
30	0.00	2.97	5.93	8.82	11.82	14.86	20.87	24.11	0.5456	1.138
31	0.00	3.10	6.17	9.17	12.29	15.44	21.70	25.08	0.5710	1.138
32	0.00	3.10	6.17	9.18	12.30	15.45	21.71	25.09	0.5712	1.138
33	0.00	3.25	6.48	9.63	12.90	16.21	22.78	26.35	0.6040	1.138
34	0.00	3.25	6.48	9.63	12.91	16.22	22.79	26.36	0.6027	1.138
35	0.00	3.45	6.86	10.19	13.66	17.17	24.12	27.88	0.6442	1.138
36	0.00	3.46	6.87	10.20	13.67	17.17	24.13	27.89	0.6429	1.138
37	0.00	3.87	7.71	11.46	15.33	19.27	27.08	31.32	0.7306	1.138
38	0.00	3.87	7.71	11.45	15.32	19.26	27.08	31.32	0.7326	1.138

Table A16. Data for Polyox P-3 at $\beta = 0.041$

RUN	P1	P2	P3	P4	P5	P6	P7	P8	Q	SG
1	0.00	4.41	8.81	13.09	17.54	22.04	30.97	35.82	0.9478	1.141
2	0.00	4.40	8.80	13.09	17.54	22.04	30.96	35.81	0.9478	1.141
3	0.00	8.60	17.18	25.59	34.30	43.04	60.47	70.43	2.0804	1.140
4	0.00	8.59	17.17	25.57	34.28	43.02	60.45	70.40	2.0794	1.140
5	0.00	14.54	29.15	43.43	58.16	72.94	102.66	121.00	4.0026	1.140
6	0.00	14.53	29.14	43.41	58.15	72.93	102.64	120.97	3.9982	1.140
7	0.00	17.97	36.16	53.81	72.07	90.39	127.29	151.29	5.2395	1.140
8	0.00	17.96	36.14	53.79	72.05	90.36	127.26	151.25	5.2381	1.140
9	0.00	20.56	41.44	61.66	82.61	103.43	145.84	174.60	6.2493	1.140
10	0.00	20.56	41.44	61.67	82.62	103.54	145.93	174.68	6.2544	1.140
11	0.00	22.54	45.45	67.66	90.68	113.65	160.23	192.94	7.0377	1.140
12	0.00	22.54	45.47	67.68	90.72	113.70	160.28	193.01	7.0450	1.140
13	0.00	22.94	46.34	69.02	92.49	115.90	163.45	197.13	7.2587	1.140
14	0.00	22.95	46.34	69.00	92.47	115.88	163.41	197.07	7.2355	1.140
15	0.00	2.82	5.64	8.41	11.28	14.19	19.96	23.07	0.5968	1.140
16	0.00	2.82	5.64	8.41	11.29	14.20	19.97	23.07	0.5969	1.140
17	0.00	2.89	5.76	8.58	11.51	14.48	20.36	23.54	0.6120	1.140
18	0.00	2.90	5.78	8.61	11.54	14.51	20.40	23.58	0.6119	1.140
19	0.00	3.16	6.33	9.42	12.64	15.88	22.31	25.81	0.6730	1.140
20	0.00	3.16	6.33	9.42	12.64	15.88	22.30	25.80	0.6727	1.140
21	0.00	3.25	6.50	9.68	12.99	16.32	22.93	26.53	0.6987	1.140
22	0.00	3.24	6.48	9.65	12.96	16.29	22.90	26.50	0.6996	1.140
23	0.00	3.47	6.94	10.32	13.83	17.39	24.44	28.28	0.7530	1.140
24	0.00	3.47	6.94	10.33	13.84	17.39	24.44	28.27	0.7509	1.140

Table A17. Data for Polyox P-4 at $\beta = 0.041$

RUN	P1	P2	P3	P4	P5	P6	P7	P8	Q	SG
1	0.00	6.44	12.88	19.18	25.68	32.26	45.28	52.33	1.0529	1.004
2	0.00	6.44	12.88	19.18	25.67	32.23	45.24	52.29	1.0530	1.004
3	0.00	9.47	18.95	28.24	37.78	47.44	66.60	77.33	1.8842	1.004
4	0.00	9.47	18.94	28.21	37.74	47.37	66.52	77.22	1.8838	1.004
5	0.00	15.21	30.57	45.61	60.99	76.41	107.49	126.62	4.1002	1.004
6	0.00	15.21	30.55	45.59	60.98	76.41	107.47	126.59	4.1005	1.004
7	0.00	18.55	37.40	55.79	74.61	93.51	131.60	157.13	5.7641	1.004
8	0.00	18.54	37.40	55.78	74.61	93.50	131.60	157.12	5.7980	1.004
9	0.00	19.91	40.18	59.91	80.16	100.43	141.49	170.04	6.5858	1.004
10	0.00	19.91	40.19	59.92	80.17	100.45	141.50	170.04	6.5794	1.004
11	0.00	22.55	45.67	68.08	91.15	114.08	160.89	196.40	8.3252	1.004
12	0.00	22.55	45.67	68.08	91.15	114.08	160.89	196.39	8.3128	1.004
13	0.00	21.64	43.72	65.14	87.19	109.14	153.95	186.99	7.7128	1.004
14	0.00	21.64	43.70	65.13	87.20	109.15	153.94	186.98	7.7275	1.004
15	0.00	6.68	13.36	19.90	26.63	33.46	46.92	54.28	1.1992	1.004
16	0.00	6.68	13.35	19.88	26.60	33.43	46.89	54.25	1.1965	1.004
17	0.00	3.78	7.54	11.25	15.07	18.97	26.66	30.78	0.5708	1.004
18	0.00	3.79	7.55	11.26	15.07	18.96	26.65	30.76	0.5704	1.004
19	0.00	3.97	7.92	11.80	15.80	19.85	27.89	32.22	0.6090	1.004
20	0.00	3.97	7.93	11.81	15.82	19.87	27.92	32.25	0.6086	1.004
21	0.00	4.18	8.34	12.41	16.61	20.87	29.32	33.89	0.6512	1.004
22	0.00	4.18	8.33	12.39	16.60	20.86	29.30	33.87	0.6517	1.004
23	0.00	4.40	8.79	13.08	17.51	22.00	30.92	35.75	0.7030	1.004
24	0.00	4.40	8.80	13.10	17.54	22.04	30.96	35.78	0.7027	1.004
25	0.00	4.68	9.36	13.92	18.64	23.40	32.86	38.01	0.7618	1.004
26	0.00	4.68	9.36	13.93	18.65	23.42	32.88	38.02	0.7619	1.004

Table A18. Data for Polyox P-5 at $\beta = 0.041$

RUN	P1	P2	P3	P4	P5	P6	P7	P8	Q	SG
1	0.00	12.57	25.18	37.56	50.33	63.06	88.76	104.48	3.6524	1.048
2	0.00	12.57	25.19	37.57	50.33	63.07	88.77	104.48	3.6572	1.048
3	0.00	17.30	34.87	51.98	69.56	87.17	122.78	147.03	5.8491	1.048
4	0.00	17.31	34.88	52.00	69.59	87.19	122.81	147.07	5.8609	1.048
5	0.00	19.77	39.94	59.52	79.67	99.80	140.70	170.38	7.1423	1.048
6	0.00	19.78	39.96	59.54	79.71	99.84	140.74	170.43	7.1557	1.048
7	0.00	21.49	43.49	64.79	86.75	108.63	153.23	187.12	8.1073	1.048
8	0.00	21.49	43.49	64.79	86.75	108.63	153.23	187.13	8.0955	1.048
9	0.00	22.03	44.64	66.52	89.05	111.48	157.28	192.61	8.4299	1.048
10	0.00	22.03	44.65	66.52	89.06	111.51	157.33	192.66	8.4136	1.048
11	0.00	4.08	8.13	12.09	16.17	20.31	28.52	32.97	0.8082	1.048
12	0.00	4.08	8.13	12.10	16.19	20.34	28.57	33.02	0.8078	1.048
13	0.00	2.98	5.94	8.85	11.86	14.90	20.94	24.17	0.5688	1.048
14	0.00	2.98	5.94	8.85	11.86	14.91	20.95	24.19	0.5673	1.048
15	0.00	3.11	6.20	9.23	12.36	15.53	21.83	25.22	0.6005	1.048
16	0.00	3.11	6.20	9.23	12.36	15.53	21.83	25.22	0.6000	1.048
17	0.00	3.32	6.59	9.80	13.13	16.49	23.17	26.78	0.6448	1.048
18	0.00	3.31	6.59	9.81	13.14	16.51	23.19	26.80	0.6449	1.048
19	0.00	3.46	6.90	10.28	13.78	17.31	24.31	28.12	0.6828	1.048
20	0.00	3.47	6.91	10.29	13.79	17.32	24.34	28.14	0.6830	1.048
21	0.00	8.45	16.89	25.16	33.70	42.29	59.47	69.25	2.1085	1.048
22	0.00	8.44	16.87	25.13	33.67	42.26	59.43	69.21	2.1071	1.048
23	0.00	12.30	24.68	36.78	49.27	61.80	86.92	102.22	3.5678	1.048
24	0.00	12.30	24.68	36.78	49.27	61.80	86.91	102.21	3.5589	1.048
25	0.00	17.30	34.87	51.93	69.54	87.13	122.71	147.05	5.8841	1.048

Table A18. Data for Polyox P-5 at $\beta = 0.041$

RUN	P1	P2	P3	P4	P5	P6	P7	P8	Q	SG
26	0.00	17.31	34.87	51.95	69.57	87.16	122.76	147.09	5.8784	1.048
27	0.00	21.07	42.61	63.45	84.97	106.40	150.11	183.06	7.9345	1.048
28	0.00	21.07	42.61	63.46	84.98	106.42	150.13	183.09	7.9129	1.048
29	0.00	18.54	37.35	55.64	74.51	93.33	131.53	158.39	6.4802	1.048
30	0.00	18.53	37.36	55.65	74.53	93.36	131.57	158.43	6.4919	1.048

Table A19. Data for Polyox P-6 at $\beta = 0.636$

RUN	P1	P2	P3	P4	P5	P6	P7	P8	Q	SG
1	0.00	6.93	13.83	20.60	27.58	34.64	48.60	56.53	0.8264	1.005
2	0.00	6.93	13.83	20.59	27.56	34.62	48.58	56.51	0.8262	1.005
3	0.00	8.71	17.40	25.92	34.67	43.61	61.15	71.20	1.1447	1.005
4	0.00	8.73	17.42	25.94	34.70	43.64	61.19	71.23	1.1654	1.005
5	0.00	10.31	20.58	30.68	41.12	51.70	72.43	84.39	1.4632	1.005
6	0.00	10.30	20.57	30.68	41.12	51.70	72.44	84.38	1.4645	1.005
7	0.00	13.81	27.59	41.12	55.10	69.11	97.07	113.32	2.2780	1.005
8	0.00	13.81	27.59	41.13	55.12	69.13	97.08	113.33	2.2830	1.005
9	0.00	17.34	34.73	51.81	69.17	86.84	122.00	142.82	3.2617	1.005
10	0.00	17.34	34.73	51.80	69.18	86.86	122.03	142.85	3.2591	1.005
11	0.00	23.17	46.53	69.38	92.85	116.55	163.85	193.04	5.3502	1.005
12	0.00	23.18	46.57	69.42	92.92	116.42	163.78	192.97	5.3064	1.005
13	0.00	23.89	47.98	71.48	95.08	120.05	168.76	198.99	5.5547	1.005
14	0.00	23.88	47.97	71.48	95.70	120.16	168.86	199.09	5.5593	1.005
15	0.00	8.28	16.53	24.61	32.96	41.36	58.09	67.59	1.0780	1.005
16	0.00	8.28	16.53	24.61	32.96	41.36	58.09	67.60	1.0778	1.005
17	0.00	4.91	9.78	14.55	19.58	24.45	34.42	39.99	0.5367	1.005
18	0.00	4.91	9.79	14.57	19.59	24.48	34.44	40.01	0.5371	1.005
19	0.00	5.72	11.43	17.01	22.78	28.55	40.23	46.79	0.6712	1.005
20	0.00	5.73	11.44	17.01	22.80	28.59	40.26	46.81	0.6704	1.005

Table A20. Data for Polyox P-7 at $\beta = 0.636$

RUN	P1	P2	P3	P4	P5	P6	P7	P8	Q	SG
1	0.00	4.42	8.85	13.17	17.65	22.17	31.11	36.20	0.9572	1.048
2	0.00	4.43	8.86	13.18	17.65	22.17	31.12	36.21	0.9568	1.048
3	0.00	4.34	8.63	12.84	17.18	21.57	30.31	35.27	0.9277	1.048
4	0.00	4.34	8.64	12.84	17.18	21.58	30.33	35.29	0.9273	1.048
5	0.00	6.33	12.66	18.86	25.20	31.63	44.42	51.80	1.4947	1.048
6	0.00	6.32	12.65	18.85	25.20	31.63	44.43	51.81	1.4938	1.048
7	0.00	9.55	19.14	28.49	38.11	47.85	67.22	78.71	2.5714	1.048
8	0.00	9.55	19.14	28.47	38.09	47.83	67.20	78.69	2.5758	1.048
9	0.00	11.31	22.68	33.75	45.21	56.65	79.73	93.60	3.2550	1.048
10	0.00	11.31	22.68	33.76	45.21	56.67	79.76	93.64	3.2501	1.048
11	0.00	14.86	29.84	44.45	59.54	74.54	105.01	124.10	4.7828	1.048
12	0.00	14.86	29.85	44.46	59.54	74.55	105.04	124.13	4.7809	1.048
13	0.00	18.00	36.29	54.07	72.39	90.73	127.86	152.19	6.3467	1.048
14	0.00	17.99	36.29	54.06	72.38	90.72	127.86	152.20	6.3567	1.048
15	0.00	19.95	40.27	60.02	80.41	100.66	141.99	169.98	7.4004	1.048
16	0.00	19.95	40.29	60.04	80.43	100.69	142.02	170.00	7.3924	1.048
17	0.00	21.72	44.01	65.52	87.70	109.94	154.98	186.47	8.4334	1.048
18	0.00	21.72	44.00	65.52	87.72	109.95	155.01	186.50	8.4509	1.048
19	0.00	22.62	45.85	68.25	91.40	114.46	161.58	194.98	8.9675	1.048
20	0.00	22.62	45.85	68.26	91.42	114.48	161.62	195.03	9.0046	1.048
21	0.00	3.34	6.73	10.01	13.40	16.84	23.67	27.52	0.6896	1.048
22	0.00	3.34	6.72	10.01	13.40	16.83	23.66	27.51	0.6899	1.048
23	0.00	3.63	7.25	10.78	14.43	18.13	25.46	29.60	0.7536	1.048
24	0.00	3.63	7.25	10.77	14.42	18.13	25.47	29.61	0.7543	1.048
25	0.00	3.85	7.67	11.42	15.26	19.18	26.93	31.35	0.8082	1.048

Table A20. Data for Poolyox P-7 at $\beta = 0.636$

RUN	P1	P2	P3	P4	P5	P6	P7	P8	Q	SG
26	0.00	3.85	7.67	11.42	15.27	19.19	26.94	31.35	0.8073	1.048
27	0.00	4.09	8.13	12.10	16.17	20.33	28.57	33.26	0.8724	1.048
28	0.00	4.09	8.14	12.11	16.19	20.35	28.60	33.29	0.8714	1.048
29	0.00	4.26	8.50	12.66	16.96	21.30	29.91	34.82	0.9186	1.048
30	0.00	4.26	8.49	12.66	16.96	21.30	29.91	34.82	0.9192	1.048
31	0.00	4.39	8.74	13.01	17.41	21.86	30.72	35.76	0.9507	1.048
32	0.00	4.39	8.74	13.01	17.42	21.87	30.73	35.77	0.9513	1.048
33	0.00	3.13	6.24	9.29	12.44	15.64	21.97	25.55	0.6402	1.048
34	0.00	3.14	6.25	9.30	12.45	15.65	21.98	25.56	0.6406	1.048
35	0.00	3.27	6.53	9.70	12.99	16.33	22.92	26.66	0.6707	1.048
36	0.00	3.27	6.53	9.70	13.00	16.34	22.94	26.68	0.6720	1.048

Table A21. Data for Separan at $\beta = 0.041$

RUN	P1	P2	P3	P4	P5	P6	P7	P8	Q	SG
1	0.00	7.39	14.81	22.06	29.32	36.77	51.26	59.77	1.0806	1.004
2	0.00	7.39	14.81	22.06	29.34	36.80	51.30	59.82	1.0770	1.004
3	0.00	7.69	15.46	23.07	30.69	38.47	53.51	62.48	1.2002	1.004
4	0.00	7.70	15.48	23.09	30.71	38.50	53.54	62.51	1.1973	1.004
5	0.00	8.58	17.39	25.71	34.10	42.72	59.44	69.60	1.5672	1.004
6	0.00	8.58	17.40	25.71	34.09	42.71	59.41	69.58	1.5692	1.004
7	0.00	9.92	20.06	29.91	39.86	49.84	69.19	81.81	2.3051	1.004
8	0.00	9.95	20.11	29.97	39.91	49.90	69.25	81.87	2.3024	1.004
9	0.00	13.20	26.89	40.08	53.48	66.92	92.57	113.38	4.7423	1.004
10	0.00	13.22	26.93	40.13	53.54	66.99	92.66	113.45	4.7416	1.004
11	0.00	5.25	10.62	15.73	20.98	26.32	36.83	42.69	0.5208	1.004
12	0.00	5.26	10.63	15.74	21.00	26.34	36.86	42.71	0.5224	1.004
13	0.00	5.47	11.03	16.35	21.81	27.36	38.27	44.36	0.5759	1.004
14	0.00	5.47	11.03	16.35	21.81	27.36	38.27	44.36	0.5727	1.004
15	0.00	5.58	11.26	16.73	22.33	28.01	39.18	45.42	0.6144	1.004
16	0.00	5.58	11.26	16.72	22.32	28.00	39.18	45.43	0.6142	1.004
17	0.00	5.96	11.96	17.83	23.79	29.84	41.72	48.41	0.7276	1.004
18	0.00	5.96	11.97	17.84	23.78	29.83	41.72	48.40	0.7251	1.004
19	0.00	6.78	13.64	20.30	27.05	33.95	47.36	55.09	0.9848	1.004
20	0.00	6.78	13.65	20.29	27.02	33.93	47.35	55.07	0.9798	1.004
21	0.00	11.55	23.40	34.77	46.32	57.95	80.77	96.57	3.5444	1.004
22	0.00	11.53	23.37	34.74	46.29	57.93	80.77	96.57	3.5502	1.004